METEOROLOGICAL FACTORS IN HIGH RESOLUTION SATELLITE IMAGERY (DMSP)

Mark Evans Schultz

NAVAL POSTGRADUATE SCHOOL
Monterey, California

THESIS

METEOROLOGICAL FACTORS IN HIGH RESOLUTION
SATELLITE IMAGERY
(DMSP)

by

Mark Evans Schultz

June 1981

Thesis Advisor: K. L. Davidson

SECURITY CLASSIFICATION OF THIS PAGE (When Data Entered)

REPORT DOCUMENTATION PAGE

READ INSTRUCTIONS BEFORE COMPLETING FORM

1. REPORT NUMBER	2. GOVT ACCESSION NO. / 3. RECIPIENT'S CATALOG NUMBER
4. TITLE (and Subtitle): Meteorological Factors in High Resolution Satellite Imagery (DMSP)	5. TYPE OF REPORT & PERIOD COVERED: Masters Thesis; June 1981 / 6. PERFORMING ORG. REPORT NUMBER
7. AUTHOR(s): Mark Evans Schultz	8. CONTRACT OR GRANT NUMBER(s)
9. PERFORMING ORGANIZATION NAME AND ADDRESS: Naval Postgraduate School, Monterey, California 93940	10. PROGRAM ELEMENT, PROJECT, TASK AREA & WORK UNIT NUMBERS
11. CONTROLLING OFFICE NAME AND ADDRESS: Naval Postgraduate School, Monterey, California 93940	12. REPORT DATE: June 1981 / 13. NUMBER OF PAGES: 106
14. MONITORING AGENCY NAME & ADDRESS(if different from Controlling Office)	15. SECURITY CLASS. (of this report): Unclassified / 15a. DECLASSIFICATION/DOWNGRADING SCHEDULE

16. DISTRIBUTION STATEMENT (of this Report)

Approved for public release; distribution unlimited.

17. DISTRIBUTION STATEMENT (of the abstract entered in Block 20, if different from Report)

18. SUPPLEMENTARY NOTES

19. KEY WORDS (Continue on reverse side if necessary and identify by block number)

Aerosol, Size Distribution, Volume Distribution, Meteorology, DMSP, Satellite, High Resolution Imagery, Boundary Layer, Marine, Ocean, Munn-Katz Model, Shettle and Fenn Model.

20. ABSTRACT (Continue on reverse side if necessary and identify by block number)

Comparisons of the predicted aerosol size distributions from the Shettle and Fenn, the Munn-Katz, and the Hybrid models are made with aerosol size distribution data sets collected off the California coast near Monterey in April and May, 1980. It is shown that the mixing volume (inversion height) is an important parameter in predictive aerosol distribution equations. The Hybrid model is determined to be inaccurate when compared with the Shettle and Fenn and the Munn-Katz models. The

DD FORM 1 JAN 73 1473 EDITION OF 1 NOV 65 IS OBSOLETE
S/N 0102-014-6601
(Page 1)

SECURITY CLASSIFICATION OF THIS PAGE (When Data Entered)

Shettle and Fenn model consistently provided the most accurate results. However, it requires an input of either total particle concentration or visibility, neither of which are easily measured or predicted. The Munn-Katz model is determined to be the most operationally useful of the three models studied. It depends only on the bulk meteorological parameters of wind speed, relative humidity and altitude. The Munn-Katz model neglects mixing volume and advection. The observed data further suggest that an aerosol model which does not include a continental distribution may be more appropriate for the open ocean environment.

Approved for public release; distribution unlimited.

Meteorological Factors in High Resolution Satellite Imagery (DMSP)

by

Mark Evans Schultz
Lieutenant, United States Navy
B.S., University of Washington, 1974

Submitted in partial fulfillment of the
requirements for the degree of

MASTER OF SCIENCE IN METEOROLOGY AND OCEANOGRAPHY

from the

NAVAL POSTGRADUATE SCHOOL
June 1981

ABSTRACT

Comparisons of the predicted aerosol size distributions from the Shettle and Fenn, the Munn-Katz, and the Hybrid models are made with aerosol size distribution data sets collected off the California coast near Monterey in April and May, 1980. It is shown that the mixing volume (inversion height) is an important parameter in predictive aerosol distribution equations. The Hybrid model is determined to be inaccurate when compared with the Shettle and Fenn and the Munn-Katz models. The Shettle and Fenn model consistently provided the most accurate results. However, it requires an input of either total particle concentration or visibility, neither of which are easily measured or predicted. The Munn-Katz model is determined to be the most operationally useful of the three models studied. It depends only on the bulk meteorological parameters of wind speed, relative humidity and altitude. The Munn-Katz model neglects mixing volume and advection. The observed data further suggest that an aerosol model which does not include a continental distribution may be more appropriate for the open ocean environment.

TABLE OF CONTENTS

LIST OF PLATES

LIST OF TABLES

LIST OF FIGURES

I. INTRODUCTION

In the early 1970's the Navy's geophysics community was called upon to provide operational environmental support for the ever-growing use of electro-optical (EO) devices. As a result of lack of experience in the field, adequate support could not be provided. In addition the civilian research community had failed to provide clear-cut guidance as to the environmental effects on EO systems. Since that time there has been an increased naval and civilian research effort to better understand and predict aerosols, and their effects on the propagation of electromagnetic radiation.

Today the Navy is still in need of reliable methods for estimating EO system performance for slant path ranges. This requires a better understanding of aerosol loading in the atmosphere along vertical paths, and more specifically, how such aerosol loading is affected by changing meteorological conditions. Once aerosol size distributions have been determined along a path through the atmosphere, estimates of extinction at different wavelengths can be calculated using Mie scattering theory.

One such effort has been the investigation of "anomalous" gray shades in DMSP (Defense Meteorological Satellite Program) VHR (very high resolution) imagery and LF (light fine) imagery (Fett and Isaacs, 1979; Isaacs, 1980). In the past, these gray shades have been attributed to low level haze and moisture, thin cirrus clouds, shallow or turbid water, ocean spray, thin fog, and sun glint (Fenn and Mitchell, 1977).

Isaacs (1980) attempted to show that gray shades commonly observed in DMSP imagery are highly dependent on the atmosphere's aerosol loading. An original objective of this thesis was to validate Isaacs' (1980) model using a unique set of satellite imagery (Plates I - III) and aerosol data obtained in April and May of 1980 by investigators at the Naval Postgraduate School. The aerosol data were gathered off the California coast near Monterey and DMSP imagery was made available for the experimental period by the Naval Environmental Prediction Research Facility (NEPRF).

From the satellite imagery, it was determined that two days, 30 April and 4 May, provided the best gray shade variation for the validation. Unfortunately, the imagery could be neither navigated nor analyzed quantitatively because the satellite data were stored in encrypted form. (Hardware was not available to transform the data into a format which was usable on equipment available to the Naval Postgraduate School.)

The above mentioned difficulties with the satellite imagery precluded determination of the azimuthal and zenith angles and quantitative radiance levels, for each investigated pixel, which are required as inputs by Isaacs' (1980) radiative transfer algorithm. It was therefore decided to restructure the thesis objective to investigate the relative accuracy of the aerosol models employed by Isaacs (1980). Size distributions determined by each model were compared to measured distributions.

A secondary thesis objective was to determine the extent to which the observed size distributions were dependent on the mixing volume, as well as on wind speed and relative humidity. The results implicate

the inversion height as an important parameter in the equations describing the size distribution.

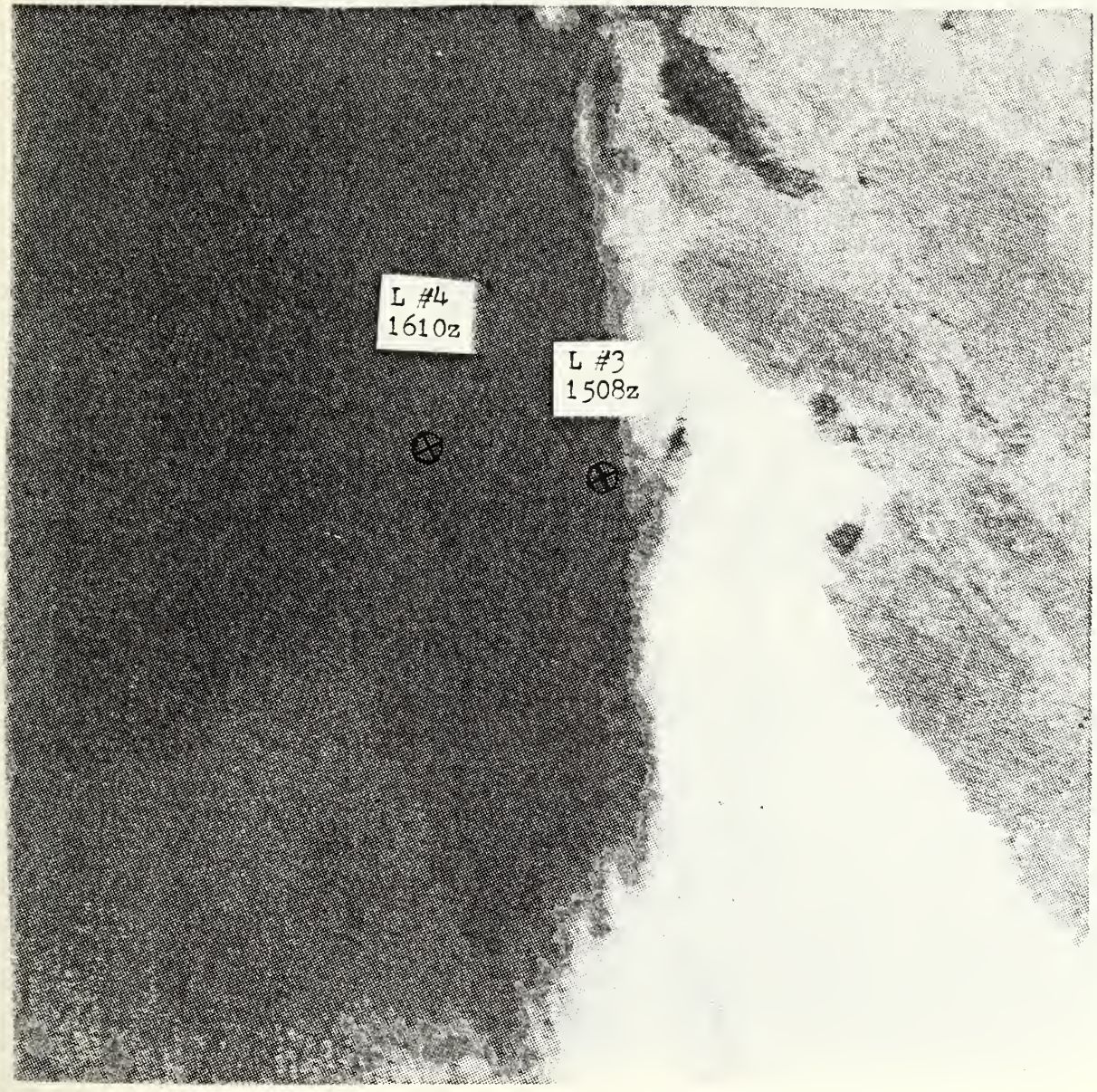

Plate I. DMSP, LF-Log Enhancement, 1911Z, 30 Apr 80
(1911Z = 1911 GMT)

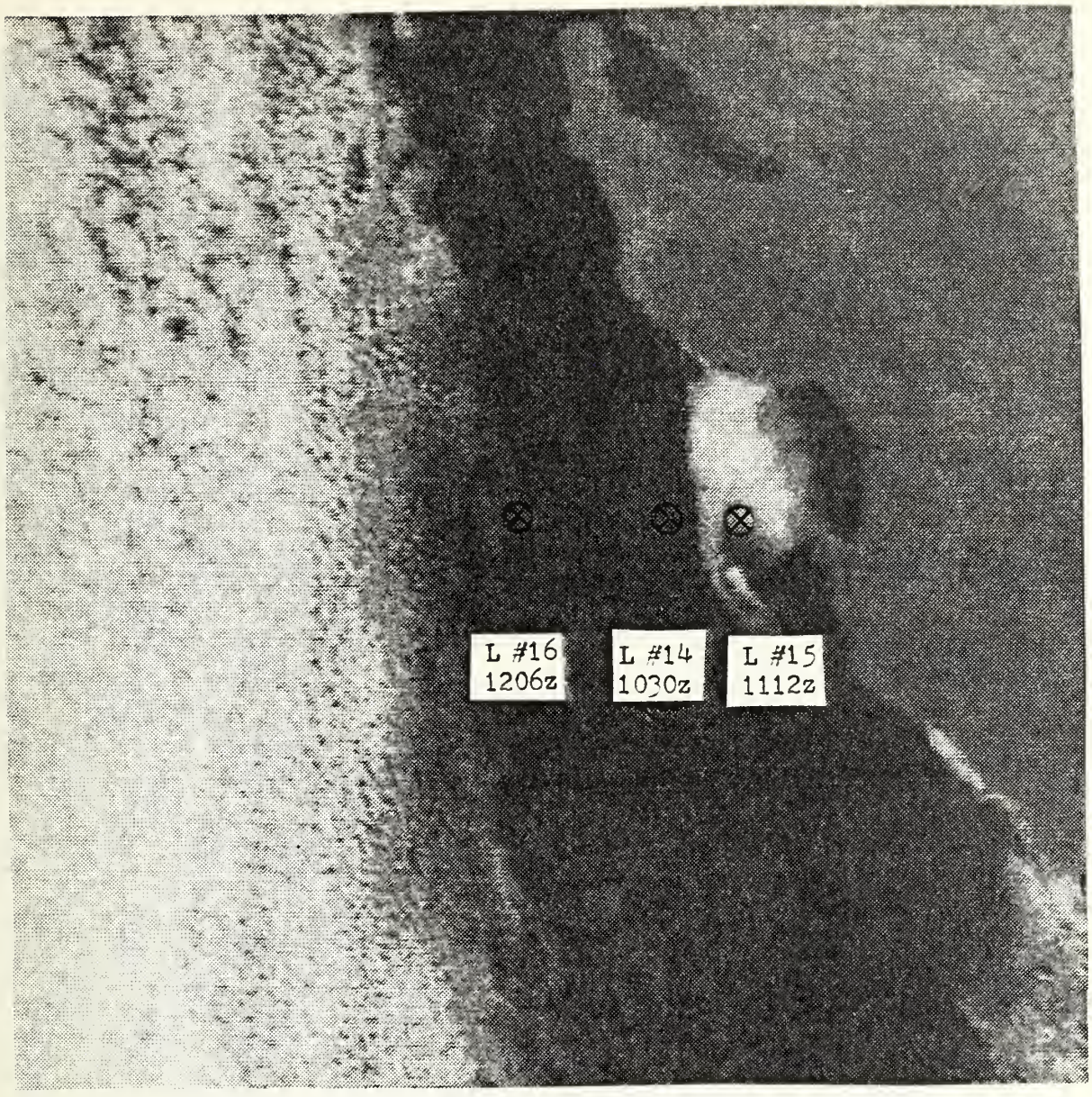

Plate II. DMSP, LF-Log Enhancement, 1753Z, 4 May 80
(1753Z = 1753 GMT)

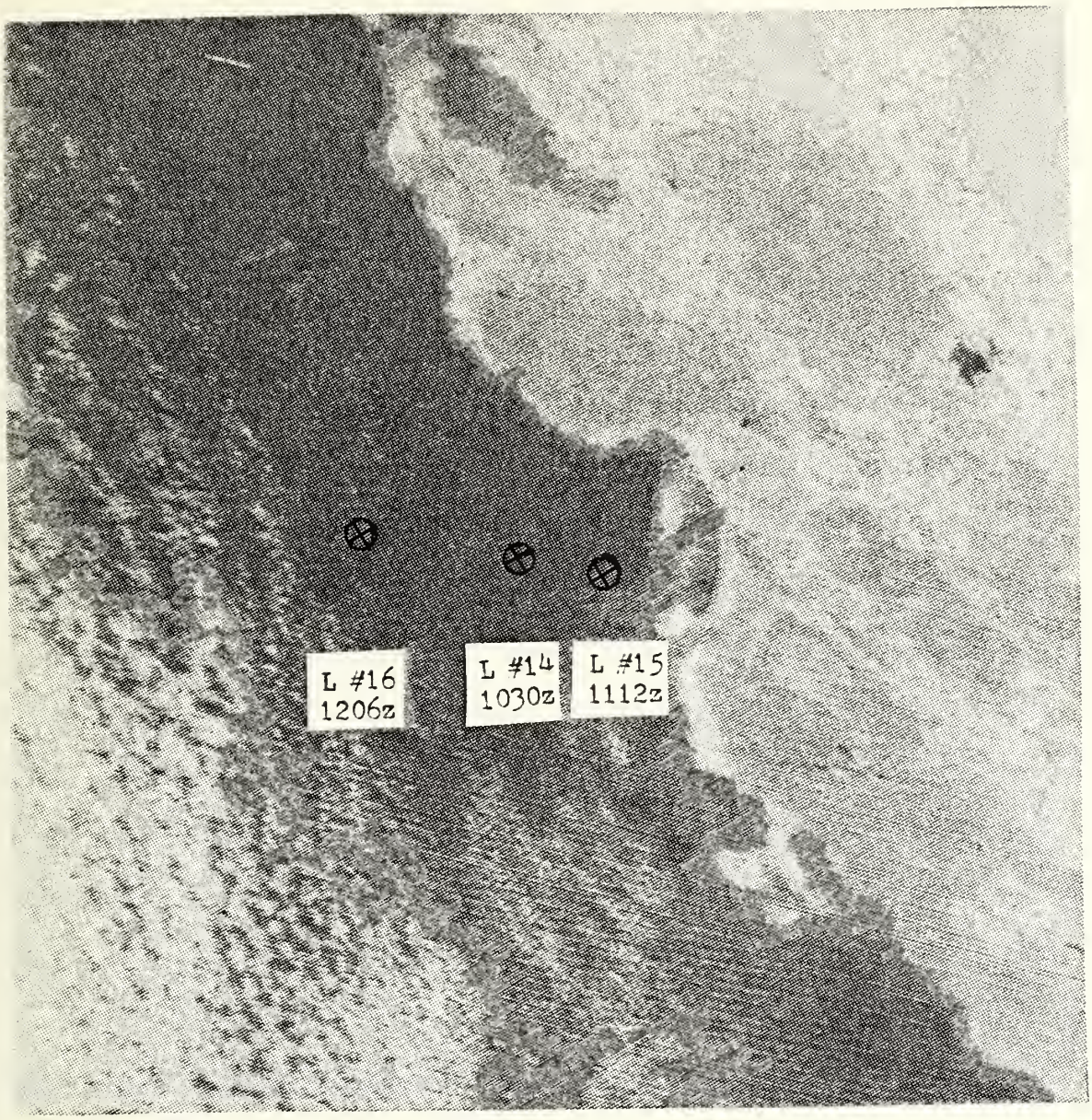

Plate III. DMSP, LF-Log Enhancement, 1933Z, 4 May 80
(1933Z = 1933 GMT)

II. BACKGROUND

Radiative transfer modeling in the visible and infrared wavelength regions requires input data defining the optical structure of the atmosphere if the model is to accurately depict observed radiative propagation conditions. The required input data are: 1) total Rayleigh optical depth, 2) absorption optical depth, 3) surface reflectivity (including sun glint effects), 4) surface emittance, 5) total aerosol optical depth, 6) aerosol height distribution, and 7) aerosol size distribution. The focus of work in this thesis was on the last three types of input data.

It has been established for some time that aerosols significantly affect remote sensing, particularly in the atmospheric boundary layer of the marine environment. A primary effort in air-ocean radiative transfer studies has been to develop models which would describe quantitatively and realistically the aerosol distribution in the planetary boundary layer. This has proven to be difficult because marine aerosols typically display spatial and temporal variability in concentration, composition, shape, index of refraction, and size distribution. Moreover, size distributions of marine aerosols are strongly influenced by wind speed, relative humidity, atmospheric stability, and air mass trajectory, all of which vary in time and space. It is necessary, therefore, to determine the dependence of aerosol size distribution on these parameters, as well as the variability of the specific parameters under various atmospheric conditions. Existing models for predicting aerosol numbers and size distributions include only effects due to wind speed

and relative humidity, and are inexact. Since aerosol particles degrade signal intensity in an amount which is proportional to their number and size, it is to be expected that the modeled aerosol effects on extinction will be imperfect.

The fundamental link between the meteorological variables and the aerosol optical properties is the size distribution, n(r), and in coastal areas, the chemical composition. The size distribution is a function describing the number density of aerosols of radius r within a size range from r to r + dr. Observational evidence indicates that the size distribution can be reproduced by three modes (Whitby and Sverdrup, 1978). These modes are: (1) the Aitkin nuclei mode ($r < 0.1$ μm radius), (2) an accumulation mode ($0.1 < r < 1.0$ μm radius, and (3) a coarse mode ($1.0 < r$ μm radius). However, the effect of Aitkin nuclei on optical properties in the 0.4 to 1.1 μm wavelength range is negligible. Therefore, we will consider only the accumulation and coarse modes. Work of Meszaros and Vissy (1974) indicates that each mode has distinct source mechanisms and compositions. For conceptual distinction by source these two modes are also referred to as the "continental" and "maritime" components respectively.

Isaacs (1980) considered two separate aerosol models in the development of a radiative transfer algorithm. The first model was a relative humidity dependent maritime model attributed to Shettle and Fenn (1979). The second model was a linear combination of the relative humidity dependent continental component of the Shettle and Fenn model and the relative humidity and wind speed dependent maritime component of the Munn-Katz model. This is referred to as the "Hybrid" model (Isaacs,

1980). A third model considered in this study is the Munn-Katz model, as described by Isaacs (1980) and Noonkestor (1980).

A. SHETTLE AND FENN MODEL

The Shettle and Fenn model (Shettle and Fenn, 1979) is the maritime aerosol optical properties model adopted by the Air Force. It is formulated on the number mean radius and standard deviation. It is based on a log normal size distribution and represents only a simple, generalized version of typical conditions since it includes only the relative humidity dependence. It neglects wind speed, stability and advection. This empirical, log normal size distribution is given, according to Isaacs (1980) and Shettle and Fenn (1979), by:

$$n(r) = \sum_{i=1}^{2} N_i[\exp(-\ln^2(\frac{r}{r_{n_i}})/2 \ln^2 \sigma_i)]/r\sqrt{2\pi} \ln \sigma_i \qquad (1)$$

where r_{n_i} is the relative humidity dependent number median radius (or mode radius), σ_i is the standard deviation, and N_i is the total normalized density of particles (cm-3). i=1 refers to the continental component and i=2 refers to the maritime component. The number median is that value, on a log probability plot, with 50% of the distribution's number above and below. Tables I and II describe the above parameters according to Isaacs (1980) and Shettle and Fenn (1979) for the maritime model.

The Shettle and Fenn model depicts a size distribution which simulates a pronounced continental aerosol background mixed with an aerosol of oceanic origin. It has been assumed that the continental component can be given by a rural aerosol model with the exclusion of the very large particles. The large particles are assumed to be lost as the air mass moves out over the ocean.

The maritime component is assumed to be composed of mainly sea salt particles which are produced by the evaporation of sea spray. These particles eventually grow large due to aggregation of water under the high relative humidity conditions of the marine boundary layer (typically above 80% relative humidity). As the relative humidity increases (decreases) the gross effect on the size distribution is to increase (decrease) the average size of the droplets. The magnitude of this change is a function of the initial size and composition of the particles (Isaacs, 1980). Size changes due to the change of liquid water in the particles produce corresponding changes in the effective composition and refractive index of the suspended droplets. This will modify the resulting effects of the aerosols on the absorption and scattering of light. The changes in particle size with relative humidity in the Shettle and Fenn model were based on results by Hänel (1976). This relative humidity dependence enters equation (1) through the number mode radius r_{n_i}, which is given explicitly for several relative humidities in Table II.

The relative humidity dependent size distributions given by the Shettle and Fenn model (eqn (1)) are illustrated in figure 1 for the continental

(accumulation) component, in Figure 2 for the maritime (coarse) component, and in figure 3 for the linear combination of the two. It is interesting to note that the increase in median size between 50 and 95 percent relative humidities is a factor of 1.75 greater in the maritime component than in the continental component (Isaacs, 1980). Also, of interest is the apparent singular point (i.e. $\partial n(r)/\partial(RH) = 0$) at $r = 0.03$ μm or at -1.5 log scale. The significance of this point will be discussed in the section on the Hybrid model (below).

The relative proportions of oceanic and continental derived aerosols will typically vary in time and space, particularly in coastal regions. The Shettle and Fenn model permits adjustment of the relative amounts of the maritime and continental components through its bimodal nature. The component proportion used for the results of this thesis, following Isaacs (1980), is that 40 particles out of every 4000 are assumed to be of marine origin. Gathman and Julian (1979) indicate that numbers on the order of 40/1000 are more typical of the open ocean case. Test computations showed, however, that the results are not sensitive to this factor of 4 difference.

One advantage of the form of the size distribution function as given by equation (1) is that it represents the bimodal nature of atmospheric aerosols. It also permits the number median radius for each mode to be modified for aerosol growth while holding the total number of particles constant. The difficult comes in determining the exact nature of the modifications.

The disadvantage of the Shettle and Fenn model is that it requires, alternately, the input of a fixed total number concentration, or the

scaling of the results by visibility. Both procedures have their drawbacks. First, to input a fixed total number concentration requires an *a priori* knowledge of the size distribution, the very quantity we are trying to predict. Second, while there is some evidence in the literature that scaling by visibility improves the size distribution predicted by aerosol models, visibility remains a very difficult meteorological parameter to measure on a routine basis. Furthermore, the prediction of visibility under present operating conditions is less than adequate.

B. MUNN-KATZ MODEL

The second model investigated was developed by the Navy Electro-Optical Meteorology program. It is a linear combination of Junge and Deirmendjian distributions for the continental and maritime components respectively. The model is based on an earlier model by Wells et al. (1977) as modified by Katz and is referred to as the Munn-Katz model. The size distribution is given by:

$$n(r) = 1.7\left(\frac{r}{\alpha}\right)^{-4} + 1.62(C_1 + C_2 V^{\delta})\exp\left[\frac{-Z}{h_o F} - 8.5\left(\frac{r}{\alpha}\right)^{\Gamma}\right]F^{-1}\left(\frac{r}{\alpha}\right) \quad (2)$$

where r = radius (μm)

z = altitude (m)

h_o = scale height set at 800 m

α = 0.81 Exp [0.066 S/1.058 - S] where

S = saturation ratio (relative humidity/100)

F = Relative humidity growth factor

= 1 + (V/60)

$$\Gamma = 0.384 - 0.00293\ V^{1.25}$$

V = wind factor scaled with surface wind V_o

= .5 m/s for $0 <= V_o <= 4$ m/s

= $(V_o - 3.5)$ m/s for $V_o > 4$ m/s

when $V <= 7$ m/s $C_1 = 350$, $C_2 = 1000$, $\delta = -1.15$

$V > 7$ m/s $C_1 = 0$, $C_2 = 6900$, $\delta = 0.29$

The first term on the RHS of eqn (2) is the continental aerosol component. It does not depend on elevation and wind speed. This specification is intuitively reasonable because the continental aerosols are expected to be well distributed throughout the atmospheric column. The continental component in both the Shettle and Fenn model (eqn (1)) and the Munn-Katz model (eqn (2)) are similar in their dependence on the relative humidity.

The second term on the RHS of eqn (2) is the maritime aerosol component. It is height, relative humidity and wind speed dependent. The maritime component decays exponentially with height, and its wind speed dependence arises due to white cap production.

This formulation is based on several assumptions: (1) the only nuclei present are salt nuclei, (2) the growth rate is independent of radius, (3) the absence of a growth rate hysteresis near a relative humidity of 70% (other models-not discussed-assume that there is a complete hysteresis at or about 70% relative humidity), (4) the aerosols are in equilibrium with the environment, and (5) clouds are absent for relative humidity <99.6%.

In support of assumption (3), measurements have shown that a sodium chloride crystal undergoes a phase transition to a saturated solution

droplet at a relative humidity between 70-75% (as the humidity is increased) and becomes supersaturated and does not crystallize until the relative humidity decreases to a value between 35-45% (Fitzgerald, 1979).

Assumption (5) is clearly unrealistic. Clouds are frequently present in observed data at relative humidities even lower than 90%. However, cloud cases are not considered in this study.

In addition to the above assumptions, the scale height h_o is assumed to be constant and according to Noonkester (1980), this assumption has only a minor effect on N(r) for $r > 1$ μm. This is because the continental component is larger than the maritime component and has no exponential decrease with elevation. However, this need not always be the case and Nilsson (1979) has pointed out that the two modes may equal each other under certain conditions. This appears to be true in a portion of the observed data.

The most significant improvement of the Munn-Katz model over the Shettle and Fenn model is the inclusion of the effects of wind speed on the maritime component. The magnitude of n(r), at large radii, is a function of the surface wind speed, V_o, as illustrated, for the fixed relative humidity of 80%, in figures 4-6. The wind speeds used are 0, 5, 7, and 10 m/s. Figure 4 emphasizes that the continental component is not dependent on wind speed. (All four wind speed curves plot exactly on top of each other.) Figure 5 illustrates the change in the maritime size distribution with wind speed. Demonstrated in figure 6 is the wind speed effect on the total size distribution, i.e. the linear combination of the continental and maritime components.

The relative humidity dependence of the Munn-Katz model was that formulated by Fitzgerald (1975, 1979) and is given by the growth factor F. The growth factor differs from that used by Shettle and Fenn in that Fitzgerald's relative humidity effects do not depend on either size or composition of the aerosol. Shown in each of figures 7, 8, and 9 is the relative humidity dependence at a fixed wind speed of 0 m/s and 0, 80, 95 and 99% relative humidity for the continental, maritime and total size distributions respectively. These figures emphasize that the primary contribution of the relative humidity in eqn (2) enters through the continental component. The maritime relative humidity contribution has little effect on the total size distribution, and at low wind speeds, the model acts as if the maritime component were not present. Results of the present study show this to be a significant deficiency in the Munn-Katz model.

The Munn-Katz model offers several conceptual advantages. It is dependent not only upon relative humidity but also on wind speed. The aerosol growth factor is independent of the radius. It does not require that the user know the total number concentration, which is a decided advantage if the model is to be utilized in a predictive sense. However, the Munn-Katz model still neglects the effects of mixing volume and advection in the planetary boundary layer.

C. HYBRID MODEL

Isaacs (1980) suggested that the differences in composition and size distribution between continental and maritime components require different growth factors for each mode. He then formulated a Hybrid

model by linearly combining the continental component of the Shettle and Fenn model with the maritime component of the Munn-Katz model, to obtain:

$$n(r) = N_1[\exp(-\ln^2(\frac{r}{r_{n_1}})/2\ \ln^2\sigma_1)]/r\sqrt{2\pi}\ \ln\ \sigma_1$$

$$+ 1.62(C_1 + C_2V^{\delta})\exp[\frac{-Z}{h_oF} - 8.5(\frac{r}{\alpha})\ ]F^{-1}(\frac{r}{\alpha}) \qquad (3)$$

The terms in this equation have been defined previously.

There are two conceptual advantages to this approach: (1) aerosol growth due to relative humidity is independent for each mode and (2) wind speed dependence is treated only in the coarse mode. The growth factor (or relative humidity dependence) of the continental component is that suggested by Shettle and Fenn (1979), while the growth factor of the maritime component is that of Fitzgerald (1975, 1979). In a formulation similar to the Munn-Katz model, the number density for the maritime mode varies with relative humidity and wind speed, while that for the continental mode is either fixed or scaled by visibility. The difficulty associated with visibility scaling is discussed above.

The relative humidity effects are presented, for low wind speed (0 m/s), in figure 10 and, for high wind speed (10 m/s), in figure 11. It is clear that the log normal" distribution, which is absent in the Munn-Katz model, is an important component of the Hybrid model. Also, the model predicts an order of magnitude increase in the larger particles (i.e. $r > 1$ μm) with an increase in the wind speed from 0 to 10 m/s. There is minimal difference, however, in the relative humidity dependence

between 50 and 80% relative humidity for both the 0 and 10 m/s wind speed cases. A relatively large change is noted when the relative humidity increases from 80% to 95%, which is as expected. Fitzgerald (1979) and others have shown that the largest change in the size distribution occurs when the relative humidity increases beyond 80% (figure 12).

Of additional interest is the apparent singular point at 0.03 μm radius where, according to the model, the size distribution is independent of relative humidity. This point is most likely an artifact of the model because relative proportions of continental and maritime components are not constant and the Aitken nuclei are not considered.

Figures 13 and 14 depict the wind speed dependence of the Hybrid model at two relative humidities, 50% and 80% respectively. We see that changes in wind speed affect only the maritime component.

The three previously described models will be examined as to their ability to accurately predict observed aerosol number and volume densities. The specific algorithms developed for these models are described below in the Technical Approach section.

TABLE I. Parameters of Maritime Aerosol Size Distribution (Shettle and Fenn, 1979)

Aerosol Model	SIZE DISTRIBUTION PARAMETERS (Log Normal) N(cm^{-3})	r_n(μm)		Type
Continental Origin i=1, (accumulation mode)	1.0	0.03	2.24	Rural Aerosol Mixture (Water Soluble Aerosol)
Marine Origin i=2, (coarse mode)	1.0	0.3	2.51	Sea Salt Solution

TABLE II. Humidity Dependent Mode Radii, Maritime Model (Shettle and Fenn, 1979)

Relative Humidity (%)	NUMBER MODE RADIUS (μm) Continental (σ=2.24) (i=1)	Maritime (σ=2.51) (i=2)
0	.02700	.1600
50	.02748	.1711
70	.02846	.2041
80	.03274	.3180
90	.03884	.3803
95	.04238	.4606
99	.05215	.7505

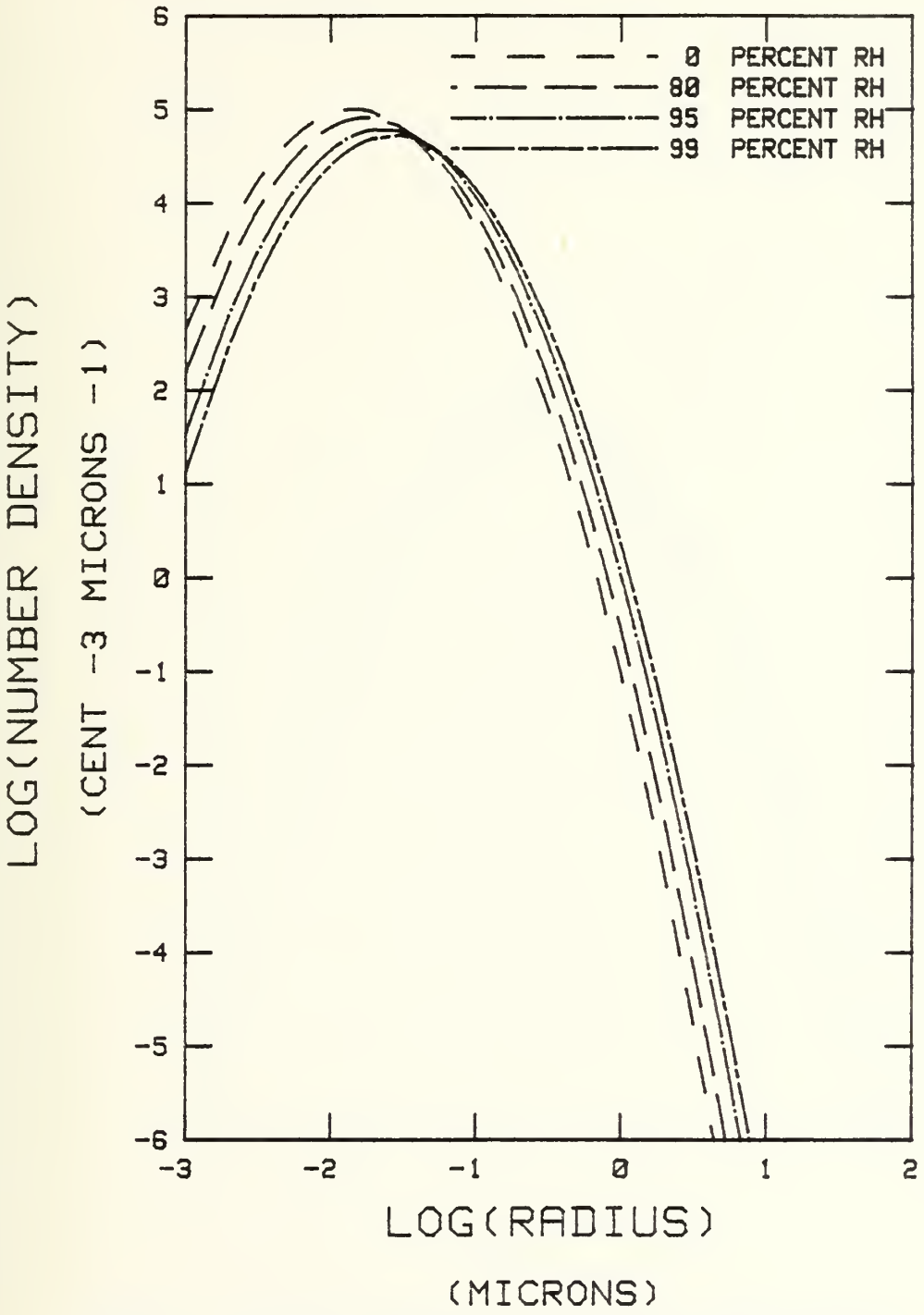

Figure 1. Shettle and Fenn Continental (accumulation) Component as a Function of Relative Humidity

PARTICLE CONCENTRATION FIXED AT 3960 CM-3

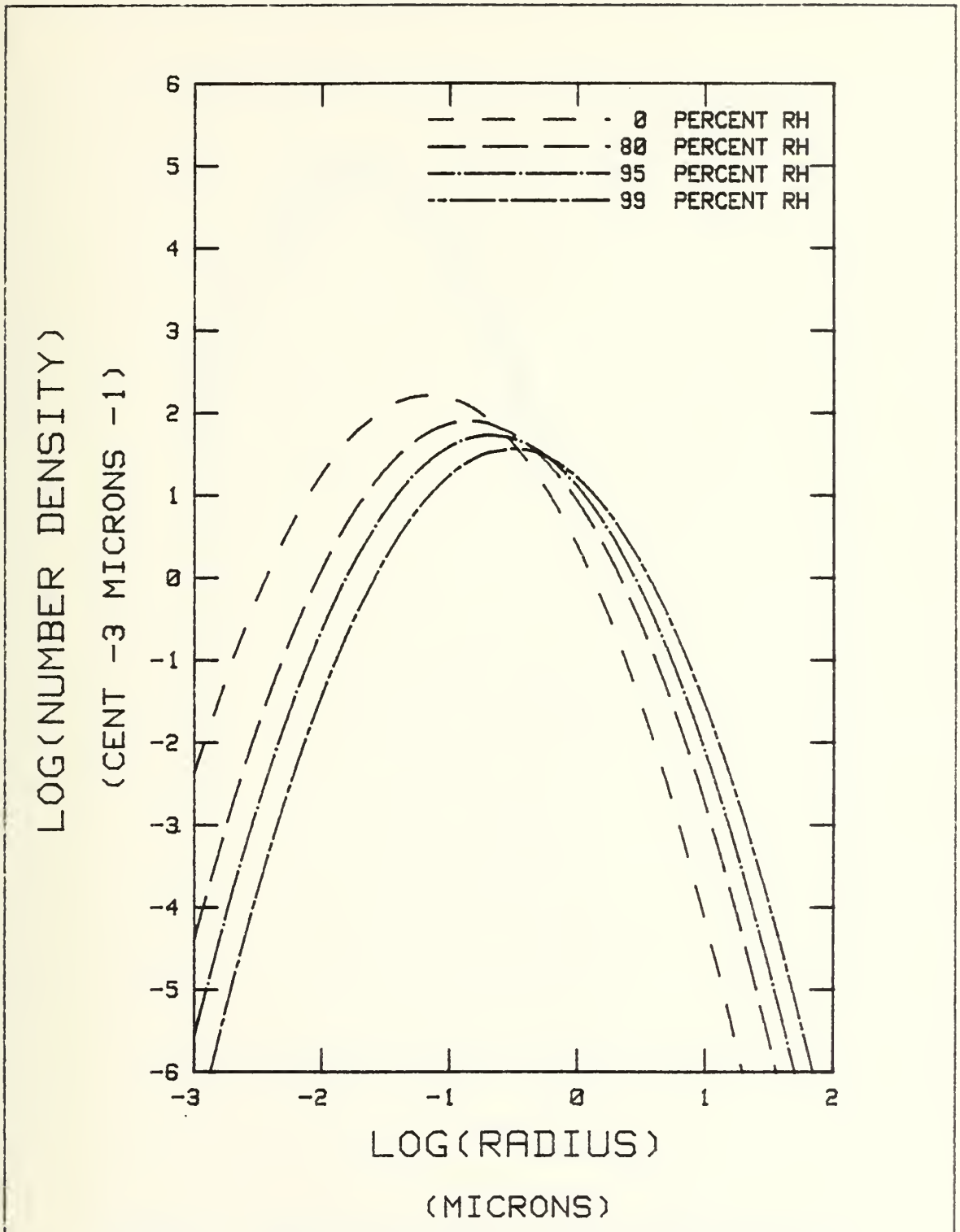

Figure 2. Shettle and Fenn Maritime (coarse) Component as a Function of Relative Humidity
PARTICLE CONCENTRATION FIXED AT 40 CM-3

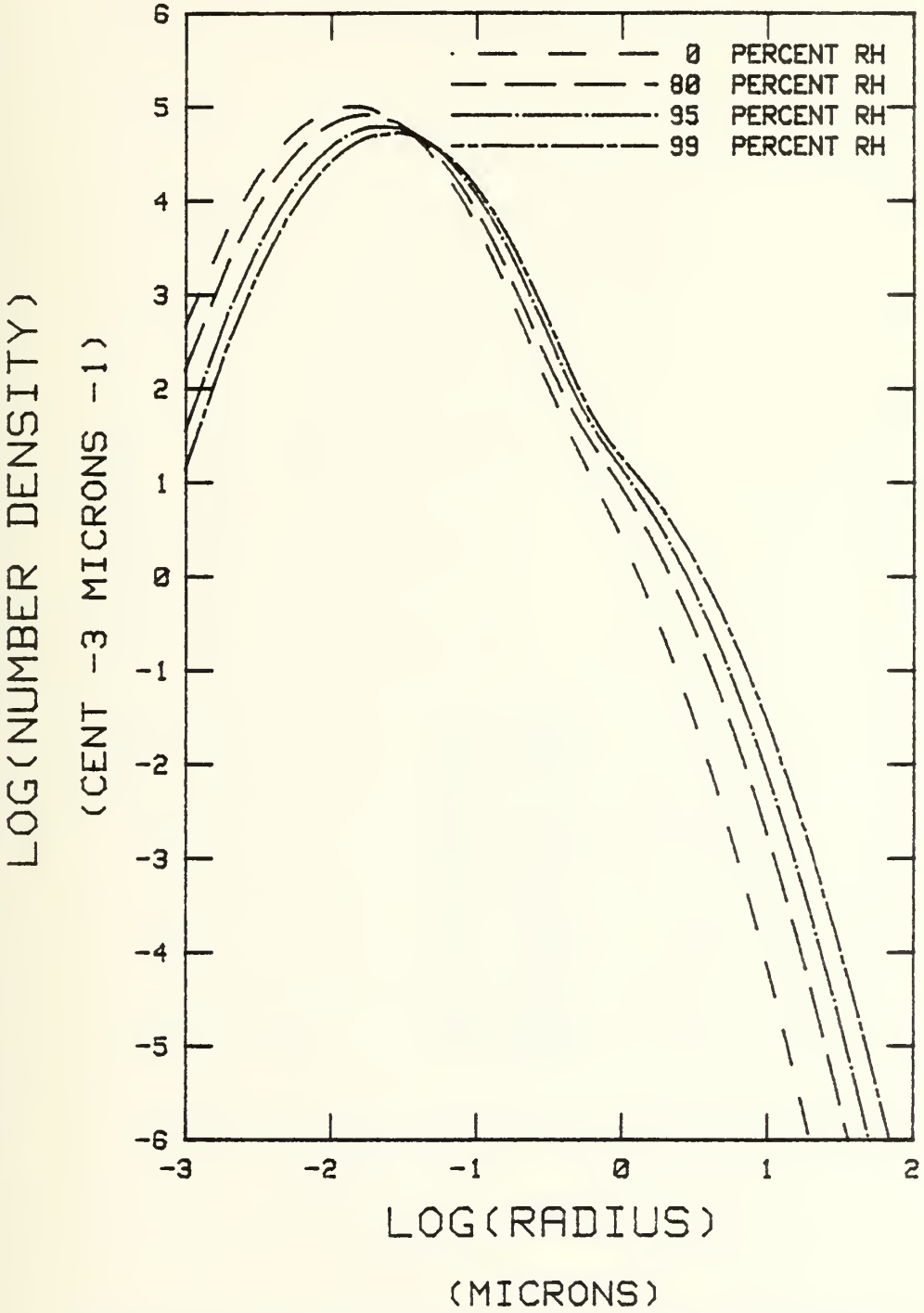

Figure 3. Shettle and Fenn Total Size Distribution as a Function of Relative Humidity

PARTICLE CONCENTRATION FIXED AT 4000 CM-3

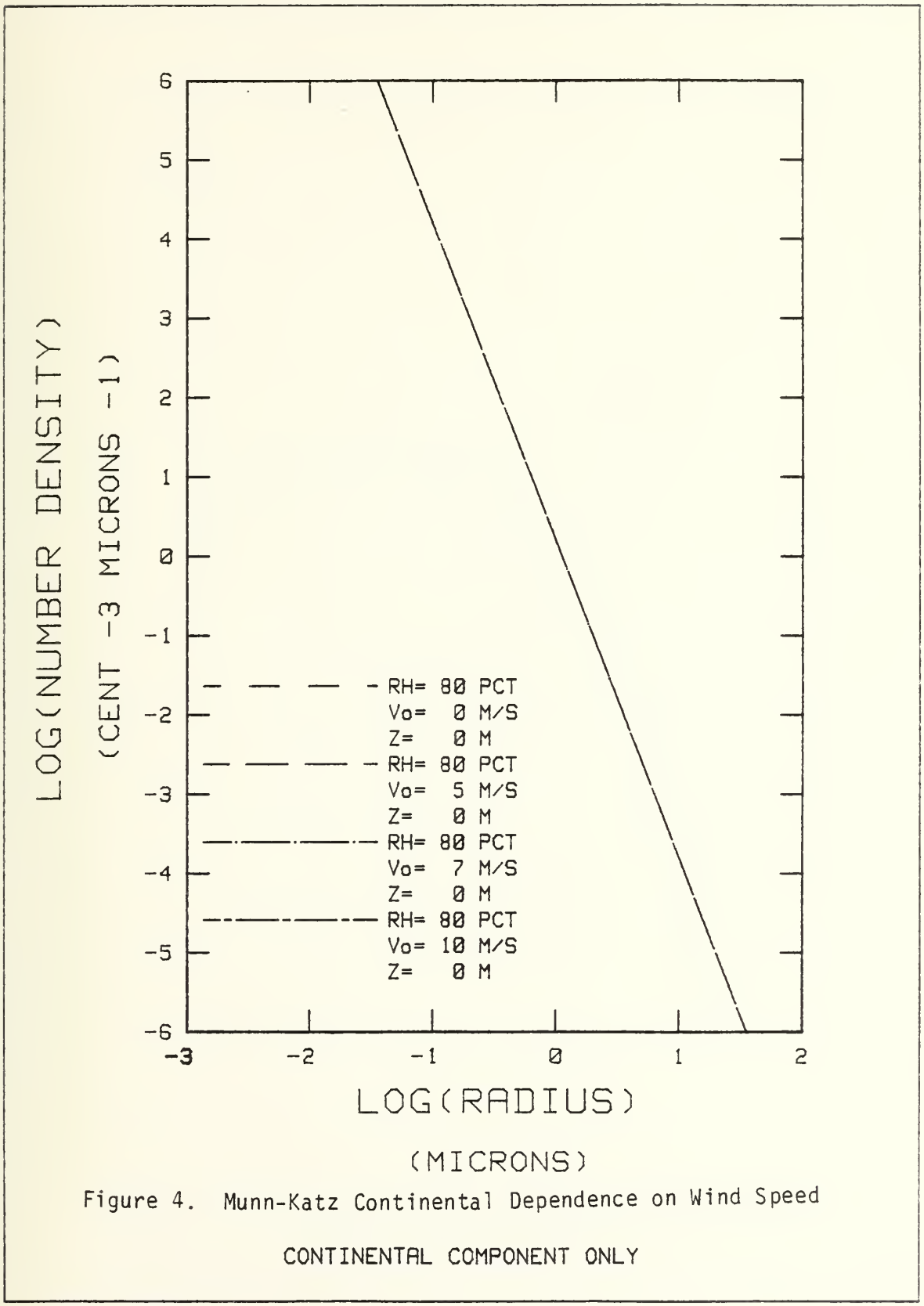

Figure 4. Munn-Katz Continental Dependence on Wind Speed

CONTINENTAL COMPONENT ONLY

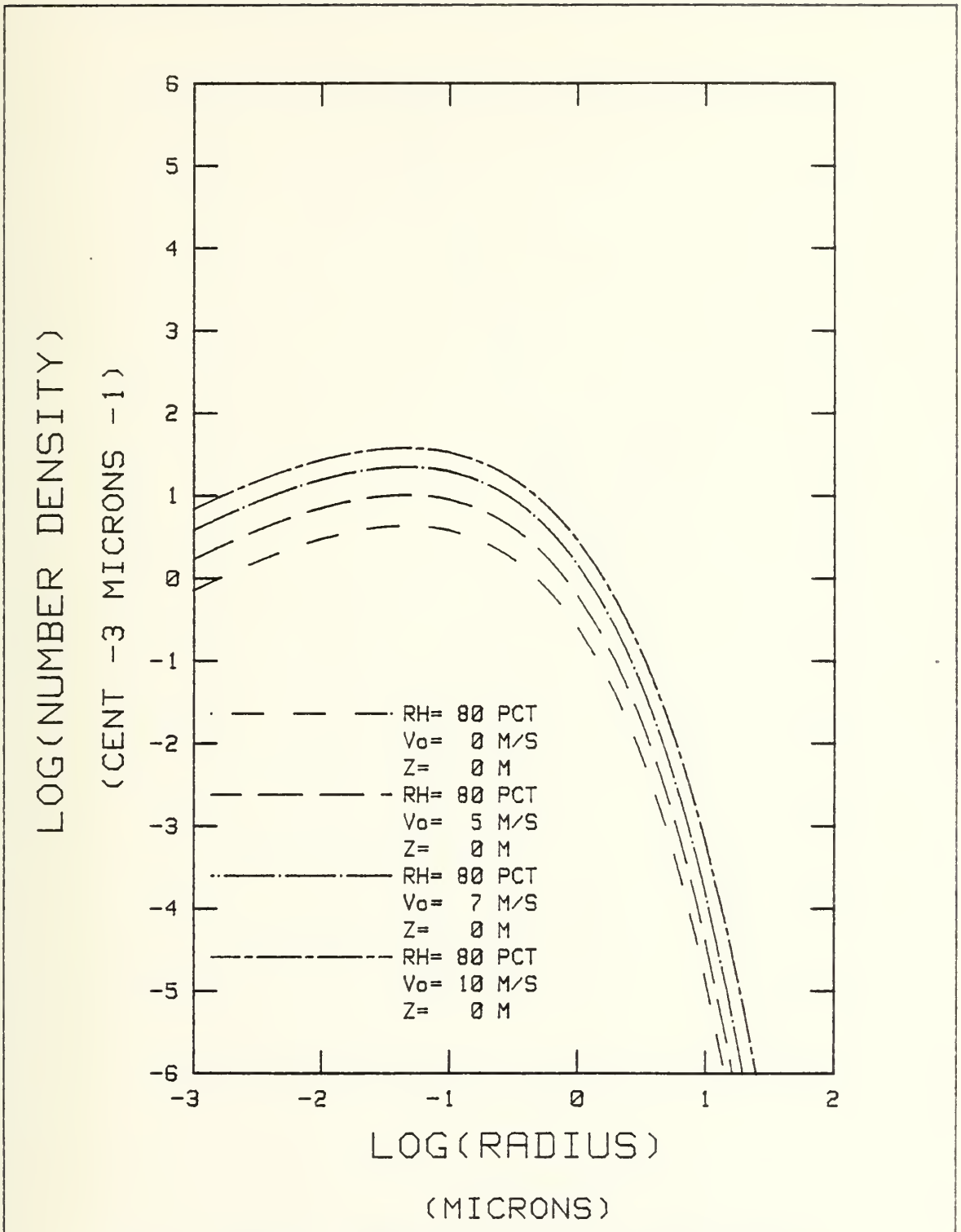

Figure 5. Munn-Katz Maritime Dependence on Wind Speed

MARITIME COMPONENT ONLY

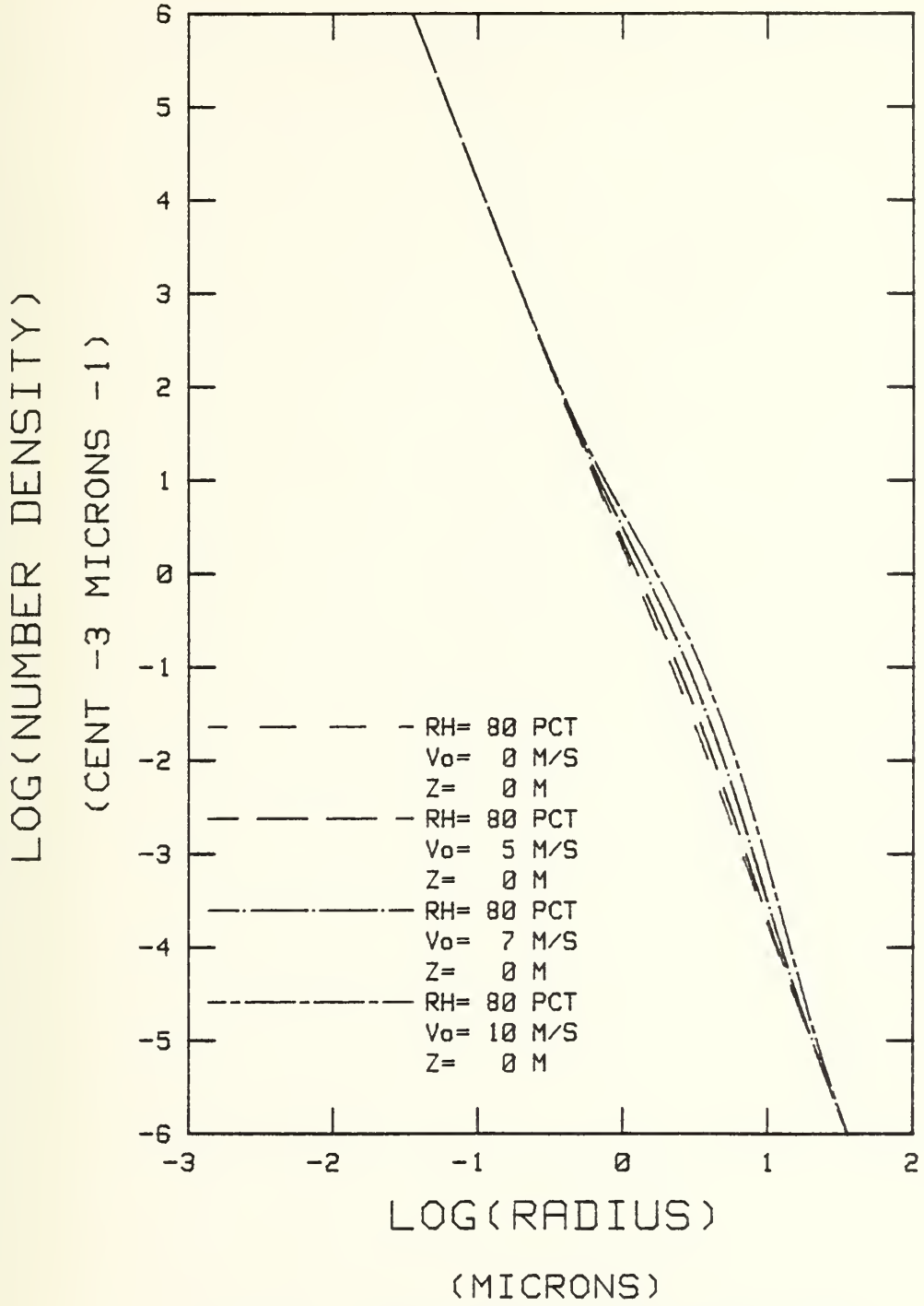

Figure 6. Munn-Katz Total Size Distribution Dependence on Wind Speed

TOTAL SIZE DISTRIBUTION

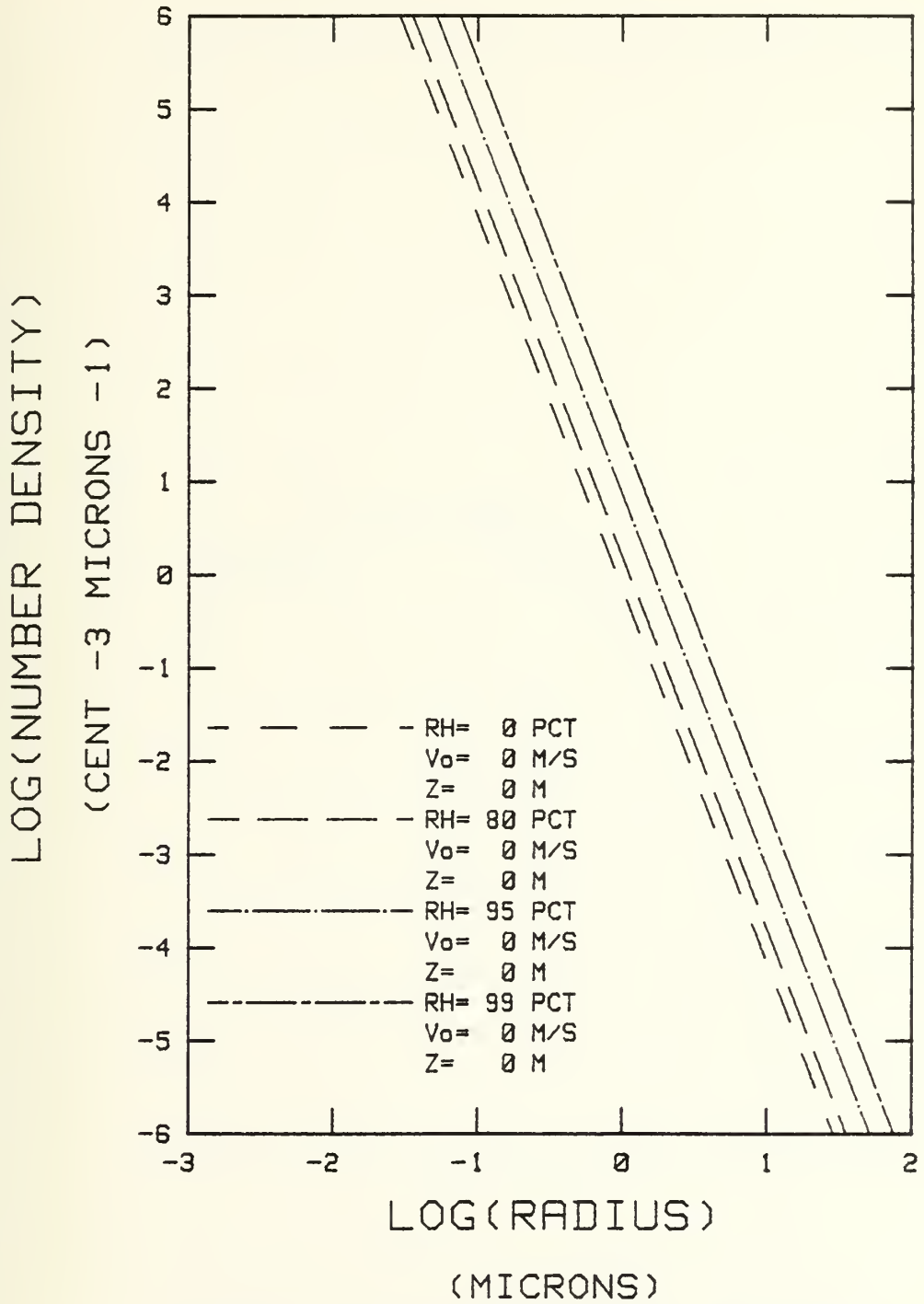

Figure 7. Munn-Katz Continental Dependence on Relative Humidity

CONTINENTAL COMPONENT ONLY

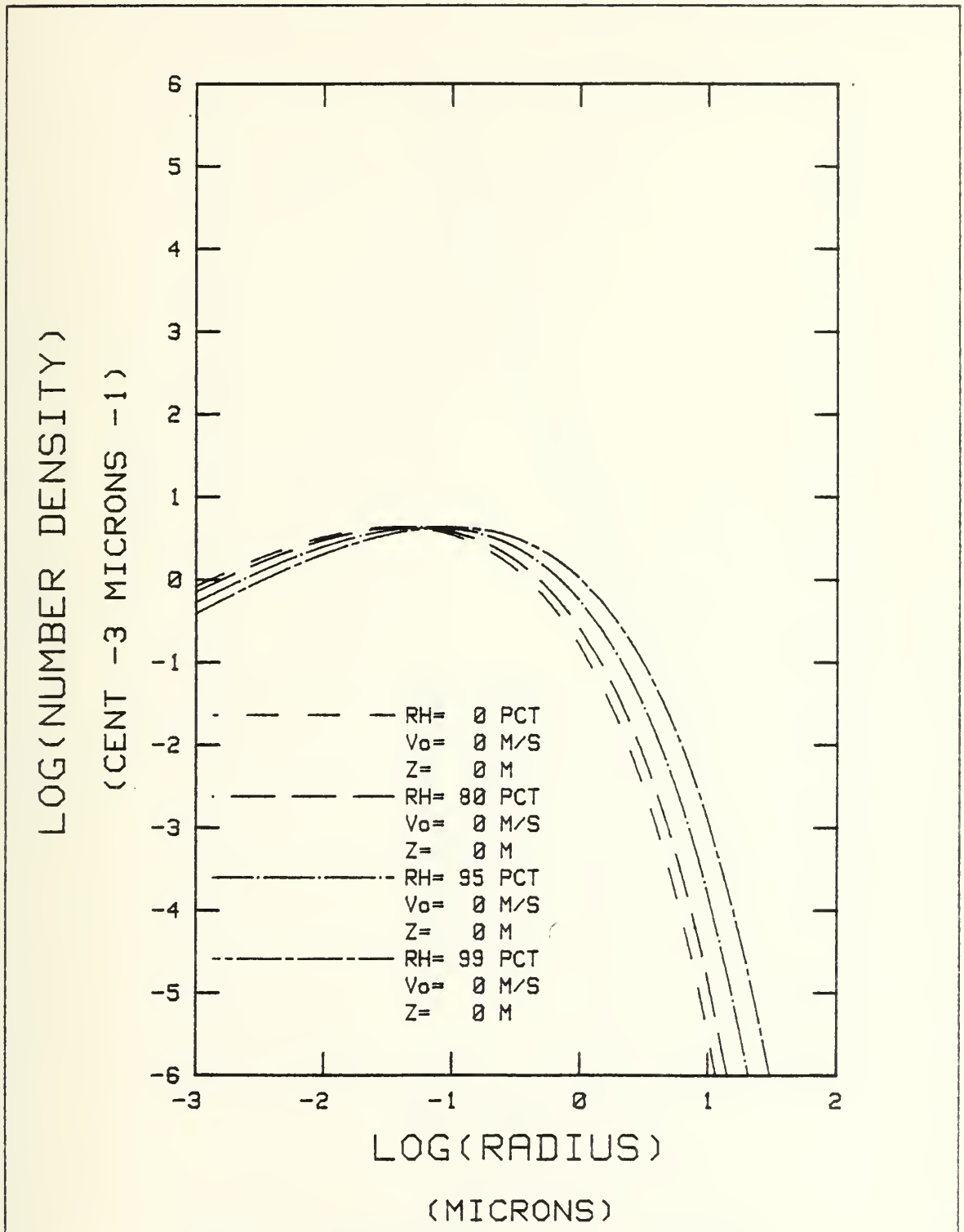

Figure 8. Munn-Katz Maritime Dependence on Relative Humidity

MARITIME COMPONENT ONLY

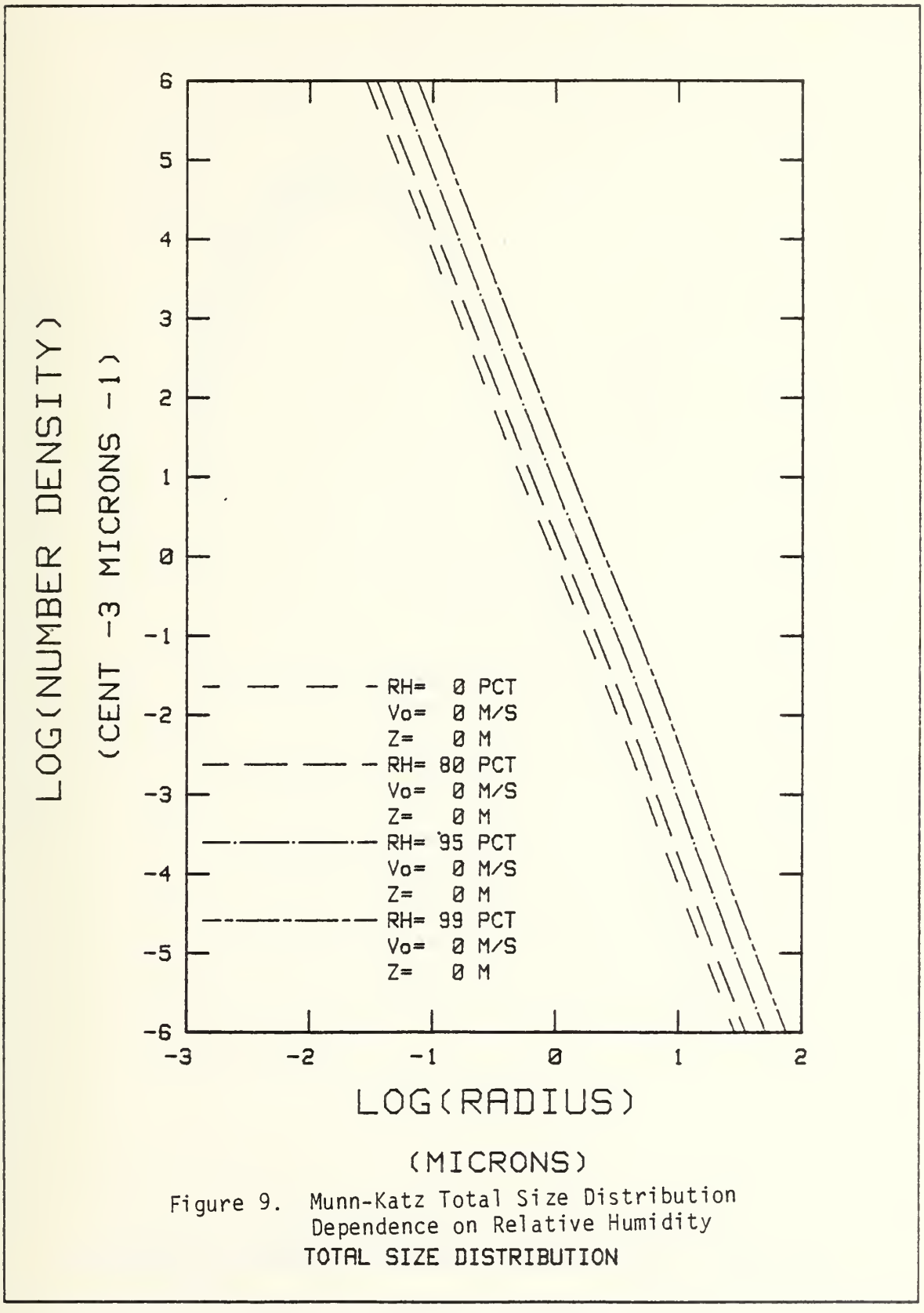

Figure 9. Munn-Katz Total Size Distribution Dependence on Relative Humidity

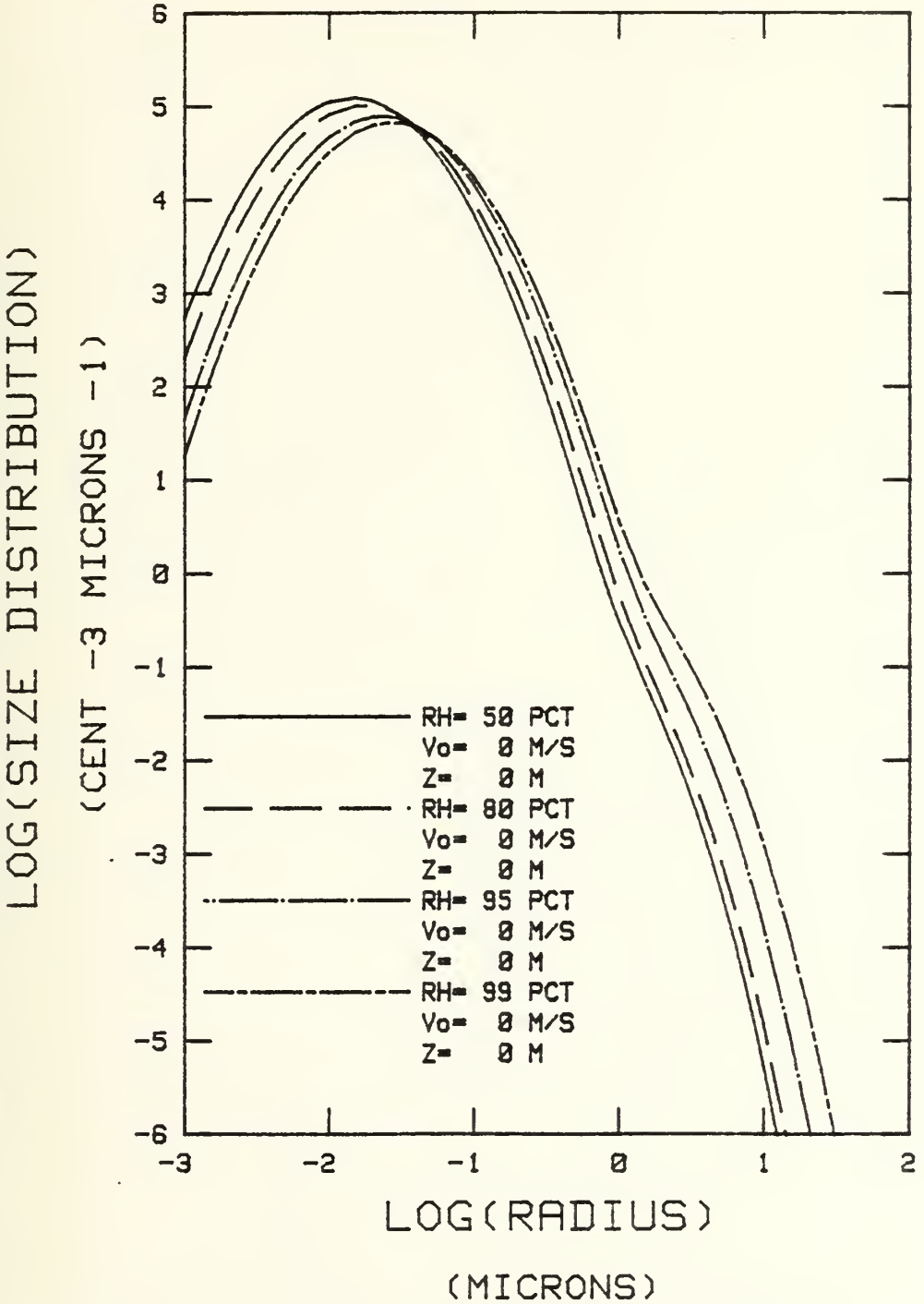

Figure 10. Hybrid Dependence on Relative Humidity at a Wind Speed of 0 m/s
CONTINENTAL COMPONENT PARTICLE CONCENTRATION IS 5000 cm-3

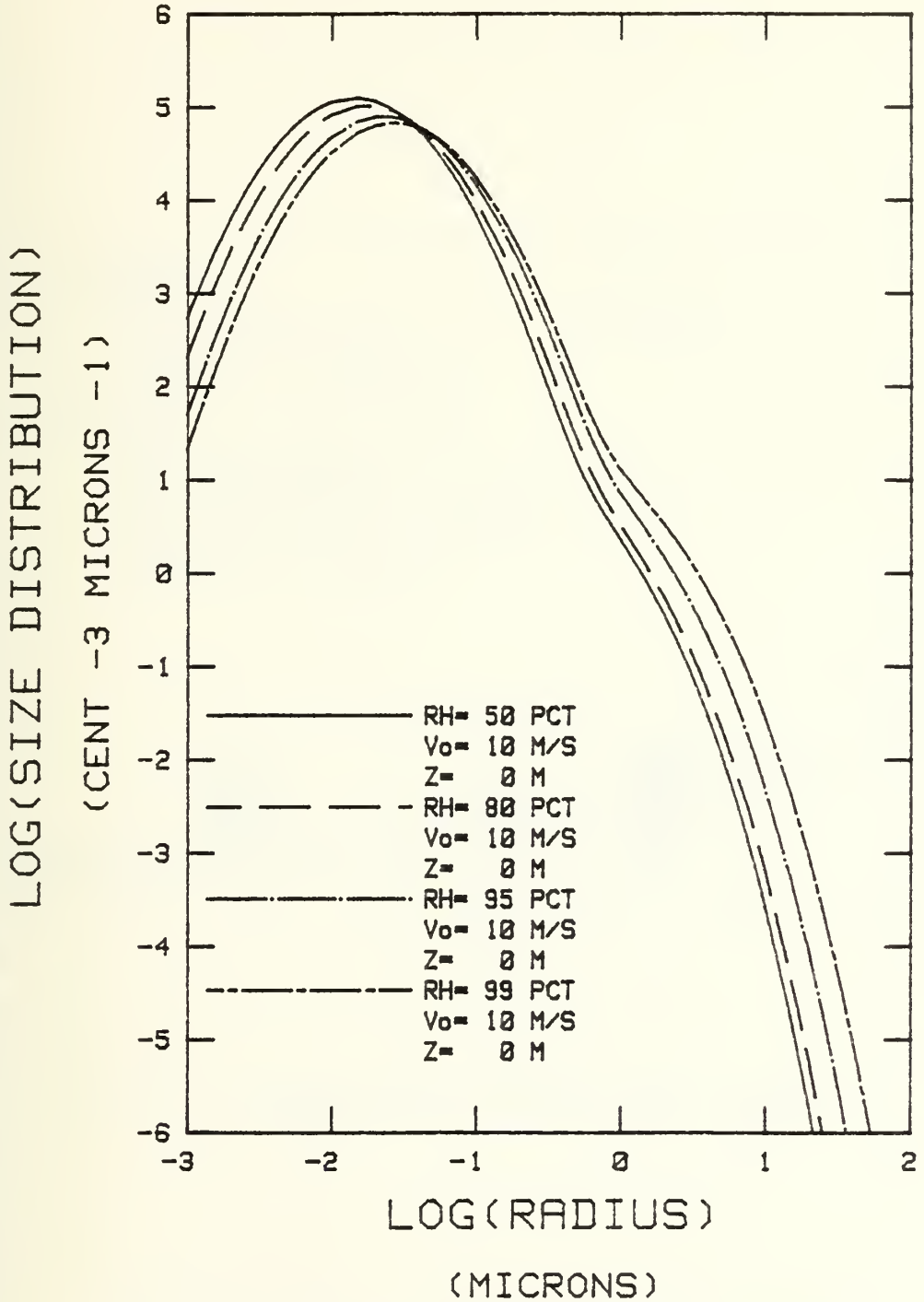

Figure 11. Hybrid Dependence on Relative Humidity at a Wind Speed of 10 m/s

CONTINENTAL COMPONENT PARTICLE CONCENTRATION IS 5000 cm-3

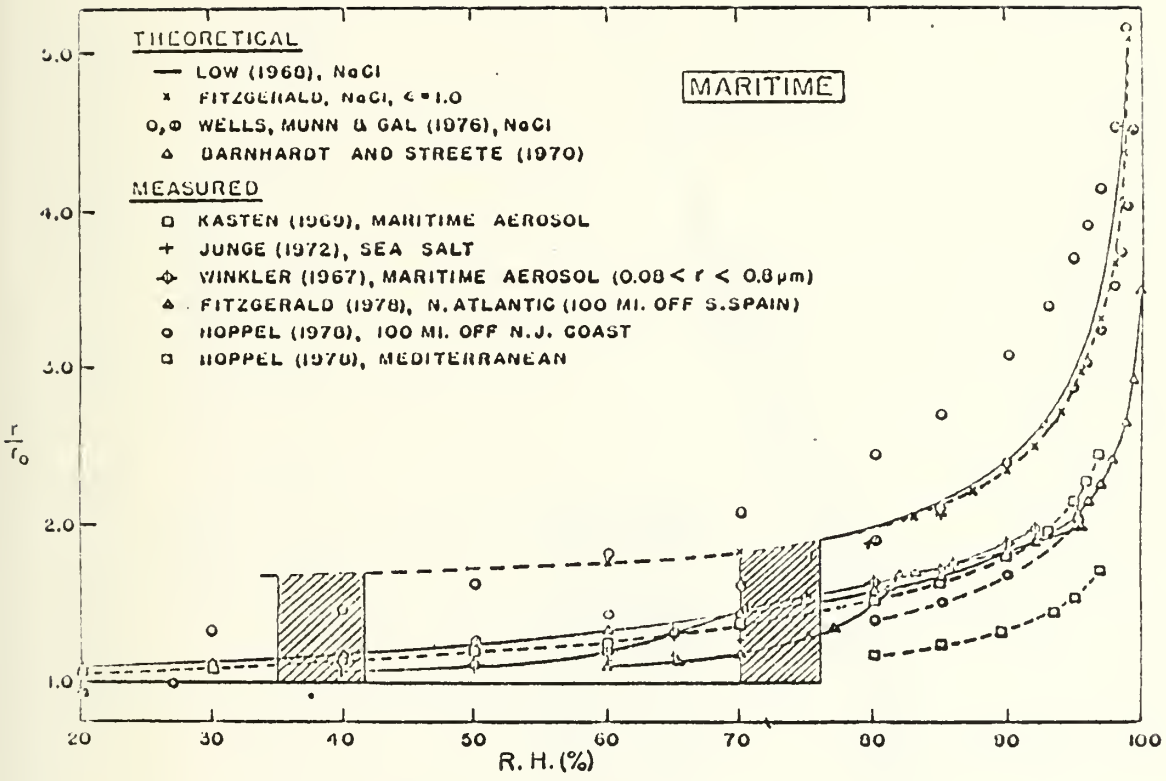

Figure 12. Measured and Calculated Growth Curves for NACL Particles and Natural Aerosols

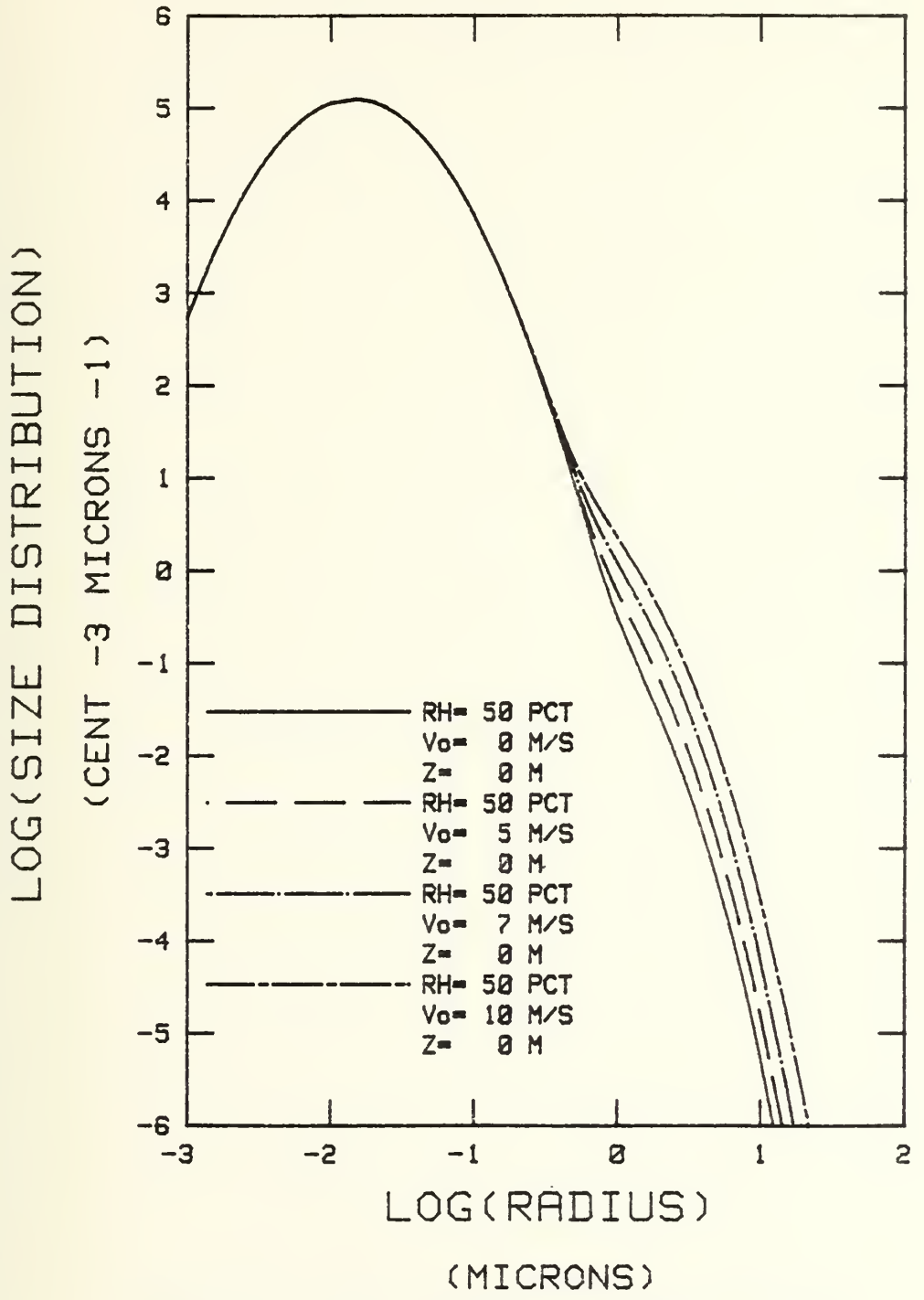

Figure 13. Hybrid Dependence on Wind Speed at a Relative Humidity of 50%

CONTINENTAL COMPONENT PARTICLE CONCENTRATION IS 5000 cm-3

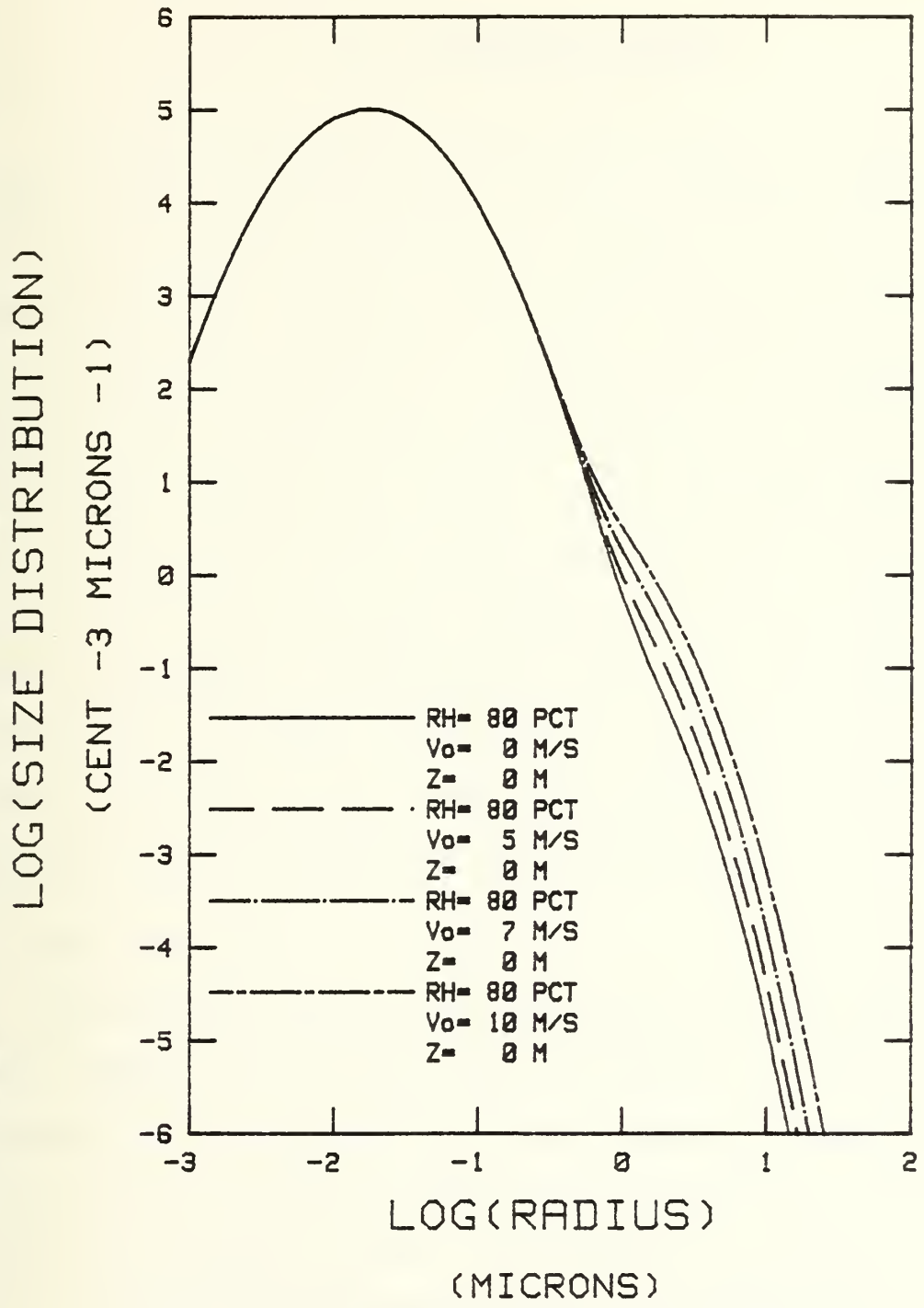

Figure 14. Hybrid Dependence on Wind Speed at a Relative Humidity of 80%

CONTINENTAL COMPONENT PARTICLE CONCENTRATION IS 5000 cm-3

III. TECHNICAL APPROACH

In the previous section the Shettle and Fenn and the Hybrid models were described in generalized form. They had to be modified in order to be used with measured meteorological variables for a specific segment of the electromagnetic spectrum. Modification included the utilization of a more general relative humidity parameter, and the introduction of a weighting factor to adjust the relative proportions of total particle concentration between the continental and maritime components. The Munn-Katz model required no modification and was utilized as described above (eqn (2)). Surface wind speed, required input to the Munn-Katz model and the Hybrid model, was determined by dividing U_* by a selected drag coefficient, $C_D = 0.035$. It was necessary to adjust or correct the aircraft data on the basis of surface measurements. Volume distribution and total particle concentration were also determined.

A. DATA ACQUISITION

The experiment, Monterey Aerosol Generation and Atmospheric Turbulence (MAGAT) was held from 28 April to 9 May 1980, in the vicinity of Monterey Bay. The experiment involved an ambitious attempt to extend dynamic models of the marine atmospheric boundary layer to include aerosol and turbulent profiles. The experiment, conducted in a region 30 to 50 nautical miles off the Monterey coast, required periodic monitoring of aerosols and meteorological variables from the surface to 5 km. These duties were shared by an aircraft and the R/V ACANIA, but only the aircraft data are utilized in this thesis.

Aerosol data were obtained using an Axial Symmetric Scattering Aerosol Probe (ASSAP) particle counter manufactured by Particle Measurement Systems (PMS) and mounted on a turbo-charged Bellanca aircraft. The data used in this study were collected in "ladder" profiles, during which the aircraft made measurements at a constant altitude for two minutes, climbed to a new altitude, and repeated the two minute measurement run. In most cases the step-like measurement procedure extended from near the sea surface, up through the well-mixed boundary layer, to a few steps above the inversion, with 10 to 14 steps in each ladder. The step heights were randomly chosen, but an attempt was made to keep each step height consistent between ladders. Air and dew-point temperatures were also measured and used to calculate relative humidity. This relative humidity data was used as an input parameter to the models.

The aircraft also flew ascending spirals (in the vicinity of the ladders) during which other meteorological parameters were collected, yielding vertical soundings similar to those provided by radiosondes. Inversion heights were determined from these soundings.

B. CORRECTION OF DATA

It was noticed, during flybys over the R/V ACANIA, that the aircraft measurements did not agree with those of the ship. The aircraft measured size distributions were consistently smaller than the ship measured distributions for radii > 1 μm. Additionally, the differences increased with radius. Two possible explanations can account for the observed differences. First, the observations may indicate spatial aerosol inhomogeneities in the boundary layer. This is unlikely, however, since

we would expect that the aircraft measurements would be higher than the ship measurements for a fraction of the flybys. Second, one or both of the measurement systems displayed a systematic measurement error. The ship system measured aerosols in 90 size channels from 0.09 μm to 14.0 μm radius while the aircraft system utilized 60 size channels from 0.28 μm to 14.0 μm radius. Since the ship system is newer and has a wider range and better sensitivity it was assumed that the aircraft measurements were in error. This assumption is reasonable if one considers that an aircraft moving at relatively high speed may not sample large radii particles as efficiently as a slower moving ship. For this reason it was decided to correct the aircraft data to match that of the ship.

Two correction factors were determined, one for use before 4 May 1980 and one for use after 4 May 1980. The correction consisted of adding a straight line, in log space, to the measured aircraft size distribution for data > 1.0 μm radius. The correction is as follows:

before 5/4/80

$$n(r) = 10^{.095}\, n(r)\, r^{1.7} \qquad (4)$$

after 5/4/80

$$n(r) = 10^{.075}\, n(r)\, r^{.8} \qquad (5)$$

Fairall (1980) has shown that extinctions calculated from ship measured size distributions compare extremely well to extinctions measured directly at various wavelengths, from 0.63 to 1.06 μm. Aircraft measured size distributions corrected to match those of the ship are, therefore, assumed to accurately describe the actual size distributions present. A more rigorous error analysis of the data is in progress.

C. MODEL MODIFICATION

The Shettle and Fenn model (eqn (1)) and consequently the continental portion of the Hybrid model (eqn (3)) was modified to utilize measured relative humidity data as input. From Table II, it is evident that values of the mode radii are given only at fixed relative humidities. Since any relative humidity between 0 and 100% could theoretically occur, a method for determining these radii at any relative humidity was devised. Based on an examination of figure 12, straight lines were fit to the values in table II between 0 and 50% relative humidity and between 50 and 70% relative humidity. Between 70 and 99% relative humidity a third order polynomial was fit. In this manner the mode radii at any relative humidity can be determined. Mode radii, so determined, are then substituted for r_n in equations (1) and (3) and, therefore, table II was not used. The equations are as follows:

RH < 50

Continental

$$r_{n_1} = 0.027 + 0.0000096(RH) \qquad (6)$$

Maritime

$$r_{n_2} = 0.16 + 0.000222(RH) \qquad (7)$$

50 < RH < 70

Continental

$$r_{n_1} = 0.02503 + 0.000049(RH) \qquad (8)$$

Maritime

$$r_{n_2} = 0.0886 + 0.00165(RH) \qquad (9)$$

$70 < RH < 99$

Continental

$$r_{n_1} = -.9440683 + .03600454(RH) - 0.000445554(RH)^2 + 1.8523192\ E - 6(RH)^3 \quad (10)$$

Maritime

$$r_{n_2} = -47.480133 + 1.753164(RH) - 0.021402461(RH)^2 + 0.00008697562(RH)^3 \quad (11)$$

An approach was devised to include the appropriate proportions of continental and maritime aerosols for the 0.28 to 14.0 μm range. It is important to include such weighting because this size range spans the region where the continental aerosol is replaced by the maritime aerosol as the dominant contributor to the number density as evident in figure 3.

The exact weighting factor for each mode was determined by integrating each model between 0.28 and 14.0 μm, assuming that 1.0% of the particles were of marine origin. The integrated values for each mode was then divided by that for the total spectrum.

$$WF1 = \frac{\int_{.28}^{14} n(r)_1}{\int_{.28}^{14} n(r)} \quad (12)$$

$$WF2 = \frac{\int_{.28}^{14} n(r)_2}{\int_{.28}^{14} n(r)} \quad (13)$$

where n(r) is given by equations (1), (2), or (3) and $n(r)_1$ refers to the continental size distribution and $n(r)_2$ refers to the maritime size distribution in each case.

The Shettle and Fenn model varies with relative humidity so its weighting factor is likewise dependent on relative humidity. The Munn-Katz weighting factors are dependent on wind speed and altitude as well as relative humidity.

Equation (12) was used to determine the Shettle and Fenn continental weighting factors for selected relative humidities. Integrations such as those in equations (12) and (13) require a large amount of computer time and, therefore, it was deemed more efficient to utilize a seventh order polynomial fit derived from the selected output of equation (12). The Shettle and Fenn weighting factor polynomial is given by:

$$WF1 = .546214374 - .0005143(RH) + .000057421(RH)^2$$
$$- .0000000685(RH)^3 - .000000119248(RH)^4$$
$$+ 3.75787E\text{-}9(RH)^5 - 4.20213E\text{-}11(RH)^6 + 1.565268E\text{-}13(RH)^6 \quad (14)$$

$$WF2 = 1.0 - WF1 \quad (15)$$

where WF1 is the weighting factor for the continental component and WF2 is the weighting factor for the maritime component. When determining the size distribution with equation (1) the total particle concentration is multiplied by WF1 (eqn (14)) and by WF2 (eqn (15)) to give the

respective particle concentrations of each mode. In this manner the proportionate amounts of continental and maritime components are determined.

A graphical depiction of this function appears in figure 15 where an unexpected minimum occurs in the curve at 75% relative humidity. It is believed that this minimum is an inaccurate depiction of changes in mode proportions with relative humidity (the curve should be smooth). It most likely represents an artifact in the Shettle and Fenn growth factor.

In a similar manner equations (12) and (13) were used to determine the weighting factors for the Hybrid model (eqn (3)). However, since these weighting factors are dependent on relative humidity, wind speed, and altitude, a simple polynomial fit could not be determined and a look-up table was developed instead. If a specific input value was between those used to develop the table, linear interpolation was utilized to arrive at the appropriate weighting factors. Weighting factors derived in this manner were then applied to equation (3), the Hybrid model, to determine the relative porportions of each component for the given conditions. Graphical depictions of the Hybrid weighting factors, as functions of relative humidity and wind speed for various altitudes, appear in figures 16 through 20. As expected the relative number of maritime particles decreases with increasing relative humidity. The larger particles have a greater affect on extinction at high humidities since their volume has increased. These five figures show a decreased influence of the maritime component with height. This leads to the possibility that the model is unable to account for the

distribution of large particles within a well-mixed boundary layer. The influence of sea spray loading is noted, but rather than occurring at the documented wind speed of 7 m/s, the effect is not evident until 10.5 m/s. This last observation is a result of the normalization which the Munn-Katz model applies to observed wind speeds.

Weighting factors were not applied to the Munn-Katz model (eqn (2)) since it determines its own relative proportions for each component.

D. VOLUME DISTRIBUTION DETERMINATION

In order to illustrate the importance of the large particles in the observed maritime aerosols it was decided to include plots of the volume distribution for each model. The volume distribution is related to the size distribution as:

$$v(r) = \frac{4}{3} \pi r^3 n(r) \tag{16}$$

where $v(r)$ represents the volume distribution, $n(r)$ is the size distribution, and r is the radius. It is similarly noted that $v(r)$ is directly proportional to the aerosol extinction which can be written as:

$$\beta_e(\lambda) = \int_0^\infty Q_e(r,\lambda,\tilde{m})\ \pi r^3 n(r)\ d\ln(r) \tag{17}$$

E. TOTAL PARTICLE CONCENTRATION DETERMINATION

Both the Shettle and Fenn and the Hybrid models require an input of the total particle concentration. The concentration was determined by fitting a least squares seventh order polynomial to the data of each

distribution and integrating it from .28 μm to the largest radius measured in each profile (up to 14 μm). The weighting factors, discussed above, were then applied to this concentration to give the relative proportions required by each mode. This value was then multiplied by N_i in equations (1) and (3) to give the total density of particles for each component.

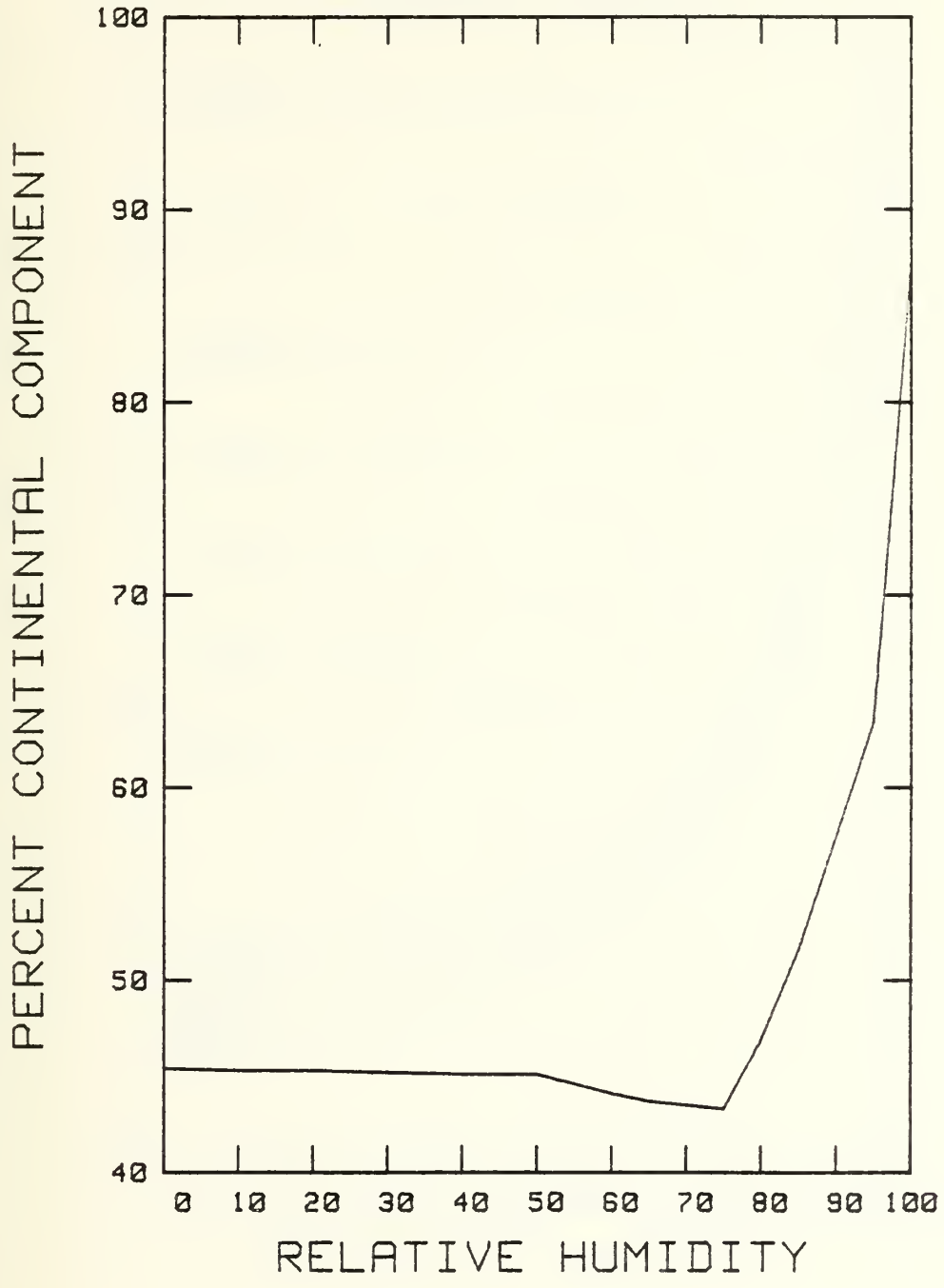

Figure 15. Shettle and Fenn Weighting Factor

PERCENT CONTINENTAL COMPONENT AS A FUNCTION OF RELATIVE HUMIDITY

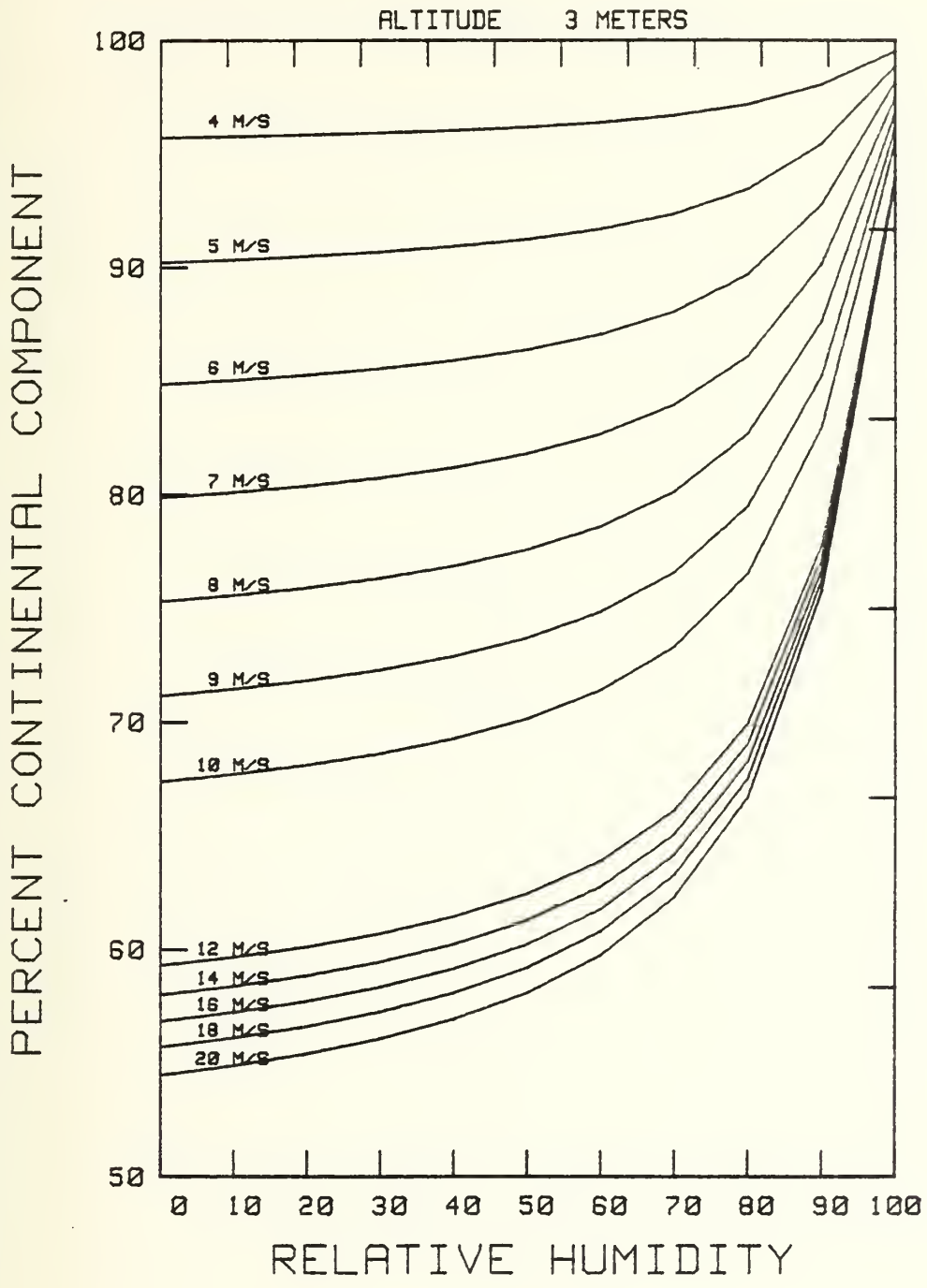

Figure 16. Hybrid Weighting Factor, 3 Meter Altitude

PERCENT CONTINENTAL COMPONENT

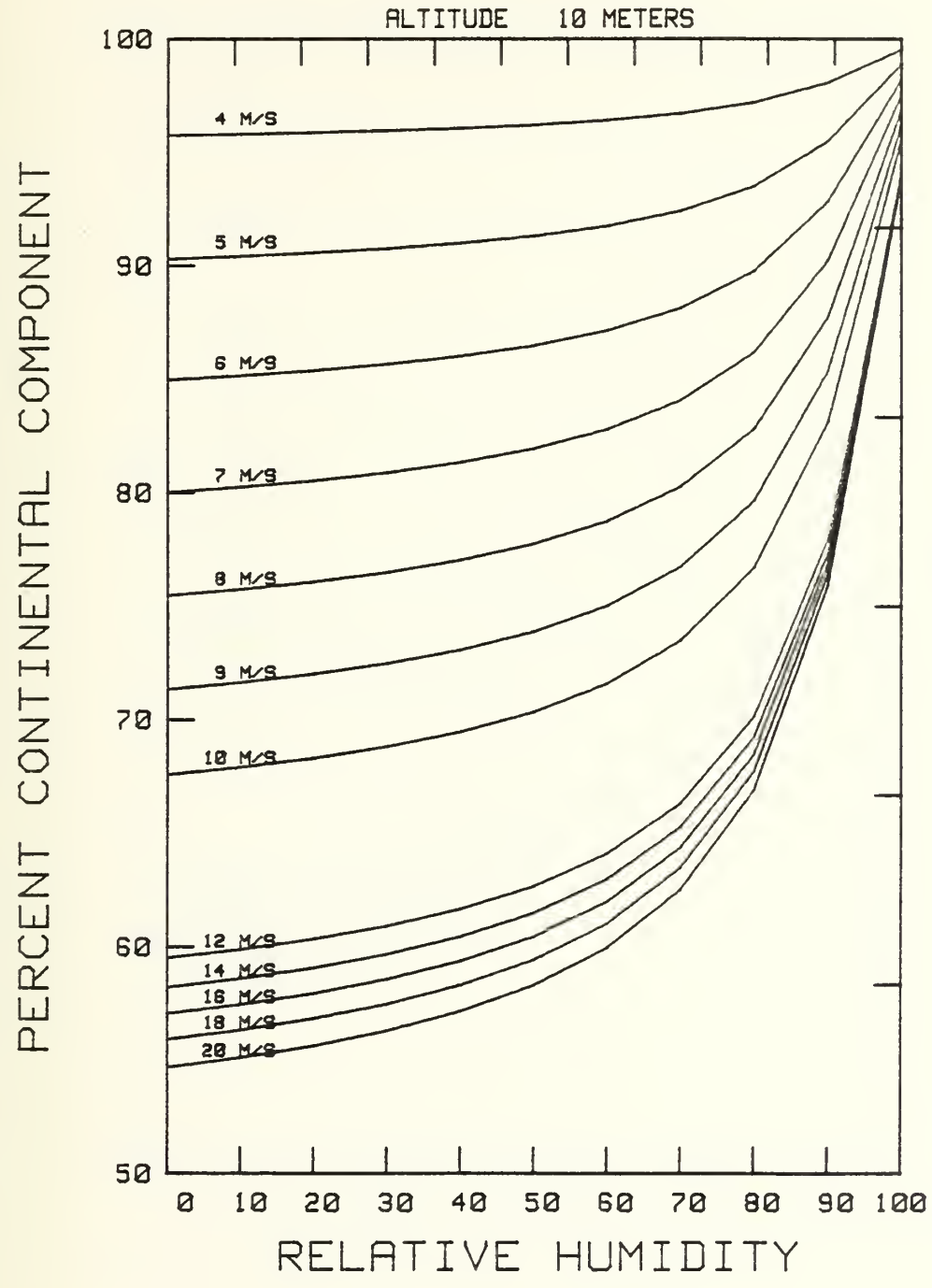

Figure 17. Hybrid Weighting Factor, 10 Meter Altitude

PERCENT CONTINENTAL COMPONENT

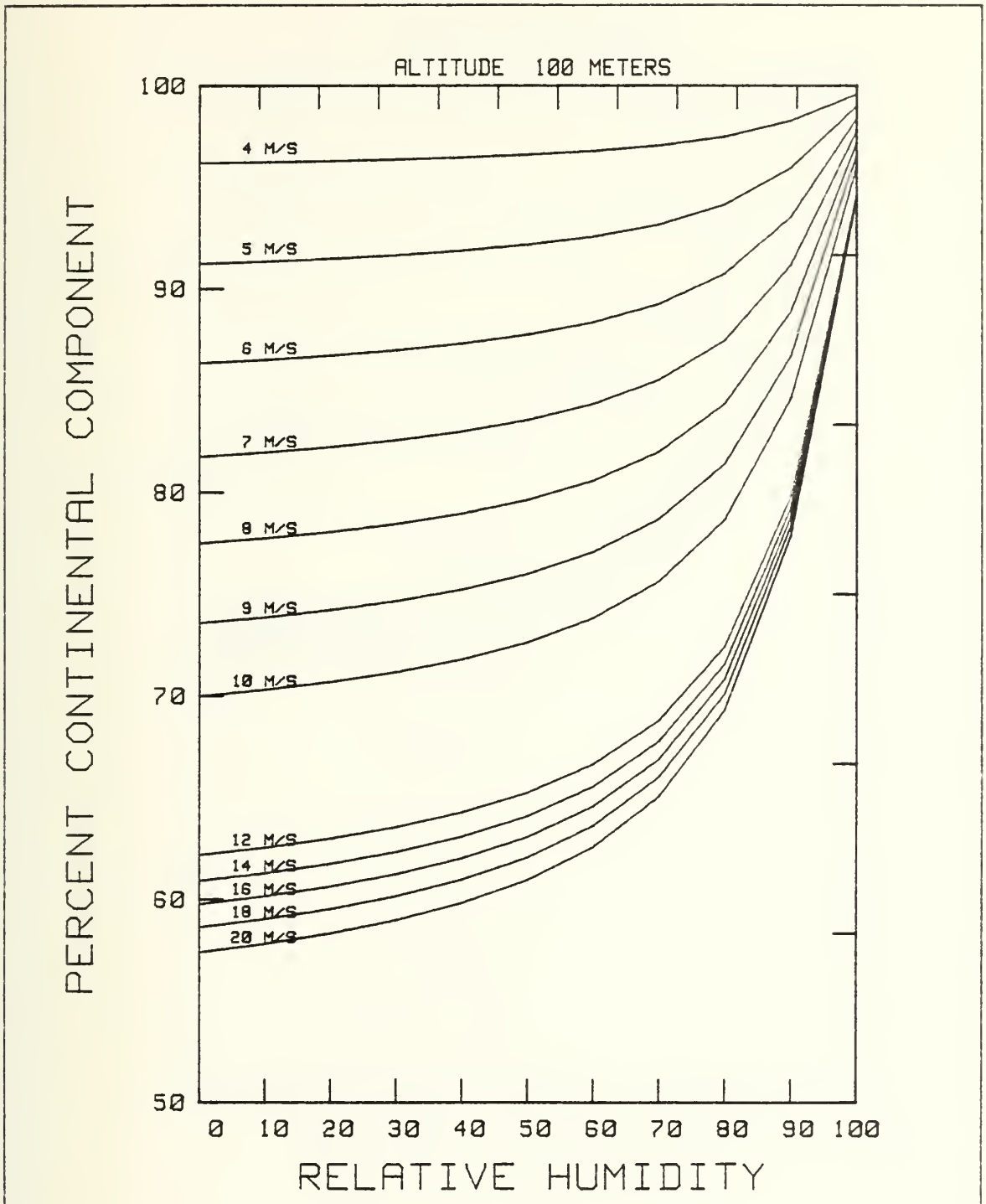

Figure 18. Hybrid Weighting Factor, 100 Meter Altitude

PERCENT CONTINENTAL COMPONENT

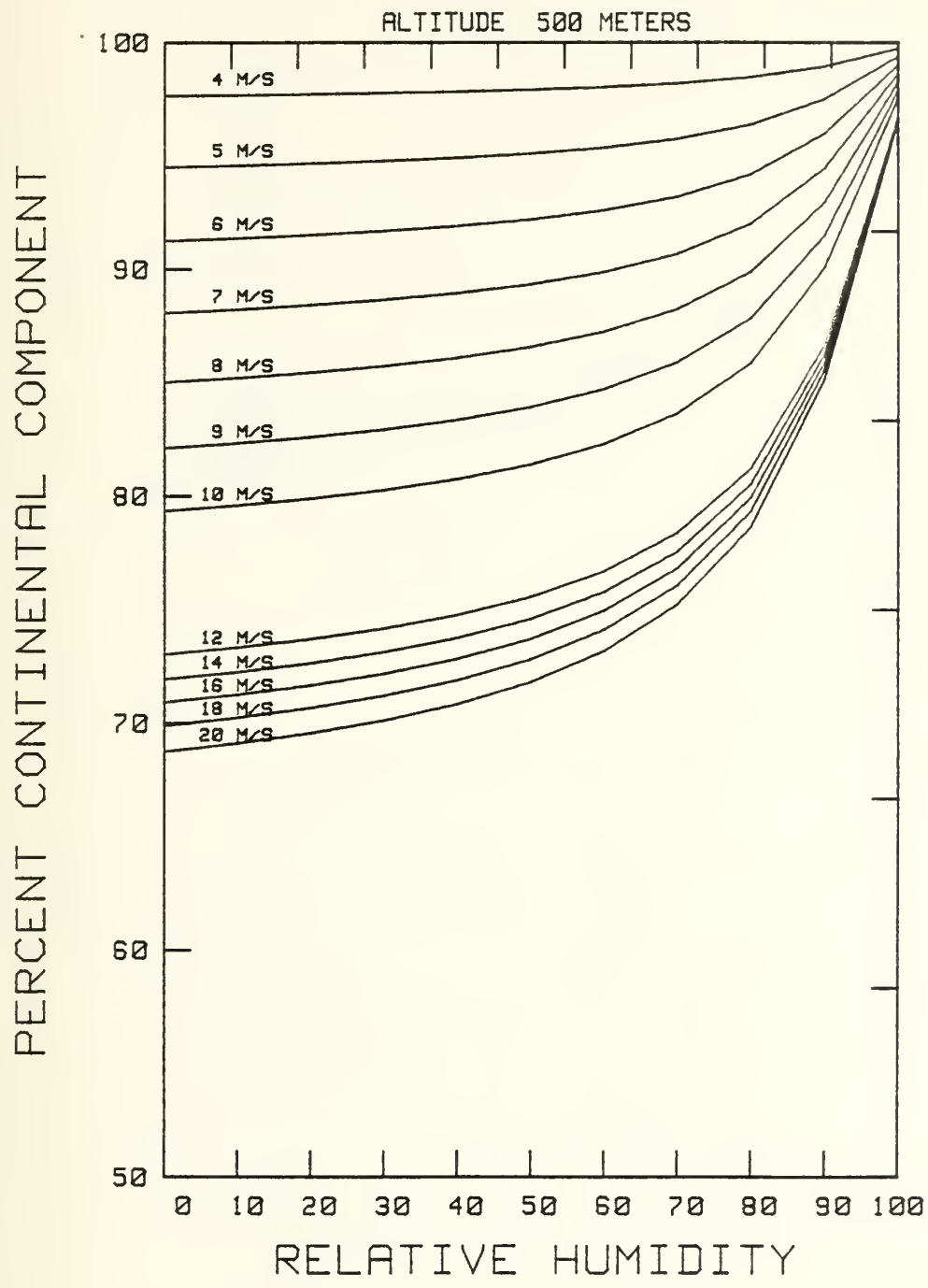

Figure 19. Hybrid Weighting Factor, 500 Meter Altitude

PERCENT CONTINENTAL COMPONENT

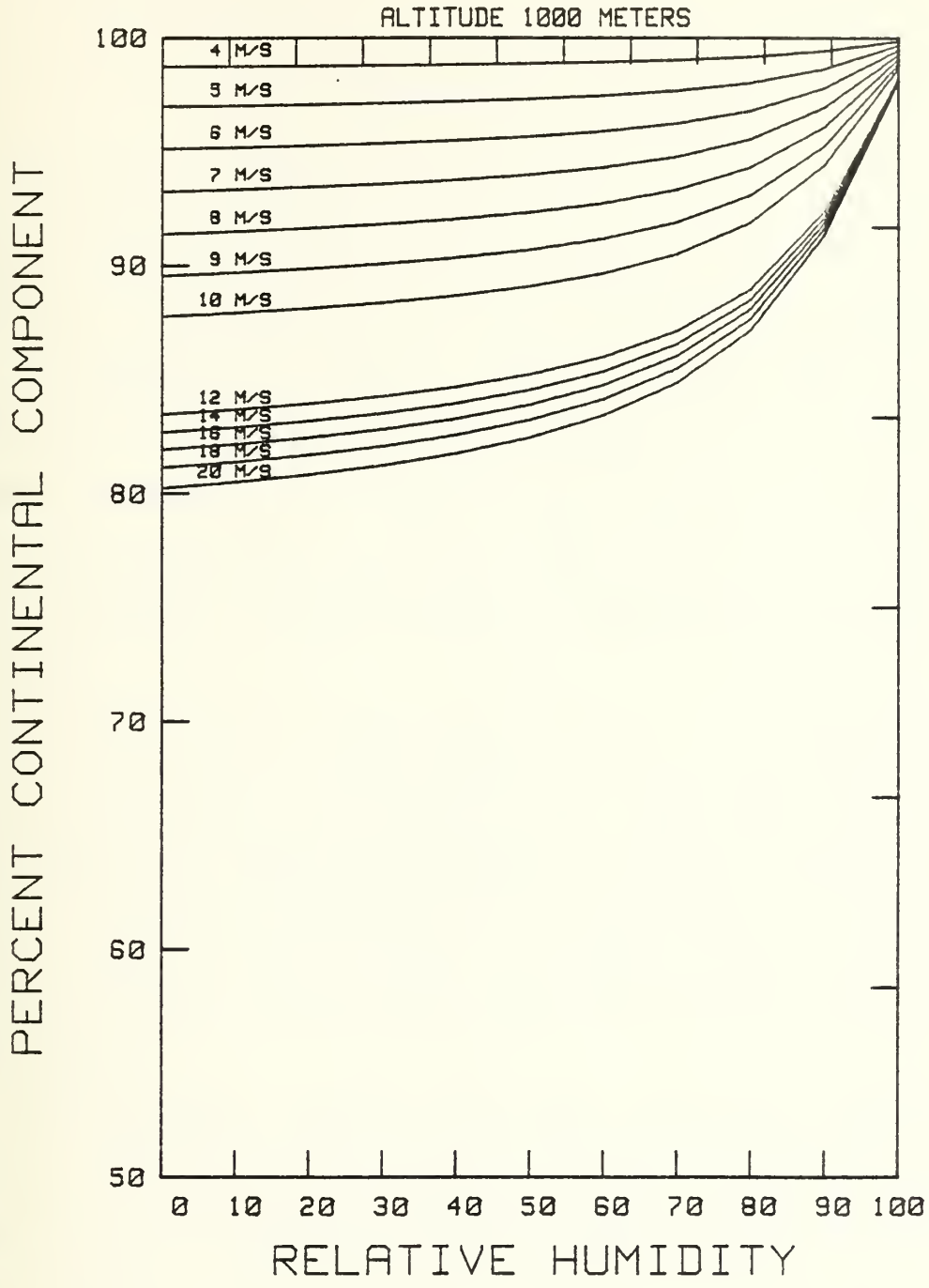

Figure 20. Hybrid Weighting Factor, 1000 Meter Altitude

PERCENT CONTINENTAL COMPONENT

IV. METEOROLOGICAL CONDITIONS

The synoptic conditions influencing the experimental area over the two-week period have previously been discussed by Heil (1981). In the interest of completeness, only a brief summary will be presented here.

As indicated by the synoptic charts the boundary layer of the experimental area was under the continuous influence of a flow regime with a westerly component. At most the flow paralleled the coast one day. Therefore, the assumption that the aerosols off the coast of Monterey were more typical of open ocean than of coastal conditions is a reasonable one.

There were several frontal passages during the experiment. Their effect on the aerosol distribution was not investigated. It is surmised that they significantly decreased the size distribution since frontal circulations would destroy the capping inversions, thus providing a much larger mixing volume through which the aerosols could be distributed.

On both 30 April, 1980 and 4 May 1980, the two days investigated in this thesis, fog or low cloudiness occurred in the early morning. Both days were influenced by slightly stable conditions with the boundary layer capped by a strong inversion. There was a weak frontal passage early on 29 April 1980. Additionally, on both days, conditions within the boundary layer were well mixed. The synoptic surface conditions for the two days in question are given in figures 21 and 22.

Plate I is a DMSP LF-log enhancement of the experimental area on 30 April 1980. Note the gray shades present. It is gray tones such as these that Isaacs is attempting to explain with his model. The circled X's indicate the location of ladders on that day. Plates II and III are LF-log enhancements for May 4 at 1753Z and 1933Z respectively. Again the circled X's depict the ladder locations. On both days low stratus fog was present. However, on the fourth little cloud cover was encountered by the aircraft.

Three out of five ladders flown over the two days will be examined. Two will not be considered. In this study thick clouds are of little interest because the models are unable to adequately describe distributions within the clouds and because "anomalous" gray shades do not occur in these regions. Therefore, Ladder #15 (denoted L #15) will not be discussed since the majority of its height was in clouds. Thin cloud situations, on the other hand, are of interest because "anomalous" gray shades will frequently appear as the cloud (or fog) evaporates. Finally, L #14 was not included because it provided no additional insight beyond that given in L #16.

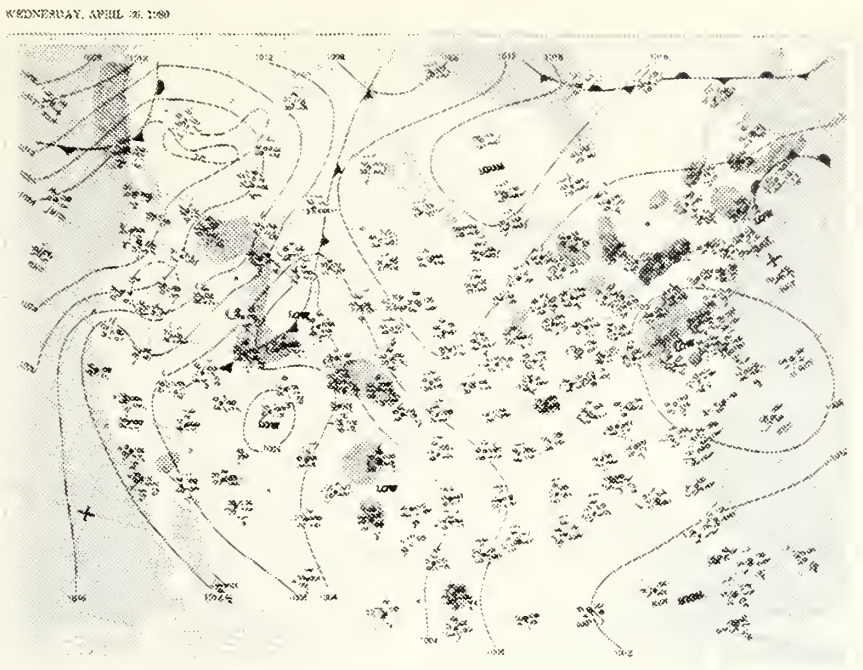

Figure 21. Surface synoptic map, 30 April 1980, 1100 GMT.

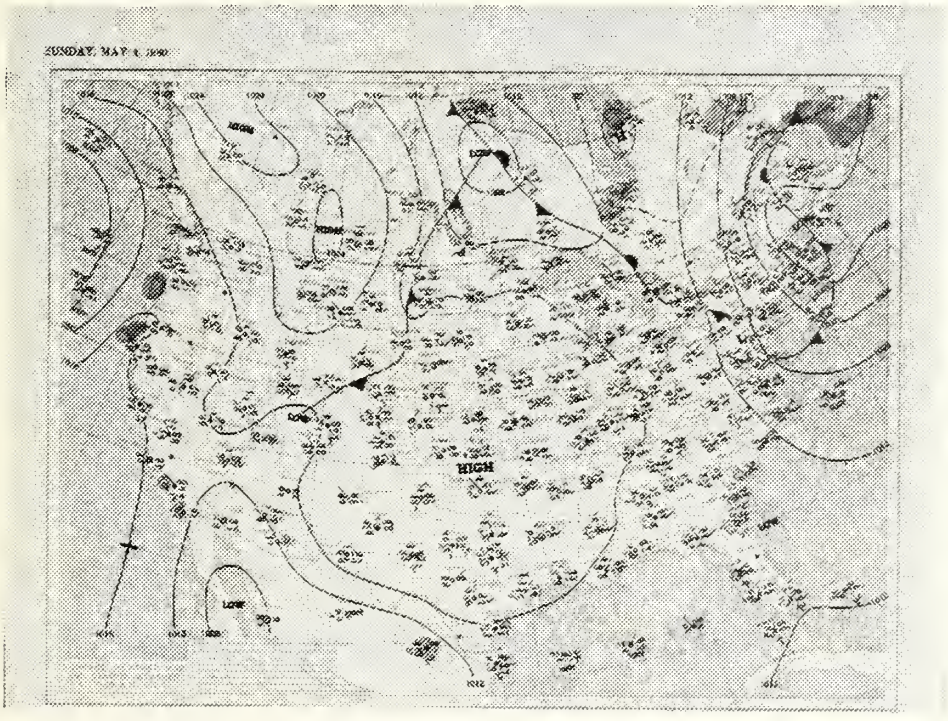

Figure 22. Surface synoptic map, 4 May 1980, 1100 GMT.

V. DISCUSSION OF RESULTS

The discussion of results from this work is broken into two major headings; (A) General Atmospheric Conditions and (B) Evaluation of Models. The first ten figures of this section illustrate comparisons of the model output with the measured data. These figures are arranged as pairs with figure (a) of each pair being the size distribution and figure (b) being the volume distribution. The volume distribution is included because it is proportional to the extinction. Also, it better illustrates the significance of the large particles. Figures 23 to 26 and 27 to 30 depict conditions at L #3 and L #4 of 30 April 1980 respectively. Circumstances at L #16 on 4 May 1980 are displayed in figures 31 and 32. Unfortunately this ladder had no information above the inversion.

A. DISCUSSION OF OBSERVATIONS

General conditions occurring within the three ladder profiles are described in the following three subsections.

1. Ladder #3

L #3 occurred during light wind; the 10 m wind was 4.1 m/s. Relative humidities in the boundary layer ranged from 80 to 95%. A stratus deck capped the boundary layer but none of the aerosol size distributions measurements were made in the clouds. The data presented in figure 24 were obtained just under the cloud deck. Total particle concentration obtained by integrating the polymial fit was 33 cm^{-3} for the 15 m altitude and 75 cm^{-3} for the 305 m altitude. Above the

inversion altitude (approximately 350 m) relative humidity dropped off significantly, to values between 20 and 32%. Likewise, the total particle concentration was reduced to 1.5 cm^{-3} at 610 m and 0.33 cm^{-3} at 1219 m.

2. Ladder #4

Conditions were generally similar to those at L #3. The inversion was found near 350 m, but the relative humidities were slightly lower and no clouds were present. The one factor which distinguished L #3 from L #4, besides lack of clouds, is the wind speed. At L #4 moderate wind speeds of 7.7 m/s were encountered compared to 4.1 m/s at L #3. Relative humidities were 80 to 86% throughout the boundary layer and again dropped off to values between 20 and 32% above the inversion. The total particles concentration (TPC) was quite constant throughout the boundary layer (32 cm^{-3} at 15 m and 29 cm^{-3} at 335 m), which was not the case for L #3. Above the inversion, the TPC decreased significantly to 0.86 cm^{-3} at 610 m and 0.36 cm^{-3} at 1219 m.

3. Ladder #16

This case compared to L #3 and L #4 was influenced by relatively drier conditions in the boundary layer and the wind speeds encountered were even higher than at L #4. Relative humidities ranged from 70 to 80%, and the 10 m wind speed was 8.7 m/s. No clouds were present throughout the profile, and the inversion was found at approximately 500 m. The TPC was determined to be, 8.0 cm^{-3} at 15 m and 11 cm^{-3} at 305 m, which is significantly less than found in either L #3 or L #4.

Three possible explanations can account for the reduction of TPC of L #16 relative to that of L #4:

First, the relative humidity was lower on the 4th of March than it was on the 30th of April. Therefore, on the basis of the relative humidity growth factor, we might expect the integrated size distribution to be smaller for lower relative humidities. However, in comparing L #4 at 335 m with L #16 at 305 m we find that the relative humidity at L #16 is higher than that at L #4, namely 88% vs 84%. The respective TPC is 11 cm^{-3} vs 29 cm^{-3}. The argument fails if we assume the slight difference in altitude (30 m) can not account for the difference in the relative humidity. Even if the relative humidities at equivalent altitudes were exactly the same in both profiles, we could not explain the drastic change in TPC simply on the basis of relative humidity.

Second and perhaps more important, inversion heights are different for the two days. On the 30th of April the inversion height was approximately 350 m, while on the 4th of May it was approximately 500 m. Such an increase in inversion height (from 350 to 500 m) greatly increases the mixing volume of the boundary layer. Furthermore, both temperature and moisture within the boundary layer of L #4 and L #16 are well mixed. Therefore, we can assume that the aerosols are also well mixed. Because the other relevant meteorological conditions are approximately same, it is reasonable to assume that the total number of particles available within the boundary layer of L #16 and L #4 are approximately equal. As a consequence of different mixing volume we should expect that the TPC of L #16 will be less than that of L #4. This is in fact what is observed. The TPC of L #16 is smaller, by a factor of 3, than the TPC of L #4. If mixing volume changes are

responsible for the observed changes in TPC then these results emphasize the importance of including the inversion height in any model describing the size distribution of the boundary layer. Failure to do so could severely impair our ability to distinguish between gray shades. None of the models considered here include inversion height.

Third, the marine aerosol production relative to L #4 may not have existed for a sufficient length of time to saturate the volume of L #16. In other words, the production which led to conditions at L #4 may have existed for an adequately long period to saturate the L #4 boundary layer with aerosols, while at L #16 the appropriate conditions may not have existed for the required length of time and we may simply have measured a pre-saturation distribution. This final point tends to discredit the second explanation; however it suggests that production time is also an important parameter neglected by the models considered here.

B. EVALUATION OF MODELS

As stated, one objective of the thesis is to determine how accurately the models describe observed aerosol size distributions. To accomplish this we will compare each model's output to observed data, evaluate all scaling factors, determine the significance of the continental and maritime components, determine the role of the Shettle and Fenn and the Munn-Katz components in the Hybrid model, and consider the treatment at the inversion. The Hybrid model might be expected to have the most accurate results since it includes distinct relative humidity growth factors for each mode, and since it includes wind speed dependence in the maritime

component. However, the results indicate that frequently it is the least accurate of the three models considered.

1. Comparison of Model Output

In the low wind speed case, figures 23-26, the Hybrid model appears to be less accurate within the mixed layer than either of the models from which its component parts were taken. This results suggests that within the boundary layer the Shettle and Fenn model and the Munn-Katz model are incompatible. This is not a surprising result since both models are empirically derived.

The Shettle and Fenn model most accurately describes the observed results relative to the magnitude and shpae of the distribution. This is particularly evident from the volume plots (figure 23b and 24b). This is not surprising either, since an input to this model was the TPC determined from the actual data.

Neither the Hybrid model nor the Munn-Katz model accurately describes either the measured size distribution or the volume distribution. The strong role of the continental component in the Munn-Katz model is apparent in the volume plots. There is a definite lack of curvature to the Munn-Katz volume plot, a clear indicator that the controlling model component is the continental aerosol.

Above the boundary layer, however, when the total particle concentrations are extremely low the Hybrid model most accurately predicts the observed size distribution. This result is consistent through all ladders and we can state that when the total particle concentration is extremely low (TPC < 3 cm^{-3}) the Hybrid model produces the most accurate

results. This situation commonly occurs above the inversion. The reason for this occurrence will be discussed in section 4 below.

Results similar to that above are found in examining the predicted and observed distributions of L #4 (figures 27-30), except that, the three models predict nearly the same results below the inversion. The Munn-Katz prediction is still strongly influenced by the continental component, as is again evidenced by the "tail" in the smaller radii of the volume plots, i.e. the model size distribution climbs unrealistically upward compared to the data. Fairall (1981) indicates that the Junge coefficient used in the Munn-Katz model is probably too large and he has determined an alternate Junge coefficient. The sensitivity of the model to changes in this coefficient will be discussed below. (The observed size distributions raise the question, however, of whether the Junge distribution is at all appropriate for the time and location of our observation.) Other than this deviation due to the unrealistically specified continental component the predicted distributions of the Munn-Katz and the Hybrid models are better in L #4 than in L #3. This improvement in model prediction can be attributed to the increase in wind speed; a characteristic which is further emphasized in L #16 (Figures 31 and 32).

2. Evaluation of Scaling Factors

Having observed the above results the question arises as to the cause of the differences. Two possibilities were considered for the differences in the predicted and observed results: (a) there may be unexpected complications with the weighting factor and (b) the Junge

coefficient of the Munn-Katz model may be in error. The second factor, however, would not effect the Hybrid model.

a. Evaluation of Imposed Weighting Factor

The weighting factors (eqns (12) and (13)) derived by integrating the Hybrid model (eqn (3)) was replaced by those derived from the Shettle and Fenn model (eqns (14) and (15)) in order to investigate each model's sensitivity to this *ad hoc* parameter. Figure 33 displays the calculated results for the 3 m height of L #16 using the original coefficient, and figure 34 displays the calculated results obtained when the Shettle and Fenn weighting factor was substituted into the Hybrid model. The negligible difference in the two plots is observed. The numerical output, as well, indicate that the Hybrid model's predictions are insensitive to this weighting factor.

b. Evaluation of Junge Coefficient

The Junge coefficient was varied to determine the effect on the Munn-Katz continental component. As in the case studied by Fairall (1981), the data suggest that a smaller Junge coefficient (perhaps 0.7) would be more appropriate for this data. Reducing this coefficient from 1.7 to .7 only reduced the influence of the continental component by approximately a factor of 2. This resulted in a better fit of the predicted distribution in the smaller radii. However, varying this parameter did not eliminate the observed continental "tail"; it simply shifted it to smaller radii. This problem will undoubtedly persist as long as the continental mode is described by a single term.

As mentioned above, Fairall (1980) has demonstrated that directly measured extinction and extinction calculated from the observed size distributions were essentially equivalent. The observed data, presented in figures 23-32, tend to fall off in the smaller radii. This fact in combination with Fairall's results suggests that an increasing continental component (Junge distribution) is incorrect. In short, the data seem to support the hypothesis that either an entirely different continental distribution, or perhaps the neglect of the continental component, is more appropriate for the open ocean planetary boundary layer. In any case, further investigation of the continental size distribution over open ocean is warranted.

3. Significance of Continental and Maritime Components

To further examine the above results, the component parts of the Shettle and Fenn and the Munn-Katz model were plotted in figures 35, 36, and 37 for L #3, L #4, and L #16 respectively. These three figures indicate that disagreements between the Shettle and Fenn model results and the observed data are attributed completely to the maritime component of the model, since the continental contribution is extremely small. The Munn-Katz model is seen to have varying dependence on both the continental and maritime components. In figure 35, which is the low wind speed case, it is seen to be strongly dependent upon the continental component. Only a slight deviation from the continental is noticed in the large radii. In figure 36, which is the 7.7 m/s wind speed case, the maritime component dominates the distribution above 1 μm radius. Its predicted distribution is not greater than that predicted by the Shettle and Fenn

model and therefore it fails short in its ability to describe the distribution for this case. Only when the wind speed is greater than 8 m/s is the maritime component of the Munn-Katz model better than that of the Shettle and Fenn model in modeling the observed distribution. This is exactly the situation in figure 37 which is the 8.7 m/s wind speed case where the influence of the continental and maritime components of the Munn-Katz model combine to give the most accurate prediction, as compared to the measured data.

4. Role of the Shettle and Fenn and the Munn-Katz Components in the Hybrid Model

In reviewing how the Shettle and Fenn continental and the Munn-Katz maritime components influence the Hybrid model we note that the continental component from the Shettle and Fenn model has a minor role at high wind speeds. The Hybrid formulation's (eqn 3) wind speed dependence is such that the entire aerosol distribution can be attributed to the maritime component of the Munn-Katz model. This result, and the better fit of the maritime component to the data, explain why the Hybrid prediction improved with wind speed, and why little difference was noted when the weighting factor of the continental component of the Hybrid model was altered.

It is obvious from the above discussion that the Shettle and Fenn model prediction (in the radius range 0.4-1.1 μm) is dominated by the maritime component. The output of the Munn-Katz model is dependent upon the relative influence of the continental and maritime components. Its influence on the Hybrid model is strongly dependent on relative humidity and wind speed. Additionally, it is clear that the Hybrid model in actuality is not a hybrid at all but simply describes

the maritime component of the Munn-Katz model. Only when the wind speed is close to zero will the Shettle and Fenn continental component influence the predicted distribution. Finally, these results indicate that the maritime component of the Munn-Katz model is less than exact, particularly under low wind speed conditions. This may be due in part to the wind speed scaling, and in part to not including the inversion height (and thus ignoring the mixing volume).

5. Treatment at the Inversion

Studies by members of the Naval Postgraduate School Environmental Physics Research Group have indicated that properties within the boundary layer are not transported through the inversion to the upper layers (Davidson et al., 1980). Instead, drier air from above the inversion is continually mixed down into the boundary layer. This prevents maritime aerosols generated within the boundary layer from being transported through the inversion. Furthermore, aerosol water droplets within the boundary layer are continuously being reduced in size due to evaporation. Given this situation, any model which does not terminate (or strongly damp) the influence of the maritime component at the inversion, and which does not account for changes in relative humidity effects due to the entrainment of warm dry air, will be incorrect in its prediction of n(r) near the top of the mixed layer.

Figure 38 has been included to illustrate the results of assuming that the size distribution above the inversion is due solely to the continental component (i.e. continental weighting factor = 1.0 and the maritime component is zeroed). When figure 38 is compared with figure 30b, a reduction in the accuracy of the Shettle and Fenn model is immediately

obvious. Its accuracy is reduced by two orders of magnitude in the small radii and by four orders of magnitude in the large radii. The Munn-Katz model, on the other hand, is affected minimally and gives the better result. However, its prediction remains somewhat high; therefore, it can be concluded that although the Munn-Katz model gives approximate results, both models need significant modification to properly specify the aerosol size distribution near the inversion.

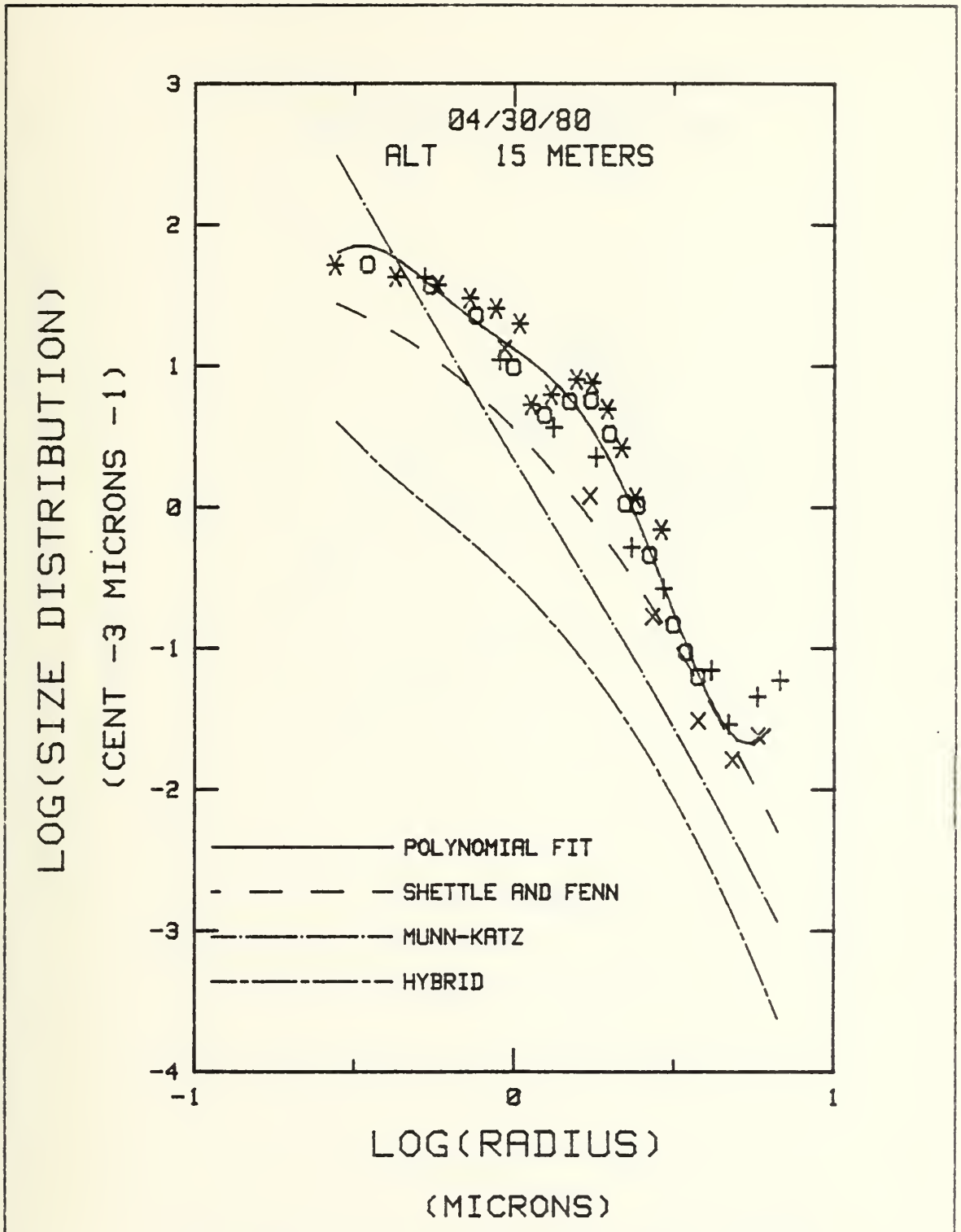

Figure 23a. Size Distribution, L #3, 15 Meters

RELATIVE HUMIDITY 82.32, MIXING RATIO 7.40, WIND SPEED 4.1

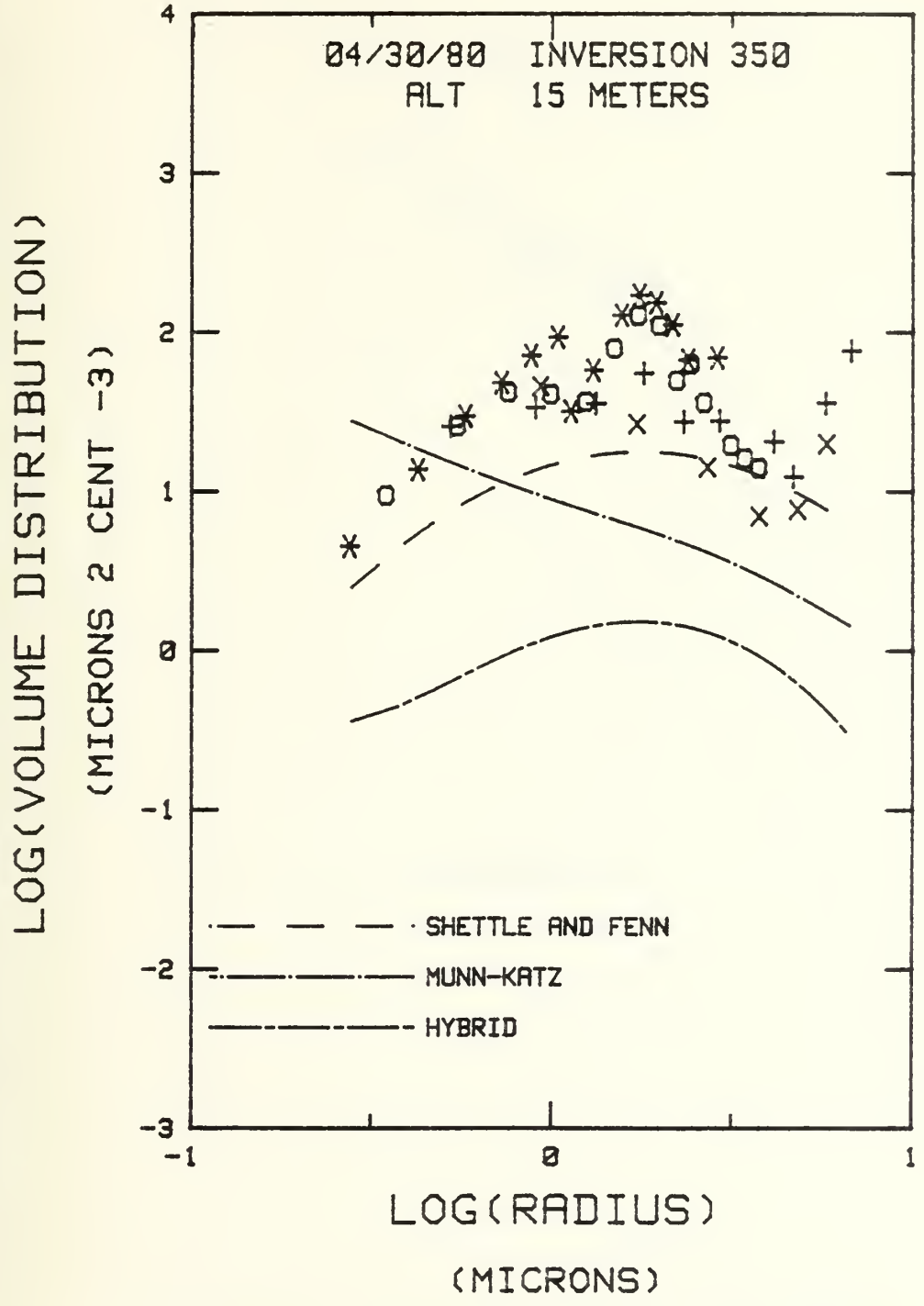

Figure 23b. Volume Distribution, L #3, 15 Meters

RELATIVE HUMIDITY 82.32, MIXING RATIO 7.40, WIND SPEED 4.1

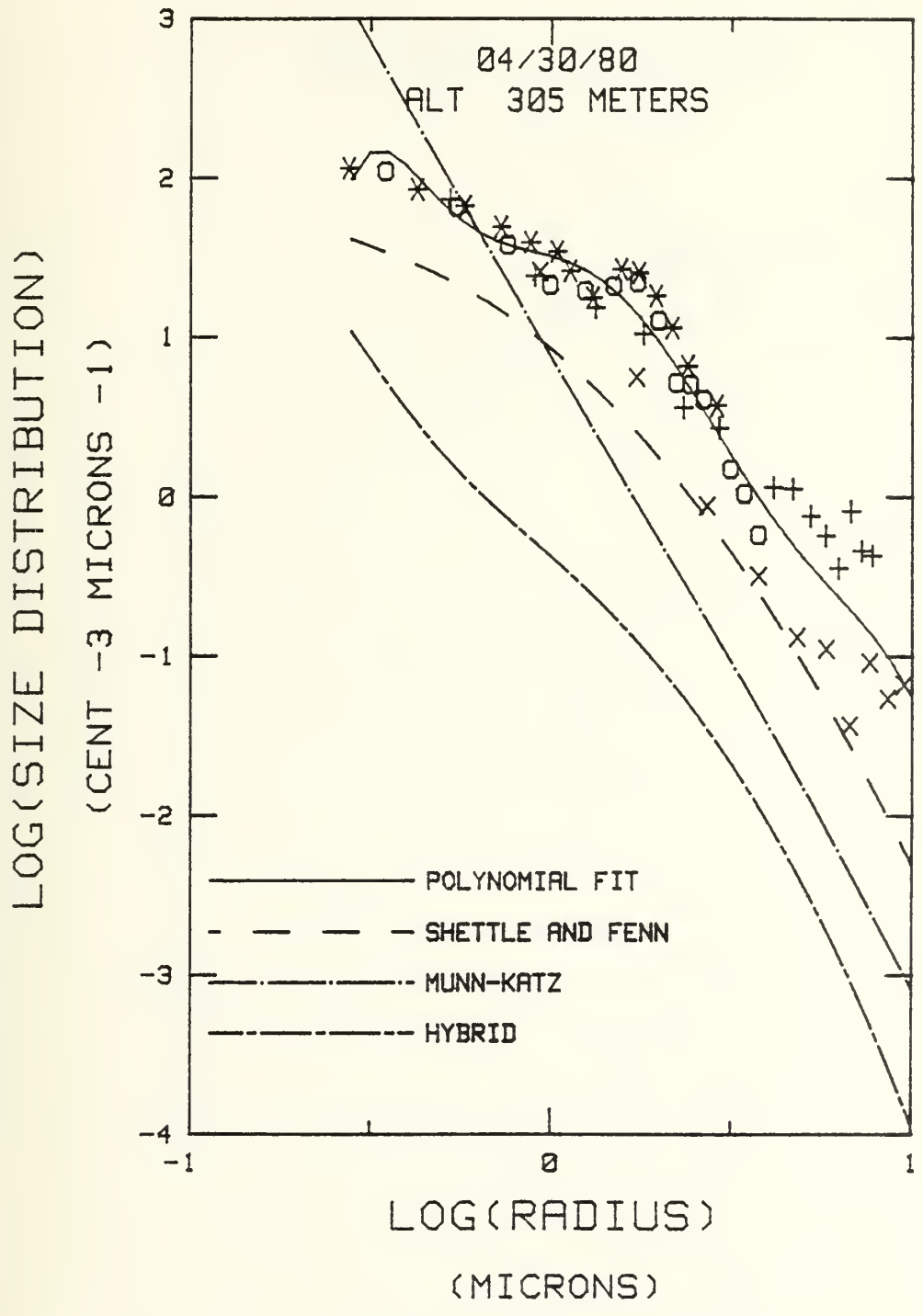

Figure 24a. Size Distribution, L #3, 305 Meters

RELATIVE HUMIDITY 94.82, MIXING RATIO 7.29, WIND SPEED 4.1

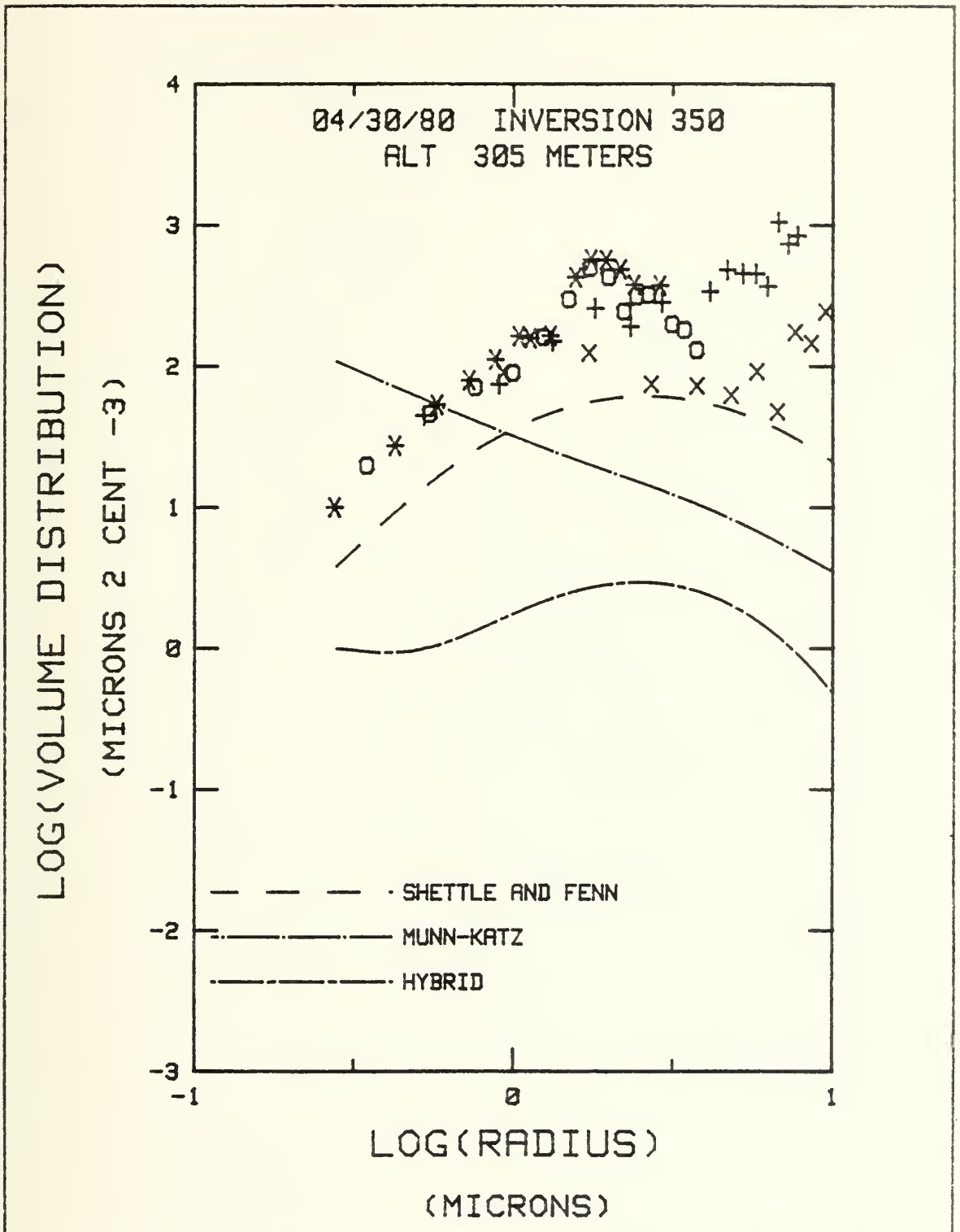

Figure 24b. Volume Distribution, L #3, 305 Meters

RELATIVE HUMIDITY 94.82, MIXING RATIO 7.29, WIND SPEED 4.1

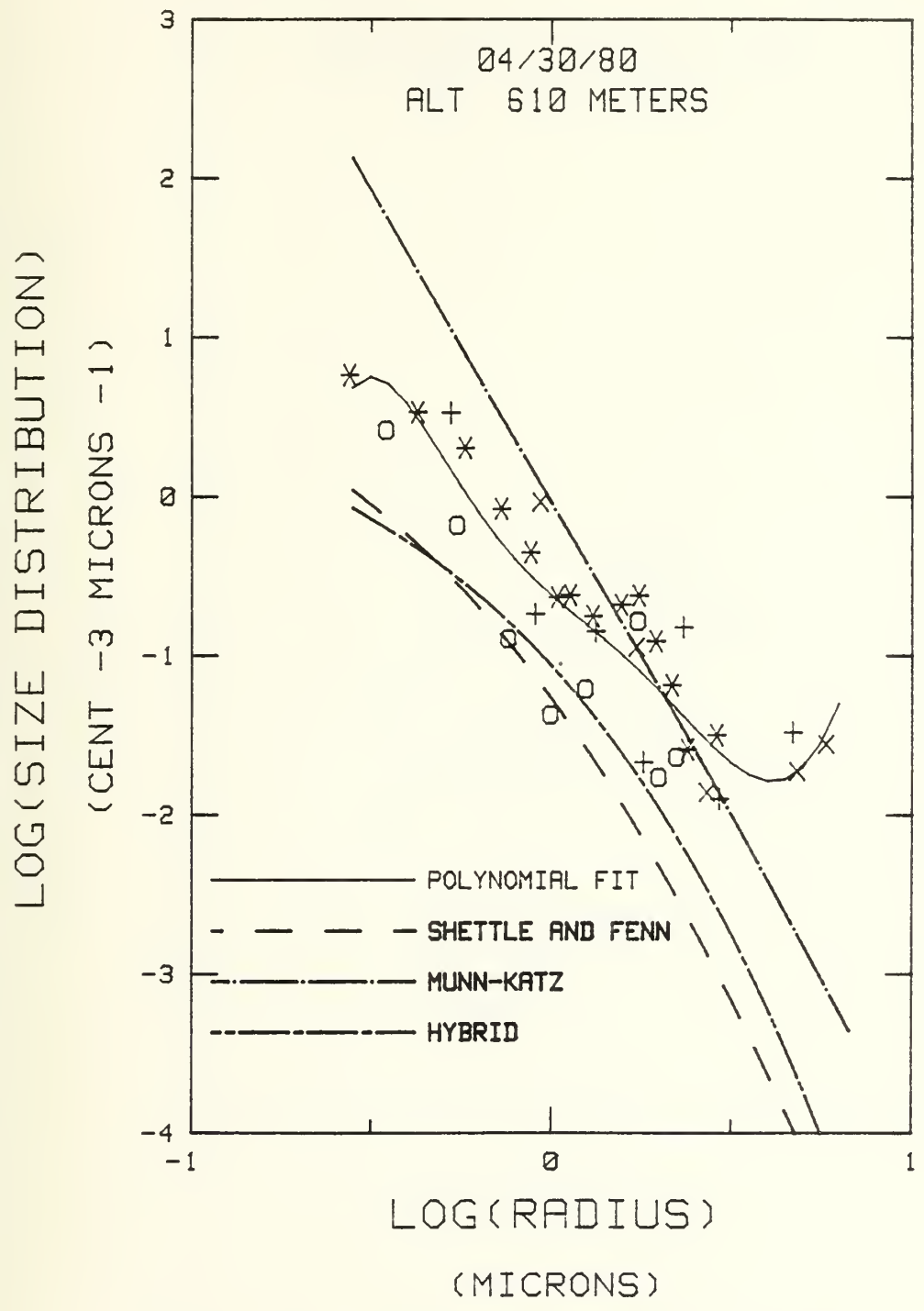

Figure 25a. Size Distribution, L #3, 610 Meters

RELATIVE HUMIDITY 31.71, MIXING RATIO 3.79, WIND SPEED 4.1

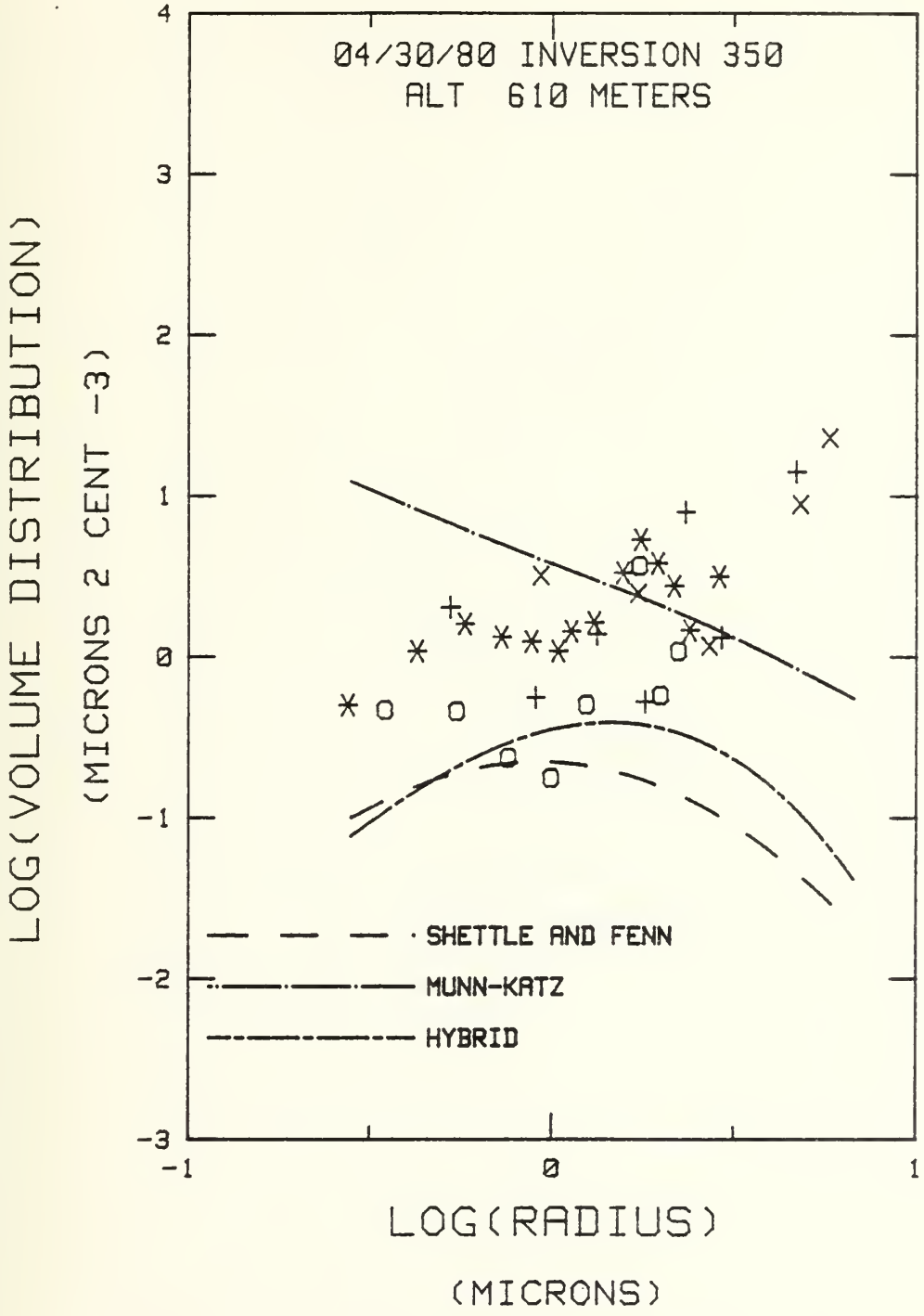

Figure 25b. Volume Distribution, L #3, 610 Meters

RELATIVE HUMIDITY 31.71, MIXING RATIO 3.79, WIND SPEED 4.1

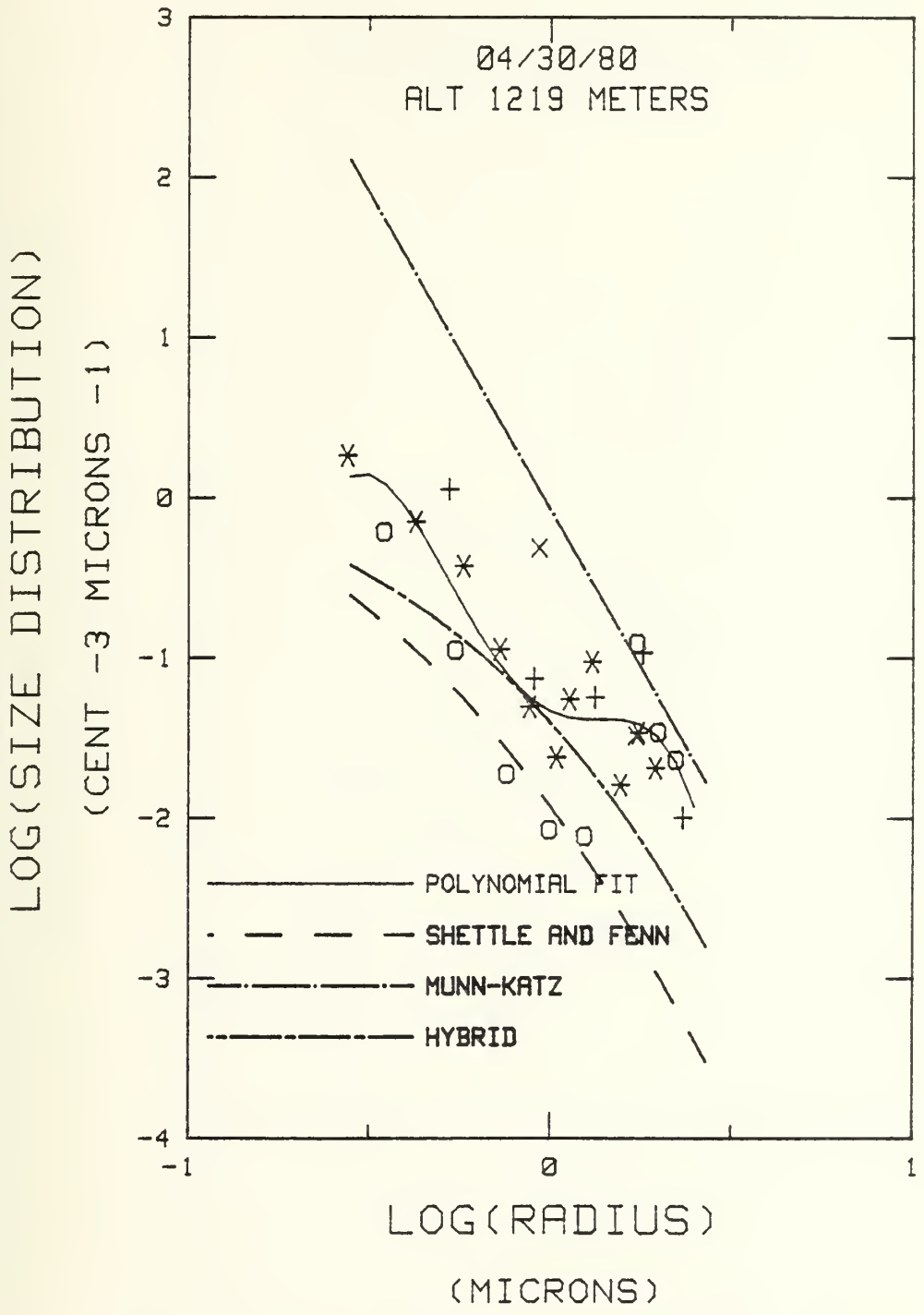

Figure 26a. Size Distribution, L #3, 1219 Meters

RELATIVE HUMIDITY 23.64, MIXING RATIO 2.76, WIND SPEED 4.1

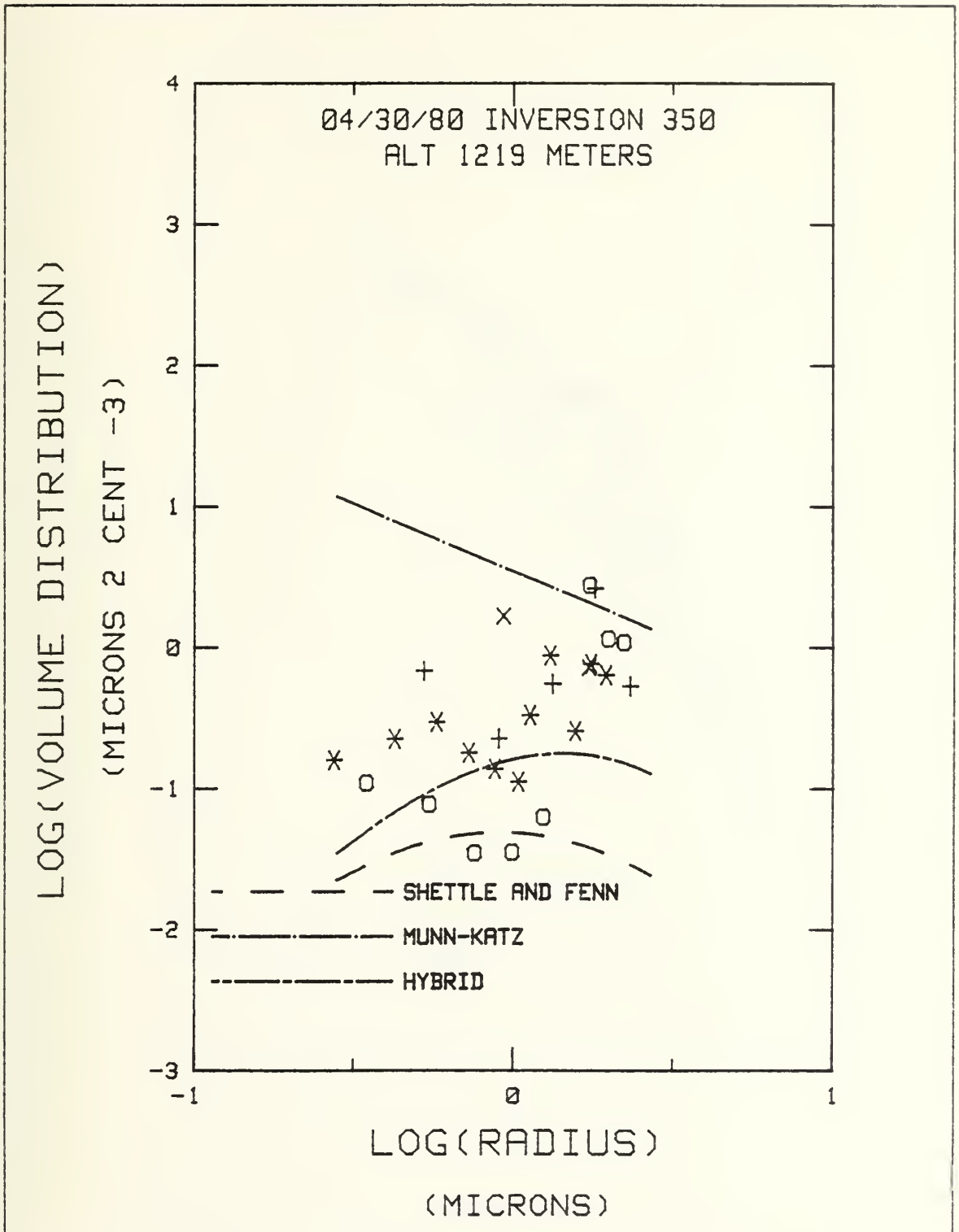

Figure 26b. Volume Distribution, L #3, 1219 Meters

RELATIVE HUMIDITY 23.64, MIXING RATIO 2.76, WIND SPEED 4.1

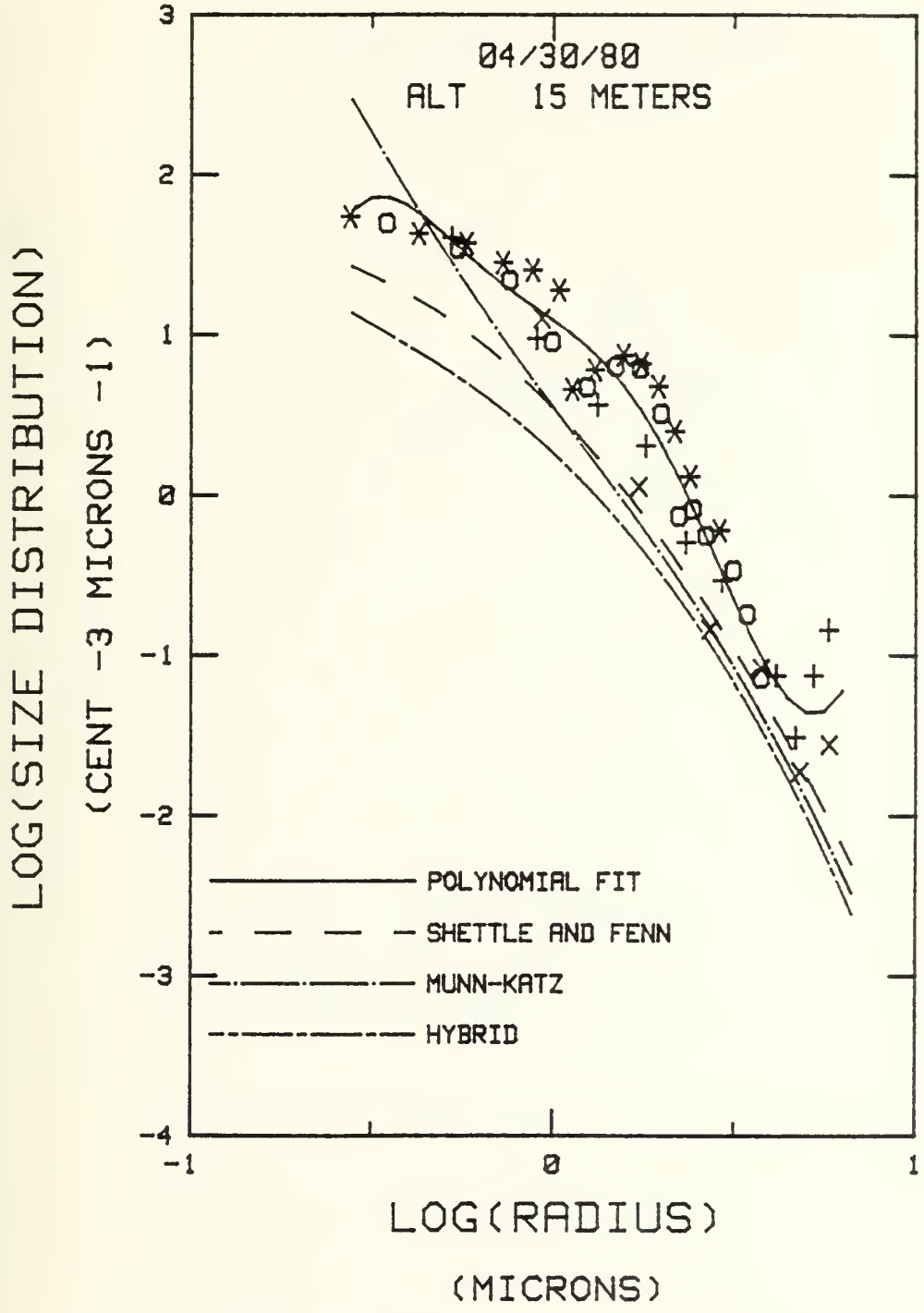

Figure 27a. Size Distribution, L #4, 15 Meters

RELATIVE HUMIDITY 81.26, MIXING RATIO 7.31, WIND SPEED 7.7

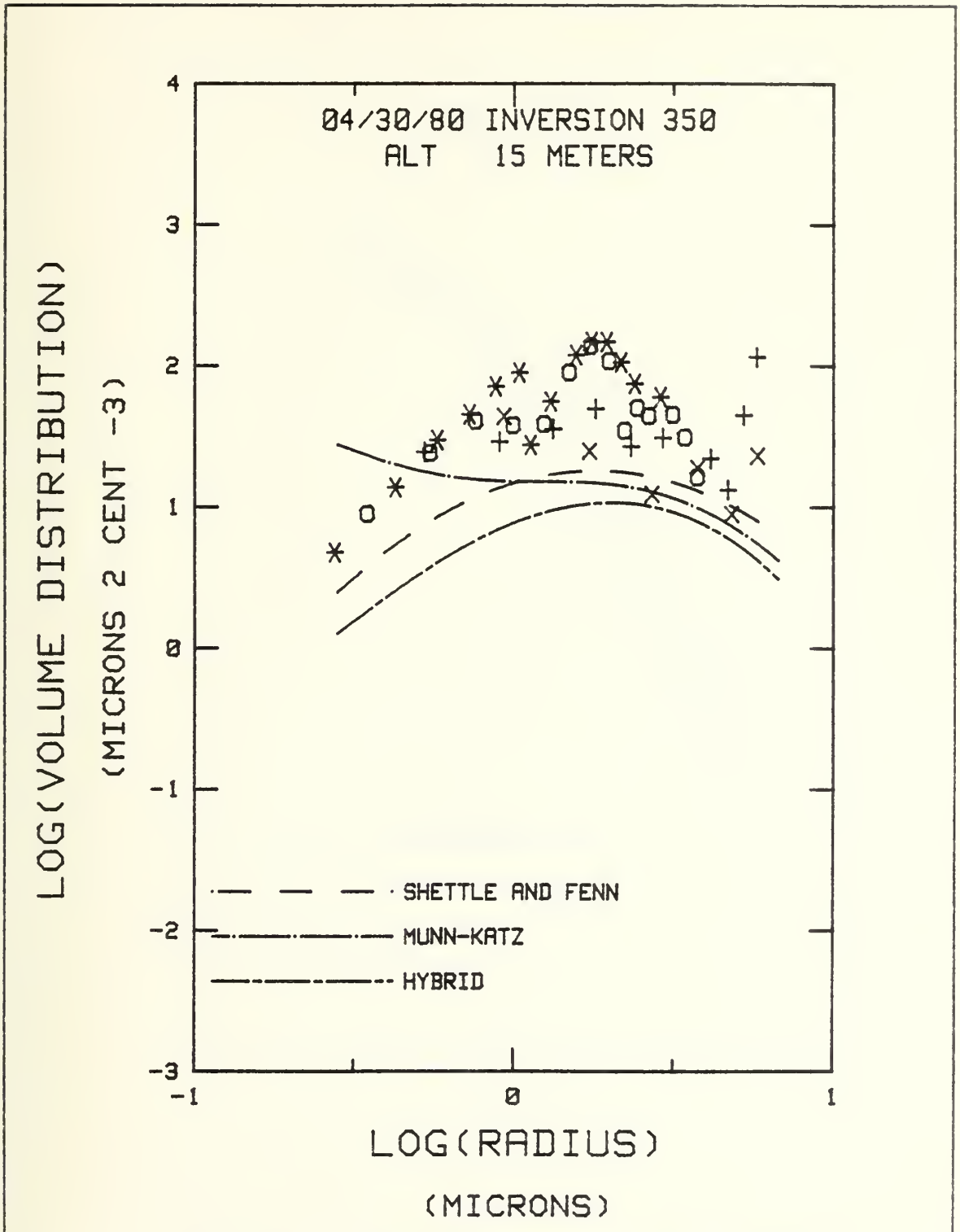

Figure 27b. Volume Distribution, L #4, 15 Meters

RELATIVE HUMIDITY 81.26, MIXING RATIO 7.31, WIND SPEED 7.7

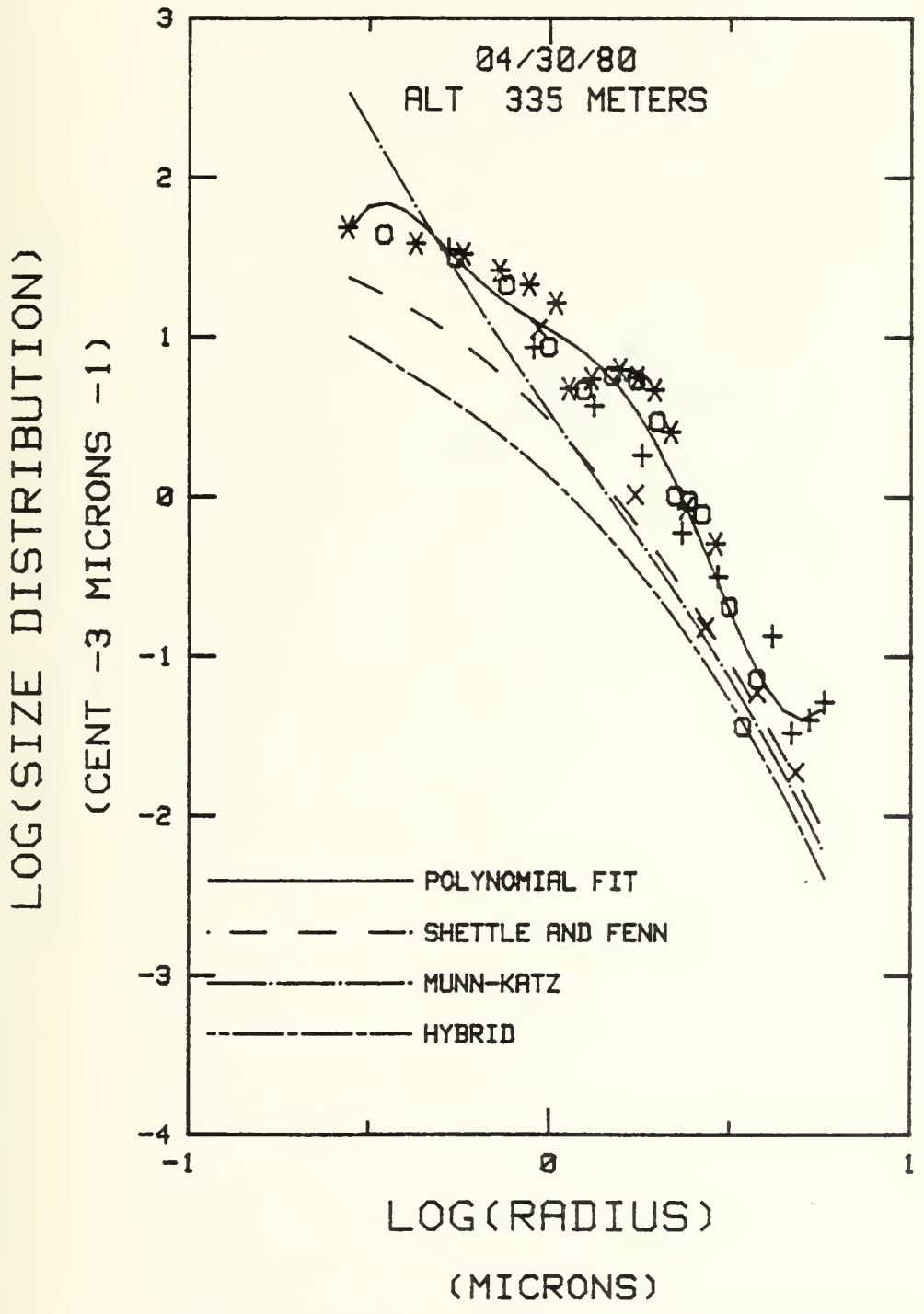

Figure 28a. Size Distribution, L #4, 335 Meters

RELATIVE HUMIDITY 84.08, MIXING RATIO 6.61, WIND SPEED 7.7

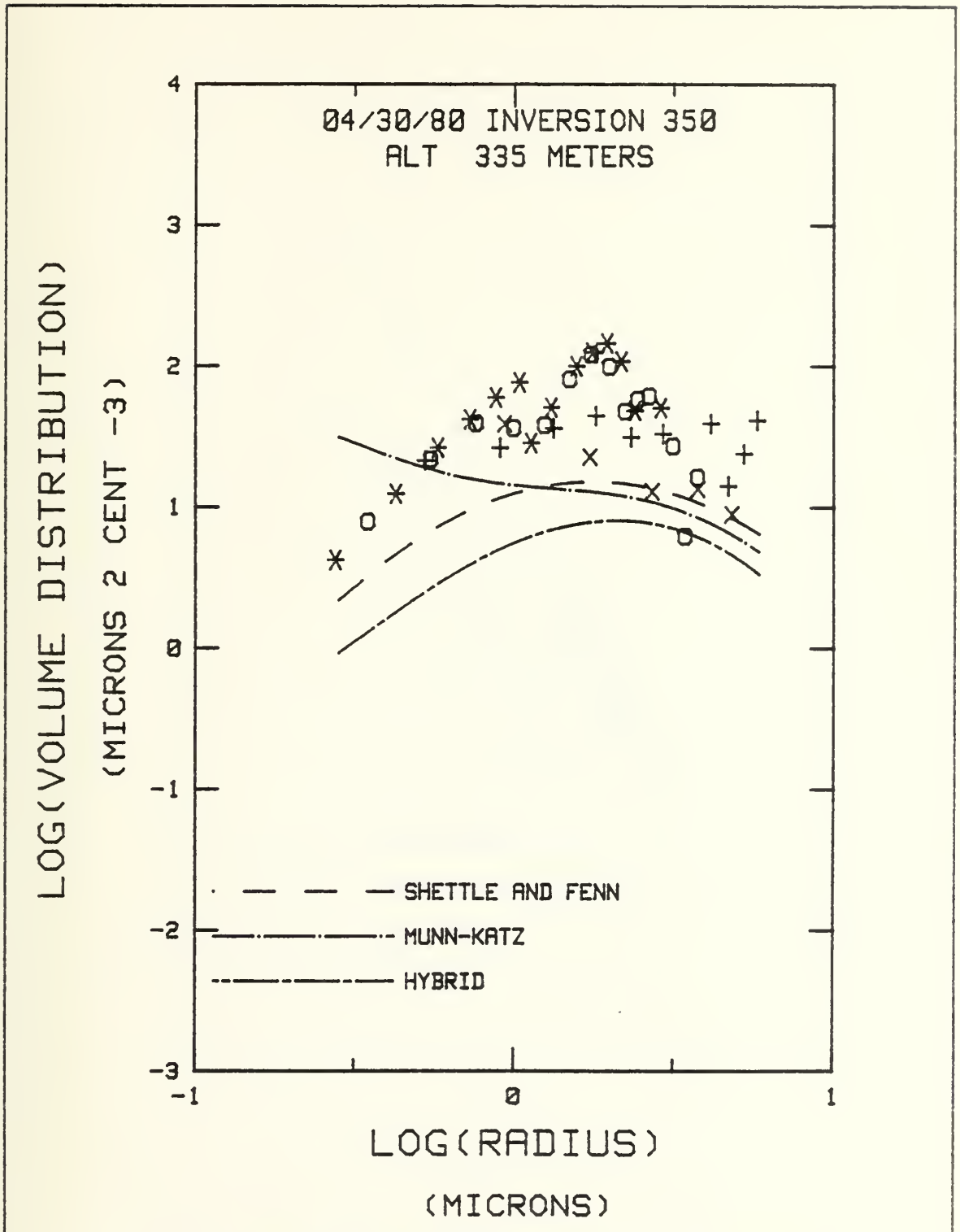

Figure 28b. Volume Distribution, L #4, 335 Meters

RELATIVE HUMIDITY 84.08, MIXING RATIO 6.61, WIND SPEED 7.7

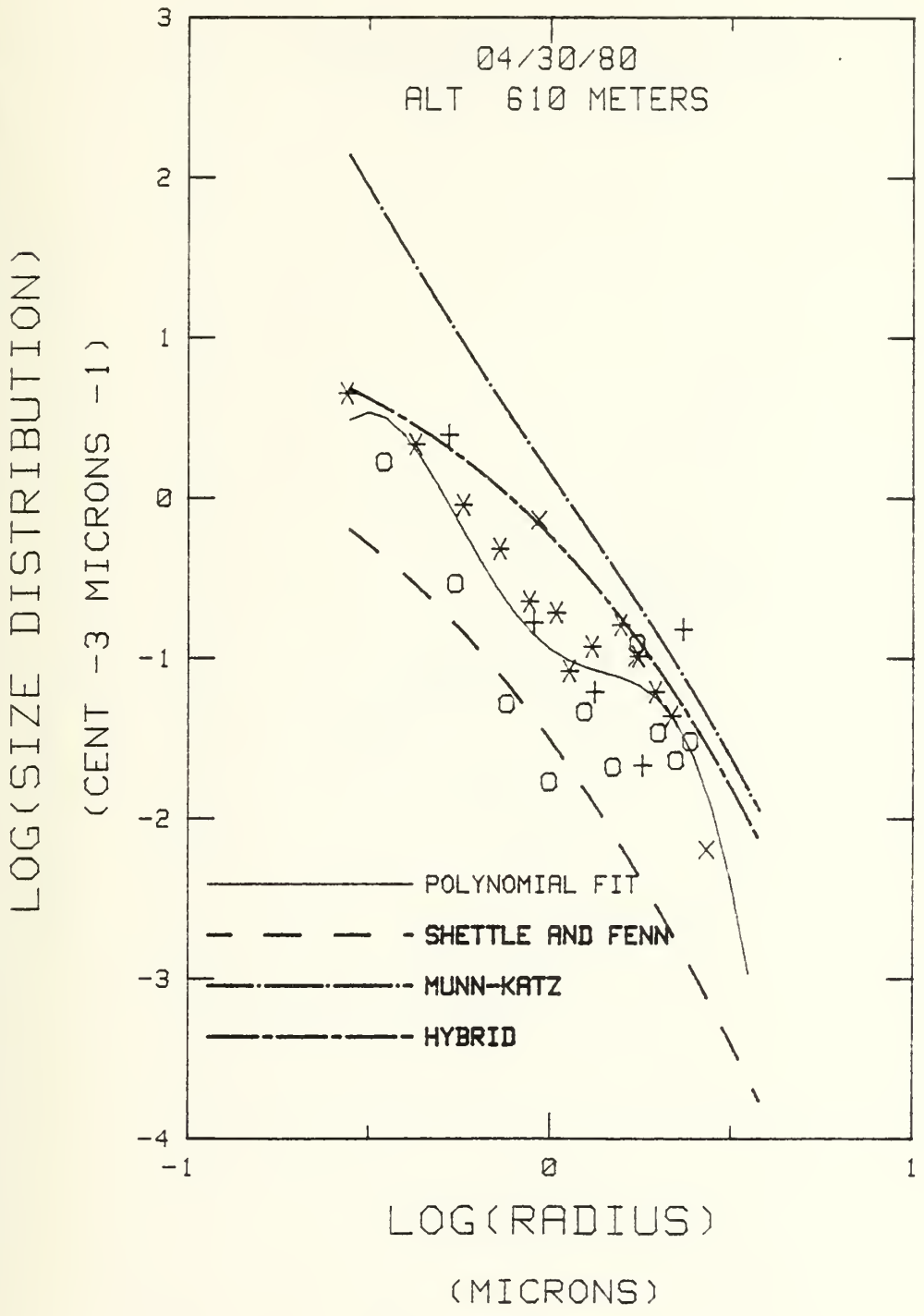

Figure 29a. Size Distribution, L #4, 610 Meters
RELATIVE HUMIDITY 30.62, MIXING RATIO 3.63, WIND SPEED 7.7

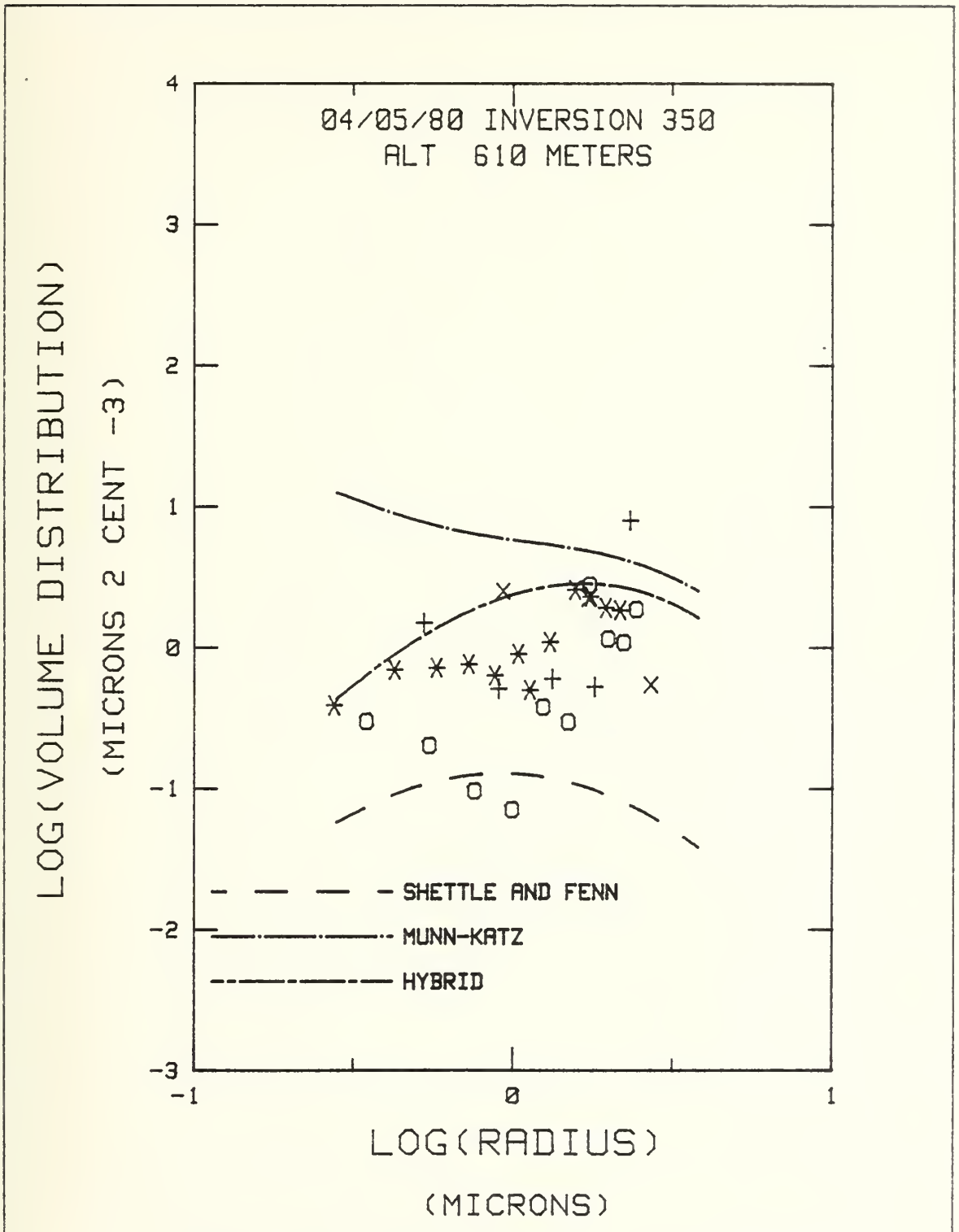

Figure 29b. Volume Distribution, L #4, 610 Meters
RELATIVE HUMIDITY 30.62, MIXING RATIO 3.63, WIND SPEED 7.7

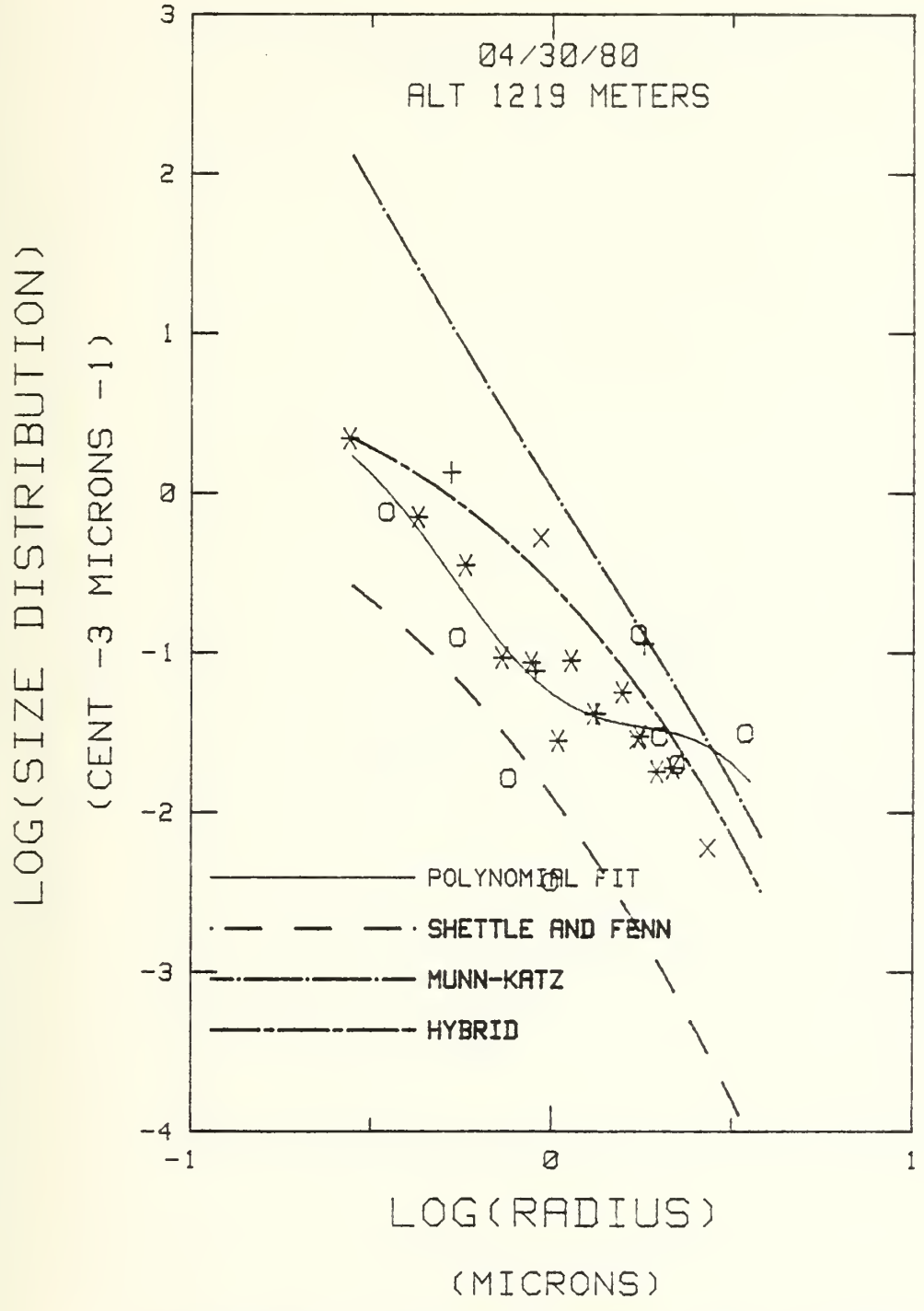

Figure 30a. Size Distribution, L #4, 1219 Meters

RELATIVE HUMIDITY 20.48, MIXING RATIO 2.37, WIND SPEED 7.7

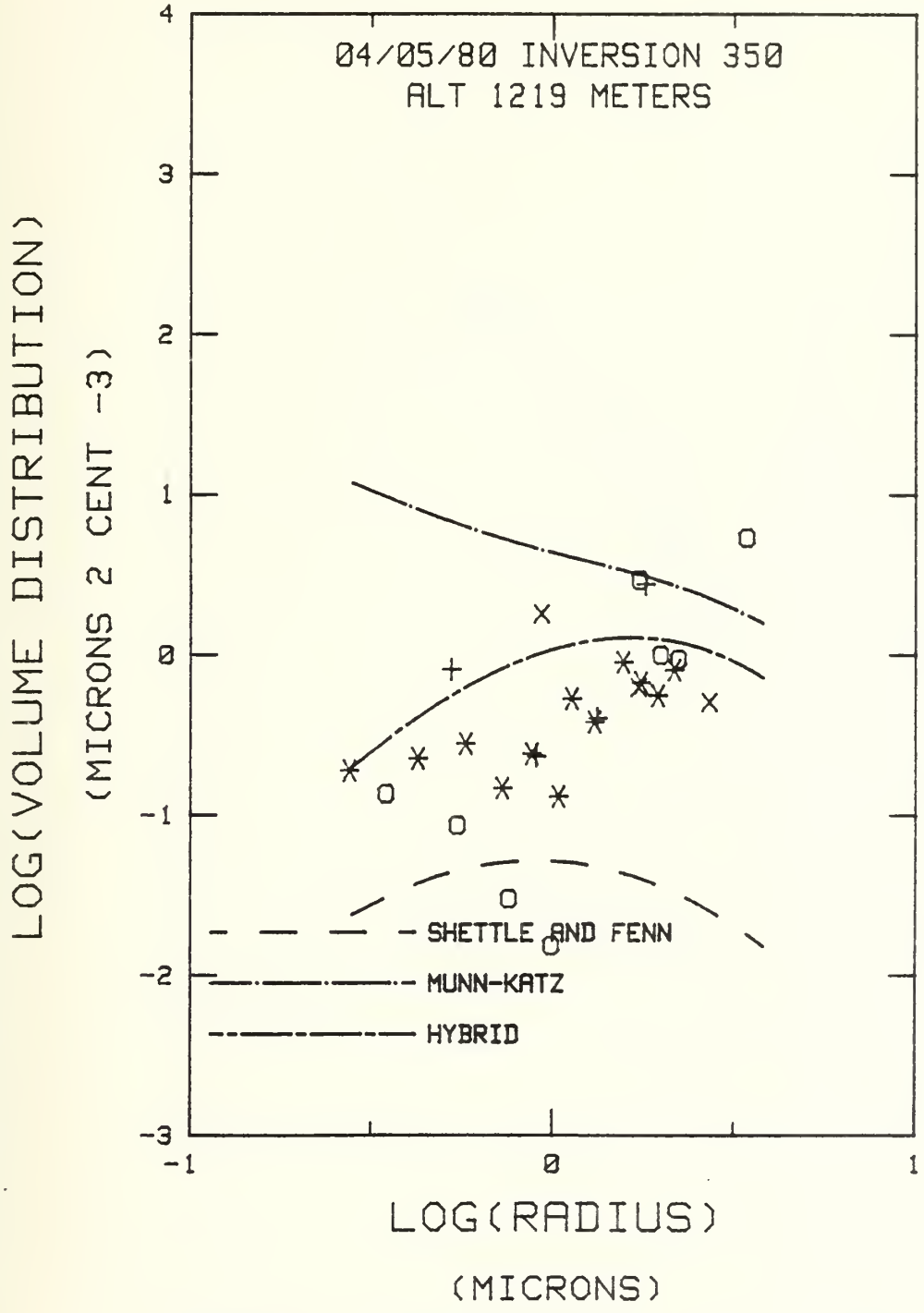

Figure 30b. Volume Distribution, L #4, 1219 Meters

RELATIVE HUMIDITY 20.48, MIXING RATIO 2.37, WIND SPEED 7.7

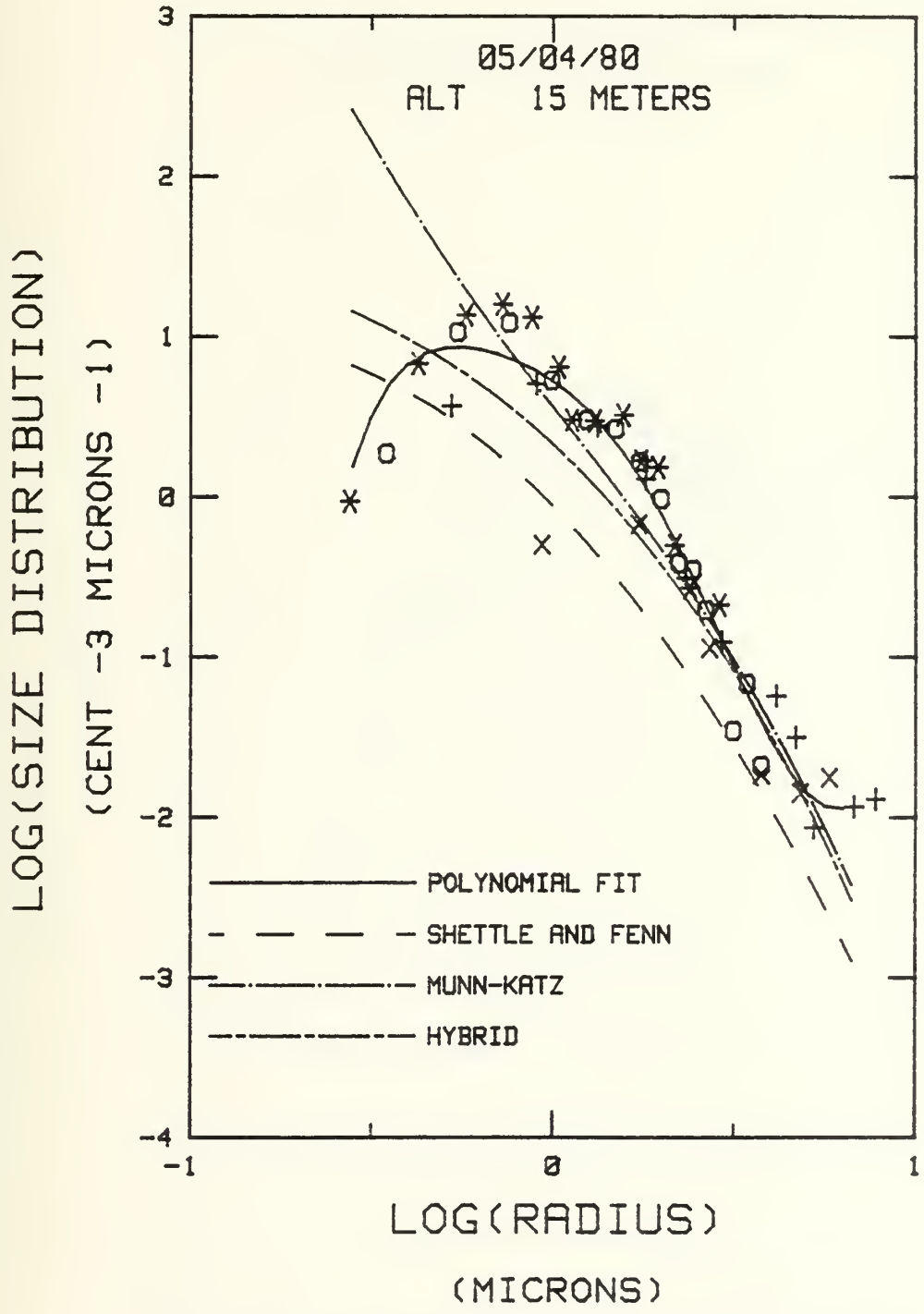

Figure 31a. Size Distribution, L #16, 15 Meters

RELATIVE HUMIDITY 77.83, MIXING RATIO 6.79, WIND SPEED 8.7

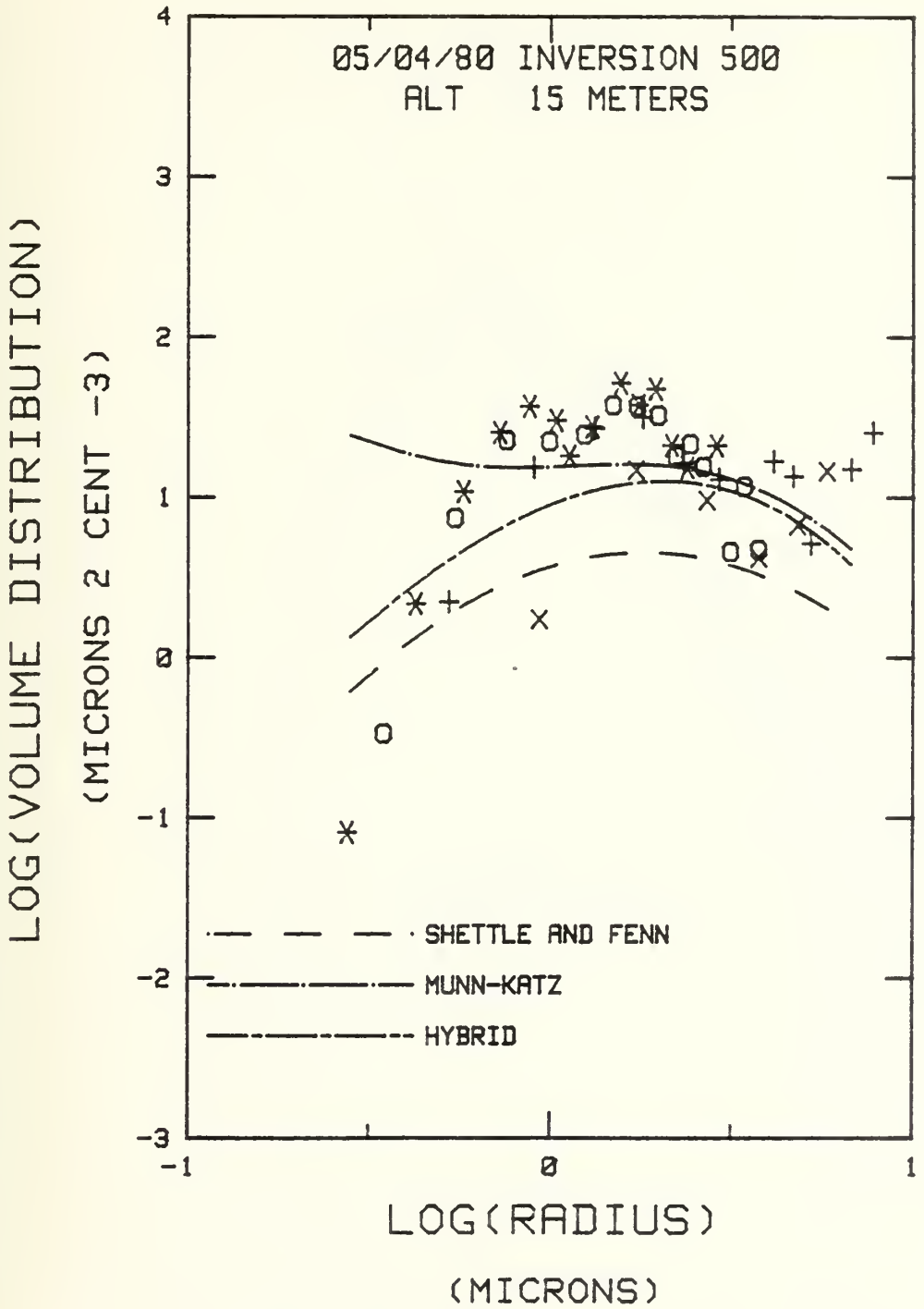

Figure 31b. Volume Distribution, L #16, 15 Meters

RELATIVE HUMIDITY 77.83, MIXING RATIO 6.79, WIND SPEED 8.7

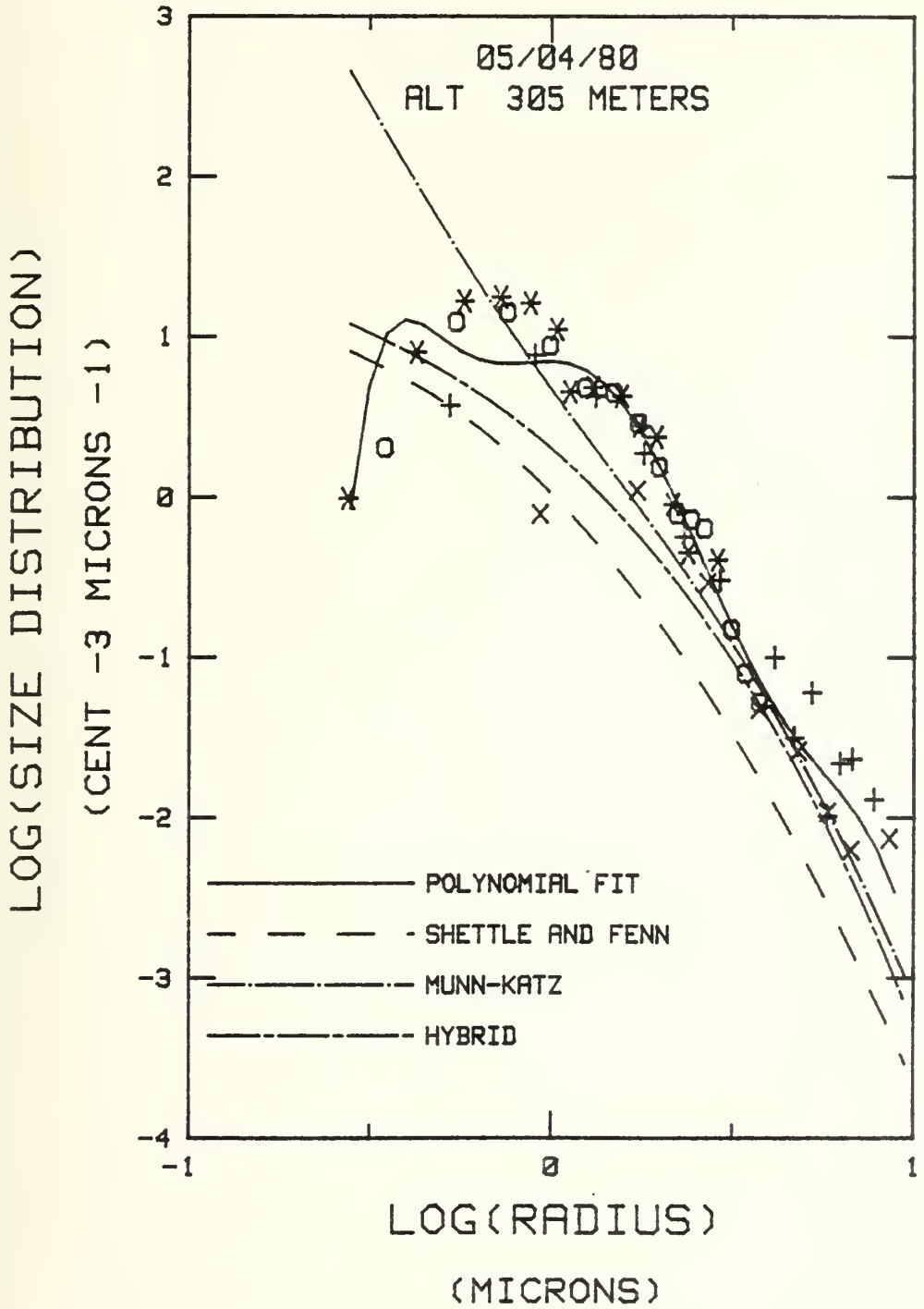

Figure 32a. Size Distribution, L #16, 305 Meters

RELATIVE HUMIDITY 88.04, MIXING RATIO 6.72, WIND SPEED 8.7

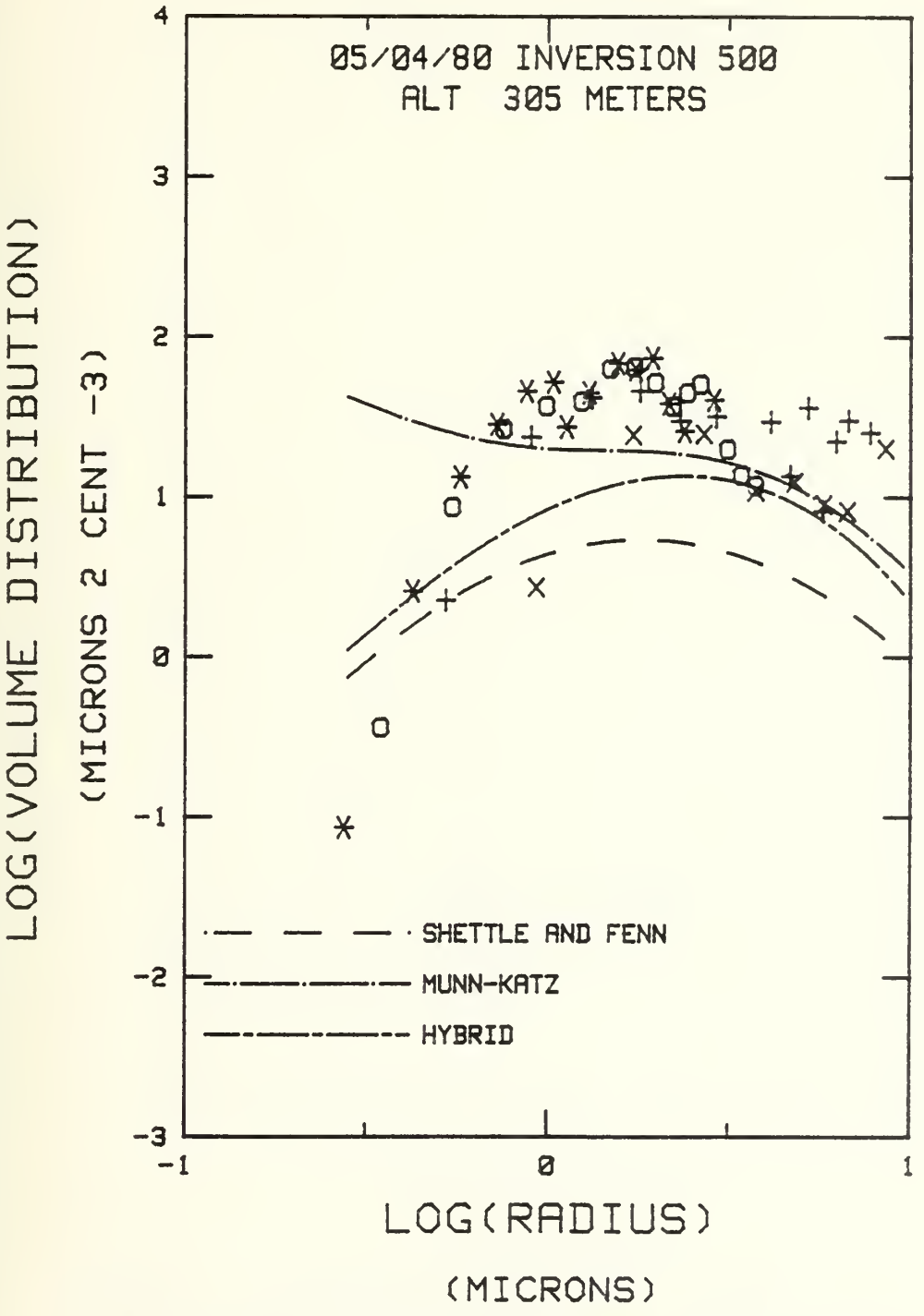

Figure 32b. Volume Distribution, L #16, 305 Meters

RELATIVE HUMIDITY 88.04, MIXING RATIO 6.72, WIND SPEED 8.7

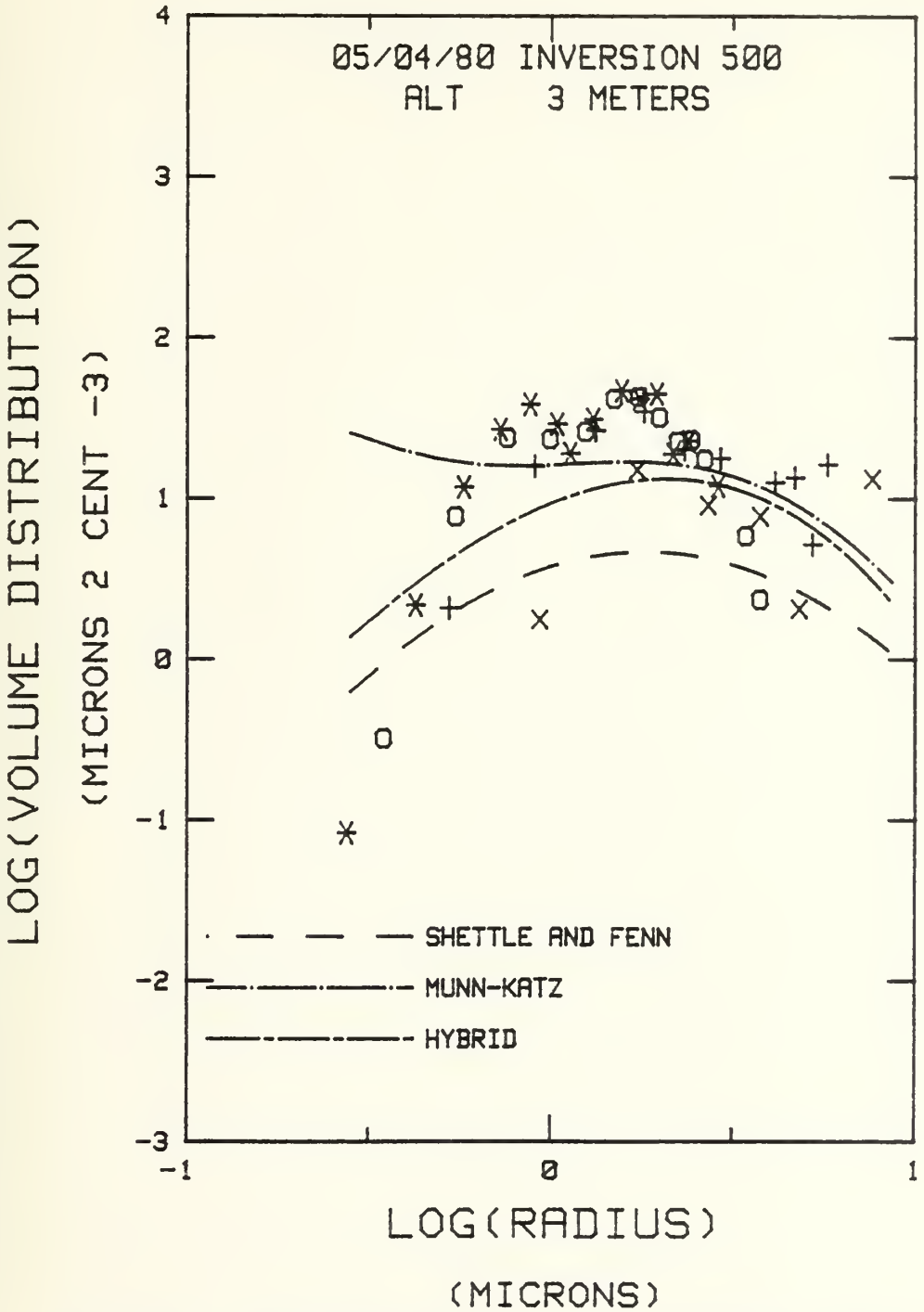

Figure 33. Volume Distribution, L #16, 3 Meters, Hybrid Weighting Factor Employed in Hybrid Model

RELATIVE HUMIDITY 79.04, MIXING RATIO 7.00, WIND SPEED 8.7

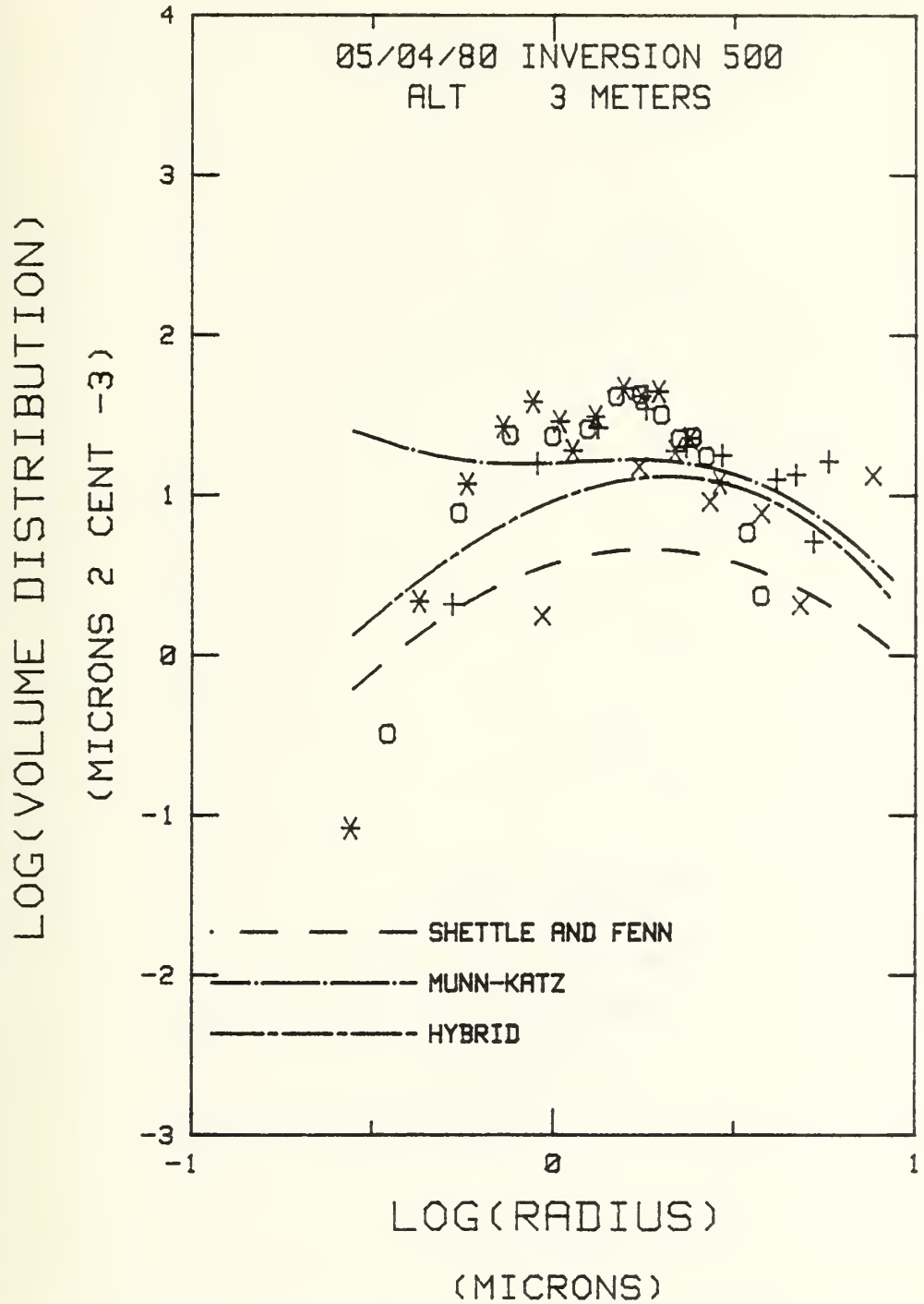

Figure 34. Volume Distribution, L #16, 3 Meters, Shettle and Fenn Weighting Factor Employed in Hybrid Model

RELATIVE HUMIDITY 79.04, MIXING RATIO 7.00, WIND SPEED 8.7

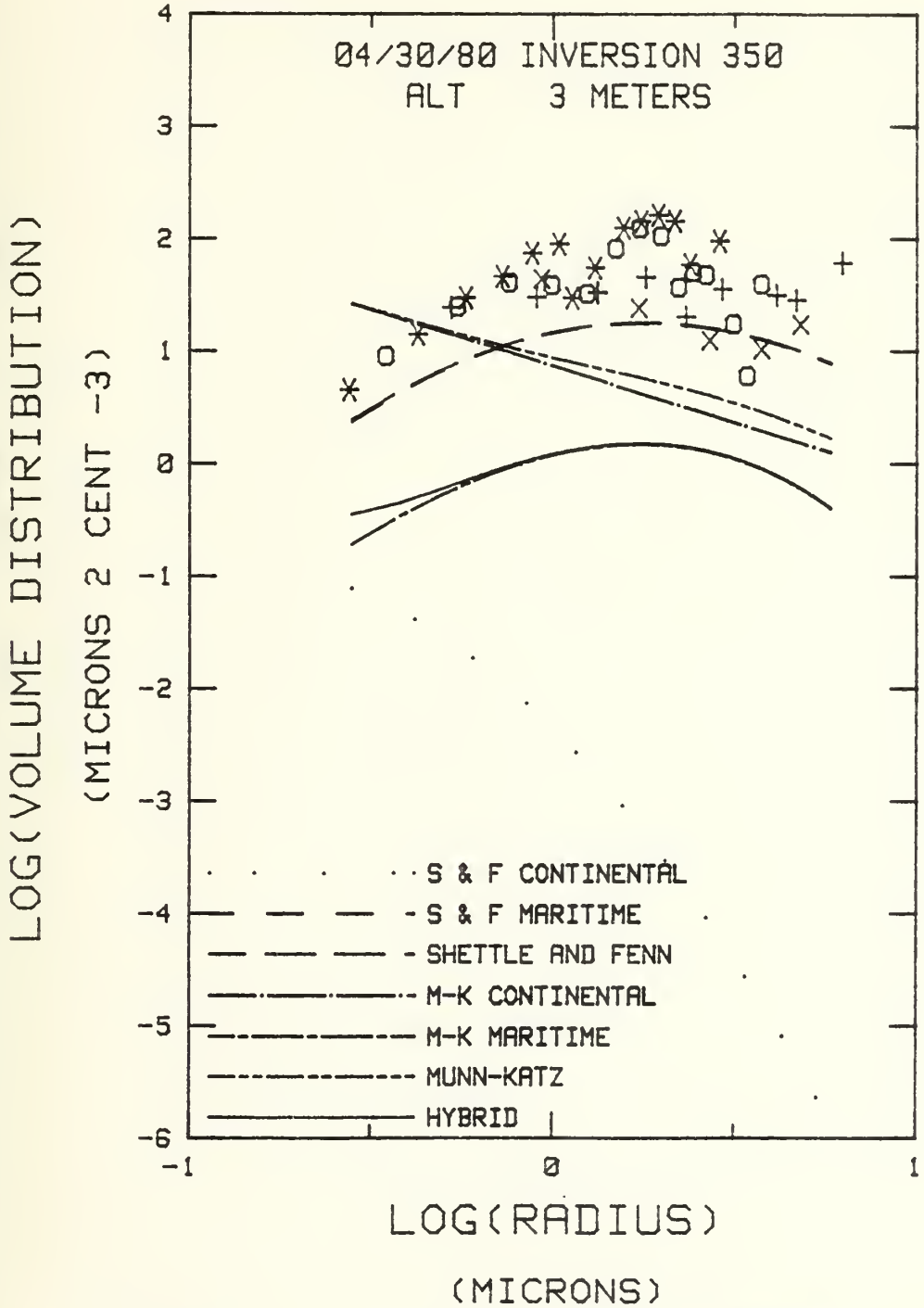

Figure 35. L #3 Volume Distribution, 3 Meters, Model Components

RELATIVE HUMIDITY 81.36, MIXING RATIO 7.34, WIND SPEED 4.1

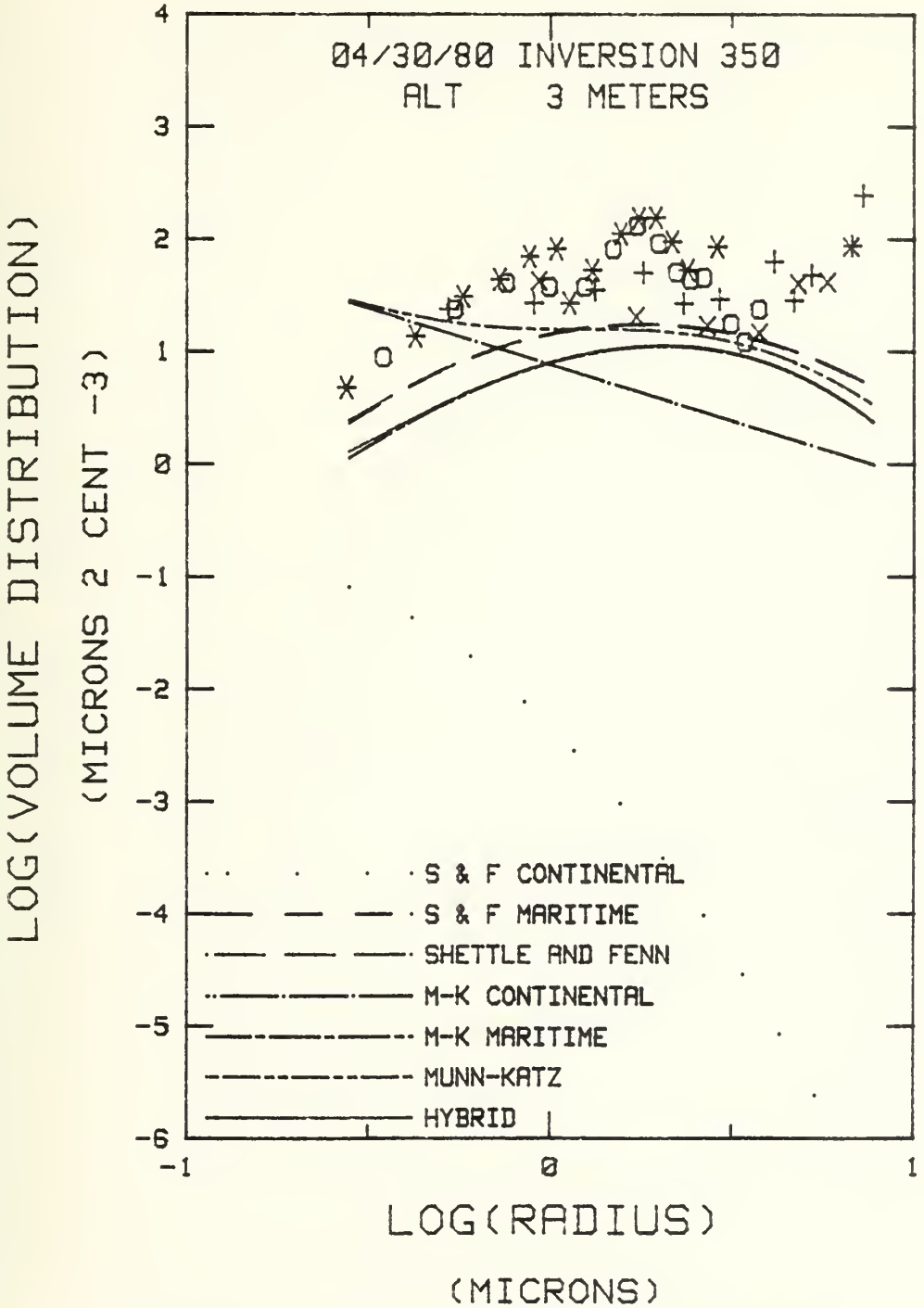

Figure 36. L #4 Volume Distribution, 3 Meters, Model Components

RELATIVE HUMIDITY 82.12, MIXING RATIO 7.41, WIND SPEED 7.7

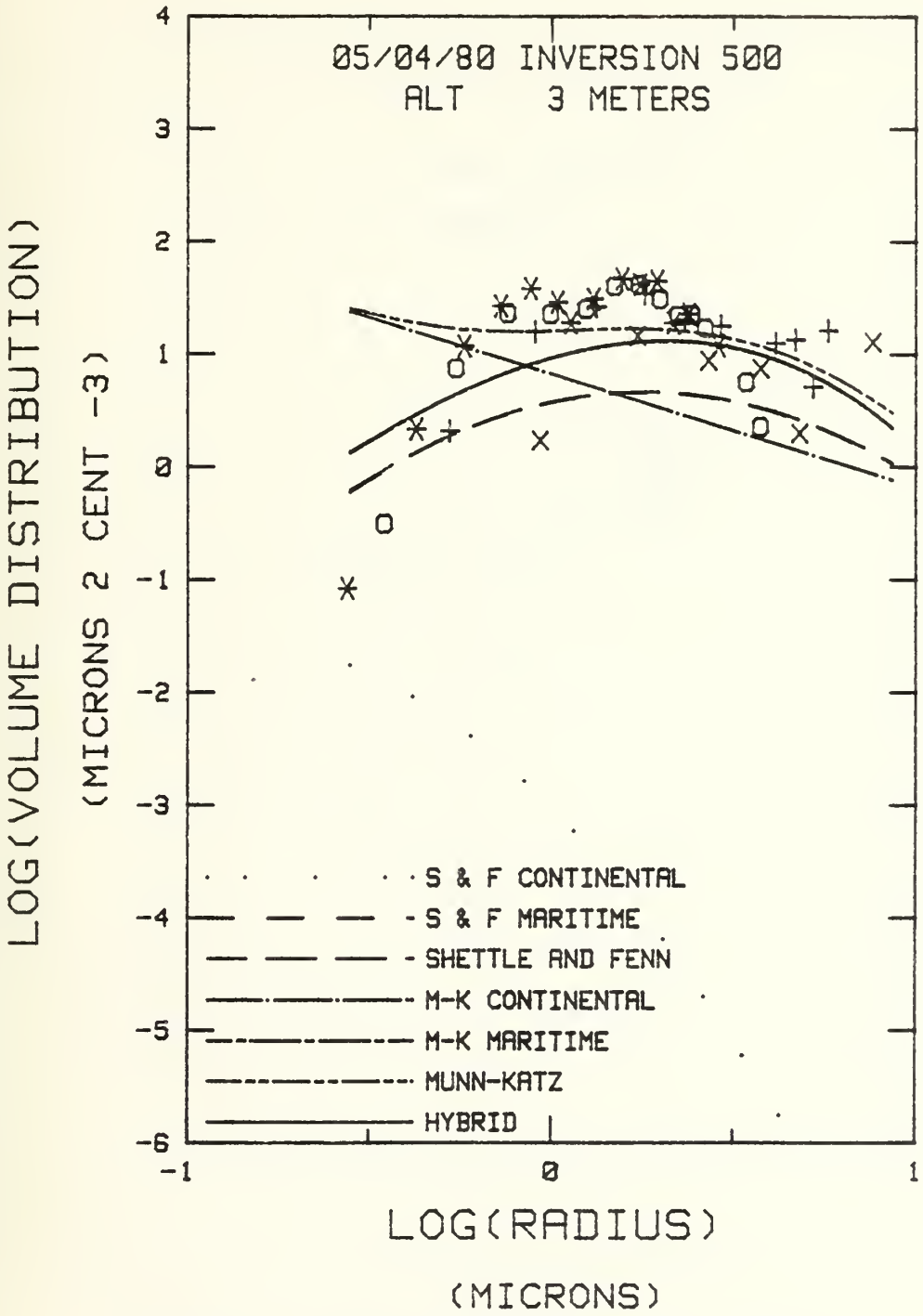

Figure 37. L #16 Volume Distribution, 3 Meters, Model Components

RELATIVE HUMIDITY 79.04, MIXING RATIO 7.00, WIND SPEED 8.7

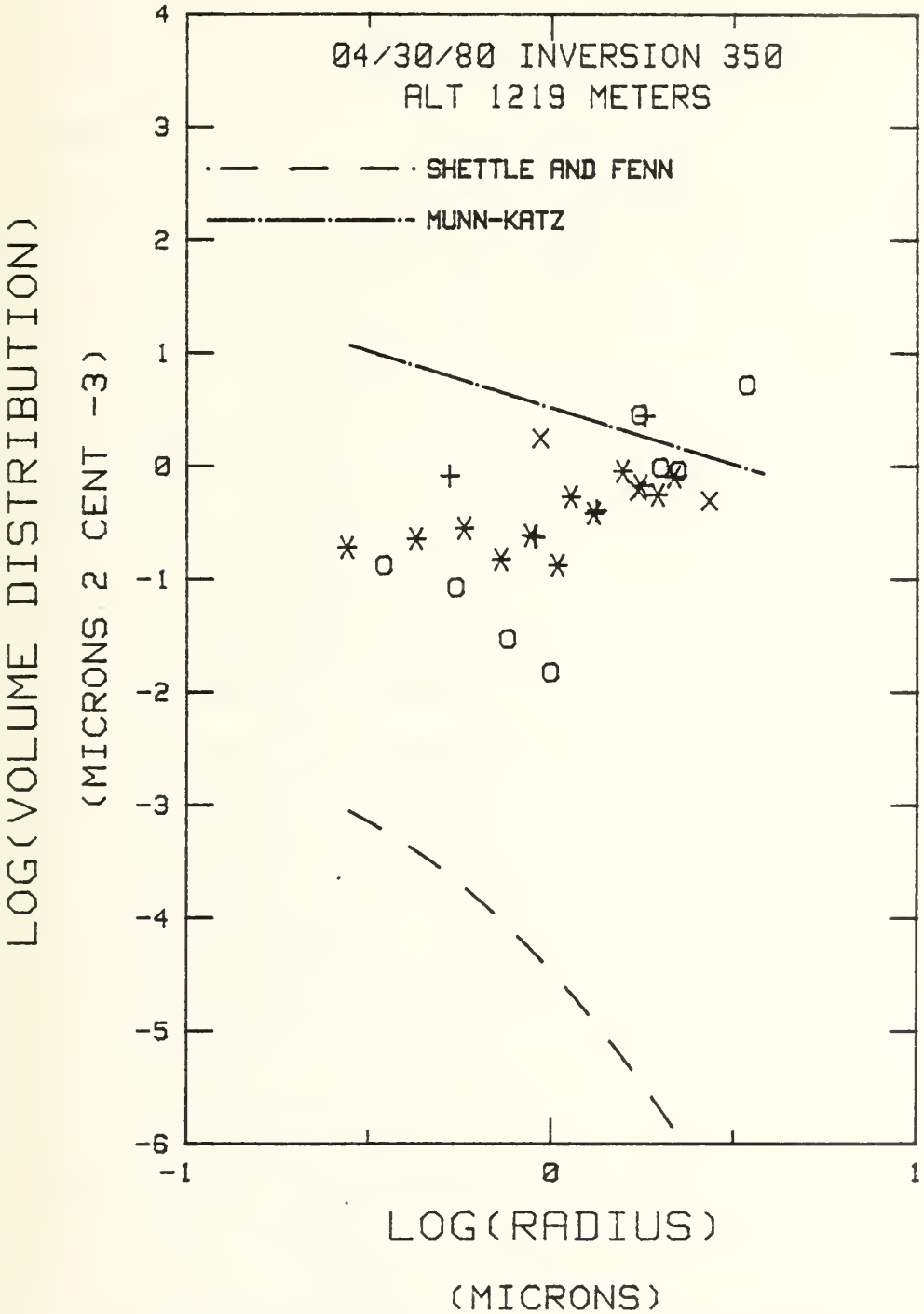

Figure 38. L #4, 1219 Meters, Size Distribution
Composed of Continental Components Only

RELATIVE HUMIDITY 20.48, MIXING RATIO 2.37, WIND SPEED 7.7

VI. CONCLUSIONS AND RECOMMENDATIONS

A. CONCLUSIONS

It must be emphasized that in a consideration of the natural variability of atmospheric aerosols, no empirical model will be consistent with all observed data and any reasonable model will only be consistent with some data. Therefore, we must employ those models which are most readily adaptable to the naval operational environment. Hence, we need a model which is dependent only upon easily measurable bulk parameters.

The main conclusions arising from this thesis are:

1) The mixing volume (or inversion height) and the production time are important parameters in observed aerosol size distributions and should be included in all models.

2) Under low to moderate wind speeds the Hybrid model is the least accurate of any of the models considered. Therefore, this model should be discarded. Under conditions of high wind speed or low total particle concentration an equivalent result to the Hybrid model can be obtained by considering only the maritime component of the Munn-Katz model.

3) The Shettle and Fenn model consistently produced the most accurate results. However, its required input parameter is either TPC or visibility, neither of which is easily predicted or measured.

4) The Munn-Katz model is the most operationally adaptable of the three models studied. Its required input data are relative humidity,

wind speed, and latitude. All of these are easily predictable and measurable bulk parameters of the marine boundary layer. The reduction of the size of the Junge coefficient, the inclusion of more terms in the continental component, and the incorporation of the inversion height effects should improve this model.

5) The fall off in size distribution of the smaller radii suggest the need of a different (from those discussed above) continental component in models describing marine aerosol size distributions. Perhaps, the omission of a continental component is the most realistic approach. Further investigation of open ocean continental aerosols is warranted.

Models such as the Munn-Katz model and modeling efforts such as that of Isaacs (1980) are a step towards an aerosol effects model usable for real time assessment of electro-optical systems performance. However, if that goal is to be attained, more work must be done to develop models which more realistically include relative humidity, wind speed and inversion height.

B. RECOMMENDATIONS

Further investigation should include a quantitative validation of Isaacs' complete radiative transfer model. The first step in such a validation should be to assess the radiometric resolution required by the EO system performance models. These findings should be compared to the radiometric resolution attainable given the DMSP quantization interval. After such a comparison, if the DMSP gray shade resolution is sensitive enough to provide the required accuracy, experiments can be

designed to validate Isaacs' model. This will require the simultaneous collection of aerosol, meteorological, and DMSP data. When it again becomes available, DMSP data should be saved on magnetic tape in decrypted form to facilitate the navigation of the imagery and the computation of required zenith and azimuthal angles. Additionally, the collection of data should begin in the areas adjacent to the fog or stratus deck and move out toward clear skies, sampling at regular intervals. This procedure will improve the probability of sampling across several gray shades.

Additionally, an investigation of the methods employed by those working with the NIMBUS-7 CZCS (coastal zone color scanner) data (Gordon, 1978) should be undertaken. Comparison of CZCS derived aerosols with measured data like those used in this thesis, may show that CZCS methods are the most accurate near-real-time operational aerosol measurements available. At the very least, existing CZCS data probably can be used to develop a climatological data base which may be used for further aerosol model development.

Attention should be given, in continued development of Isaacs' model, to the possibility of sunglint and ocean turbidity contamination. Ocean turbidity problems are probably insignificant because the uncertainties due to other assumptions probably outweigh the variation due to turbidity. Geometric considerations cause sunglint contamination to most certainly be significant in some DMSP gray shades.

These results also point out the need for continued work in the development of aerosol generation models. Specifically, the continental

component of the Munn-Katz model should be examined to provide a better description of the distribution of smaller aerosols. (The Hybrid model represents an unsuccessful attempt to meet this need.) At the very least, improvements in the Junge coefficient can be made.

The present results suggest that taking account of inversion height will yield improved predictions of aerosol size distributions. Therefore, effects on variations in aerosol loading due to changes in the inversion height should be investigated and modeled. The inversion height could then be included as an additional input variable for the Munn-Katz model, perhaps drawing on existing mixed layer models to predict inversion height.

LIST OF REFERENCES

Davidson, K. L., G. E. Schacher, C. W. Fairall, and T. M. Houlihan, 1980: Observations of Atmospheric Mixed-Layer Changes Off the California Coast. Proceedings of 2nd Conference on Coastal Meteorology, Los Angeles, CA, Jan 1980, 63-76.

Fairall, C. W., 1980: Atmospheric Optical Propagation, Comparisons during MAGAT-80. The BDM Corporation Report, BDM/M-010-80, Monterey, CA, 143 pp.

Fairall, C. W., 1981: Aerosol Extinction over the Ocean: A Field Evaluation of the Wells-Munn-Katz Model. The BDM Corporation Report, BDM/M-TR-0001-81, Monterey, CA, 26 pp.

Fett, R. W., and R. G. Isaacs, 1979: Concerning Causes of "Anomalous Gray Shades" in DMSP Visible Imagery. J. Appl. Meteor., 18, 1340.

Fett, R. W., and W. F. Mitchell, 1977: Navy Tactical Applications Guide: Vol. 1. Technique and Applications of Image Analysis (DMSP). NEPRF Applications Report 77-03, Tactical Applications Department, NEPRF, Monterey, CA.

Fitzgerald, J. W., 1975: Approximation Formulas for the Equilibrium Size of an Aerosol Particle as a Function of Its Dry Size and Composition and the Ambient Relative Humidity. J. Appl. Meteor., 14, 1044-1049.

Fitzgerald, J. W., 1979: On the Growth of Aerosol Particles with Relative Humidity. NRL Memorandum Report 3847, Naval Research Laboratory, Washington, DC.

Gathman, S. G., and B. J. Julian, 1979: The EOMET Cruise of the USNS HAYES, May-June 1977, NRL Memorandum Report 3924, Naval Research Laboratory, Washington, DC.

Gordon, H. R., 1978: Removal of Atmospheric Effects from Satellite Imagery of the Ocean. Appl. Optics, 17, 1631-1636.

Hänel, G., 1976: The Properties of Atmospheric Aerosol Particles as Functions of the Relative Humidity at Thermodynamic Equilibrium with the Surrounding Moist Air. Advances in Geophysics, 19: 73-188. Edited by H. E. Landsberg, and J. Van Mieghem, Academic Press, New York.

Heil, J. N., 1981: Synoptic Scale Features Associated with Vertical Distributions of IR Aerosol Extinction, M.S. Thesis, Naval Postgraduate School, Monterey, CA.

Isaacs, R. G., 1980: Investigations of the Effect of Low Level Maritime Haze on DMSP VHR and LF Imagery. Office of Naval Research, Arlington, VA.

Meszaros, A., and K. Vissy, 1974: Concentration Size Distribution and Chemical Nature of Atmospheric Aerosol Particles in Remote Oceanic Areas. Aerosol Sci., 5, 101-109.

Nilsson, B., 1979: Meteorological Influences on Aerosols in the 0.2 - 40.0 μm Wavelength Range. Appl. Opt., 18, 3457-3473.

Noonkester, V. R., 1980: Offshore Aerosol Spectra and Humidity Relations Near Southern California. Preprints Second Conference on Coastal Meteorology, American Meteor. Soc., Los Angeles, CA, Jan 1980, 113-119.

Shettle, E. P., and R. W. Fenn, 1979: Models for the Aerosols of the Lower Atmosphere and the Effects of Humidity Variations on the Optical Properties. AFGL-TR-79-0214, Air Force Geophysics Laboratory, Hanscom AFB, MA.

Wells, W. C., G. Gall, and M. W. Munn, 1977: Aerosol Distribution in the Maritime Air and Predicted Scattering Coefficients in the Infrared. Appl. Opt., 16, 543.

Whitby, K. T., and G. M. Sverdrup, 1978: California Aerosols: Their Physical and Chemical Characteristics. Publ. No. 347, Particle Technology Lab., University of Minnesota, Minneapolis, MN.

INITIAL DISTRIBUTION LIST

		No. Copies
1.	Defense Technical Information Center Cameron Station Alexandria, Virginia 22314	2
2.	Library, Code 0142 Naval Postgraduate School Monterey, California 93940	2
3.	Commander Naval Oceanographic Command NSTL STation, Mississippi 39529	1
4.	Commanding Officer Fleet Numerical Oceanography Center Monterey, California 93940	1
5.	Commanding Officer Naval Environmental Prediction Research Facility Monterey, California 93940	1
6.	Prof. R. J. Renard, Code 63Rd Naval Postgraduate School Monterey, California 93940	1
7.	Prof. C. N. K. Mooers, Code 68Mr Naval Postgraduate School Monterey, California 93940	1
8.	Department of Meteorology Library, Code 63 Naval Postgraduate School Monterey, California 93940	1
9.	Dr. E. E. Hindman Department of Atmospheric Science Colorado State University Fort Collins, Colorado 80523	1
10.	Mr. R. W. Fett Naval Environmental Prediction Research Facility Monterey, California 93940	1

11. Atmospheric Sciences Lab — 1
DELAS-AS-P
White Sands Missile Range, New Mexico 88002

12. Lt. Mark E. Schultz — 5
Naval Environmental Prediction Research Facility
Monterey, California 93940

13. Lcdr. T. E. Callaham, Code N341 — 1
Naval Oceanographic Command
NSTL Station, Mississippi 39529

14. Lt. J. W. Raby — 1
NOCF
NAS North Island, California 92135

15. Dean of Research, Code 012 — 1
Naval Postgraduate School
Monterey, California 93940

16. Assoc. Prof. K. L. Davidson, Code 63Ds — 10
Naval Postgraduate School
Monterey, California 93940

17. Adj. Prof. J. L. Mueller, Code 68My — 1
Naval Postgraduate School
Monterey, California 93940

18. Asst. Prof. C. H. Wash, Code 63Wy — 1
Naval Postgraduate School
Monterey, California 93940

19. Dr. A. Goroch — 1
Naval Environmental Prediction Research Facility
Monterey, California 93940

20. Dr. A. Weinstein — 1
Director of Research
Naval Environmental Prediction Research Facility
Monterey, California 93940

21. Cdr. K. Van Sickle — 1
Code AIR-370
Naval Air Systems Command
Washington, DC 20360

22. Dr. A. Shlanta — 1
Code 3173
Naval Weapons Center
China Lake, California 93555

23. Dr. E. J. Mack 1
Calspan Corporation
Buffalo, New York 14221

24. Dr. R. G. Isaacs 1
Atmospheric and Environmental Research, Inc.
872 Massachusetts Avenue
Cambridge, Massachusetts 02139

25. Dr. J. Richter, Code 532 1
Naval Ocean Systems Center
San Diego, California 92152

26. Lt. Bauke Houtman 1
Officer in Charge
NAVOCEANCOMDET AGANA Box 81
FPO San Francisco 96654